COLLEGE OF NATURAL SCIENCES

SCHOOL OF EARTH SCIENCES

PETROGRAPHY AND DEFORMATION HISTORY OF BILA (GIDANO KING) AREA, WOLLEGA, WESTERN ETHIOPIA

BY: DEREJE KENEA

ID. No. : GSR/0425/08

ADVISOR: MULUGETA ALENE (Dr.)

A thesis submitted to the School of Graduate Studies of Addis Ababa University in partial fulfilment of the requirements for the degree of Master of Science in Earth Sciences (Petrology)

May, 2017

Addis Ababa, Ethiopia

ADDIS ABABA UNIVERSITY

COLLEGE OF NATURAL SCIENCCES

SCHOOL OF EARTH SCIENCES

PETROGRAPHY AND DEFORMATION HISTORY OF BILA (GIDANO KING) AREA, WOLLEGA, WESTERN ETHIOPIA

BY

DEREJE KENEA

APPROVED BY EXAMINING BAORD

Dr. Balemwal Atnafu	_______________	______________
Head, School of Earth Sciences	Signature	Date
Dr. Mulugeta Alene	_______________	______________
Advisor	Signature	Date
Prof. Gezahegn Yirgu	_______________	_____________
Examiner	Signature	Date
Dr. Bekele Abebe	_______________	______________
Examiner	Signature	Date

Declaration of Originality

I hereby declare that this thesis is my original master‘s degree work under the supervision of Dr. Mulugeta Alene, School of Earth Sciences, Addis Ababa University during the year 2016/2017. This thesis is my original work and has not been presented for a degree or diploma in any other university, and all sources of materials used for the thesis have been duly acknowledged.

Dereje Kenea ______________ ________________

Signature Date

This is to certify that the above declaration made by the candidate is correct to the best of my knowledge.

Dr. Mulugeta Alene (Advisor) ______________ ________________

Signature Date

Acknowledgment

First of all I am deeply thankful to my advisor Dr. Mulugeta Alene for his special assistance, guidance, encouragement, comments and suggestions in this study from the beginning to the end of the research work. Next I would like to give my gratitude to Addis Ababa University School of Earth Sciences for funding my study. At the last gratitude goes to all of my friends who directly or indirectly helped me for the success of this research work and peoples of Boji Dirmaji Wereda for allowing and helping me during the field work.

Abstract

Bila area is located in the metamorphic terrains of West Ethiopian Shield. It covers an area of about 56 Km^2. The main objective of this study is to understand lithology, petrography, structures, deformation history and geochemistry of the basement rocks. To accomplish the objectives; an integrated descriptions of field work, petrographic investigations, structural and geochemical data analysis have been carried out. The area consists varieties of rock units; slate, marble, phyllite, quartzite, graphite schist, metabasalt, chlorite schist, serpentinite, talc schist and actinolite-tremolite schist. The metasedimentary rock group contains chlorite, muscovite, biotite, sericite, quartz and feldspar whereas the metaultramafic and metavolcanic rocks composed the minerals; sericitized plagioclase, chlorite, epidote, actinolite, feldspar, opaque, quartz, calcite and talc with some relict of igneous origin. Based on their mineral assemblages, relict igneous texture and the existence of primary bedding the rocks of the area experienced low grade green schist facies metamorphism. Field structural data and petrographic investigations from this area demonstrate that, at least three deformational phases are recorded in the area. D1 and D2 phases are mostly responsible for the formations of ductile deformations whereas, post D2 deformational phases may be responsible for the formations of the latter brittle deformations during which the faults, veins and joints were developed. The major oxides and trace elements Harker variation diagrams, REE and multi element patterns of Bila metavolcanic rocks demonstrate the rocks are linked with fractional crystallization process. The Zr-Y-Nb and Th- Ta- Hf triangular discrimination diagrams revealed that most of the Bila rocks are within the tectonic environment of volcanic arc basalts.

Key words: Bila area, metavolcanic rocks, meta-ultramafic rocks, metasedimentary rocks, deformation history, metamorphism, fractional crystallization.

Table of Contents

List of Figures

List of Table

List of Acronyms

ANS	Arabian Nubian Shield
DSZ	Didessa shear zone
EAO	East African Orogeny
F	fold
GPS	Global Positioning System
GSE	Geological Survey of Ethiopia
ICP-AES	Inductively Coupled Plasma–Atomic Absorption Spectrometry
ICP-MS	Inductively Coupled Plasma– Mass Spectrometry
HREE	heavy rare earth elements
LOI	Loss of Ignition
LREE	Light Rare Earth Element
MB	Mozambique Belt
MORB	mid-ocean ridge basalt
OIB	Ocean island basalt
PPL	Plane Polarized Light
REE	Rare Earth Element
S	Foliation
TD	Tulu dimtu
TDB	Tulu Dimtu Belt
TDTZ	Tulu Dimtu thrust fault/ shear zone
UTM	Universal Transversal Mercator
WEB	Western Ethiopian Belt
WE	Western Ethiopian

WES	Western Ethiopian Shield
XPL	Cross Polarized Light

CHAPTER ONE

Introduction

1.1 Background

The exposures of the basement rocks in Ethiopia are found in the areas not highly affected by Cenozoic volcanism, rifting and where the Phanerozoic cover rocks have been eroded away (Mengesha Tefera et al., 1996). This study identifies four major regions where the Precambrian basement rocks of Ethiopia are exposed. These area include in Tigray region in the north; Gojam, Wollega, Ilubabor and Kefa regions in the west, in Sidamo and Bale regions in the south and in Harerghe region in the east. The Ethiopian basement is Neoproterozoic in the age ranging from 880 to 550Ma that constitutes wide exposures in the southern and western part and, to a lesser extent, in the northern part (Abbate et al., 2015). The Precambrian rocks of Ethiopia categorised under gneissic rocks of Mozambique Belt, to the south and the low grade rocks of the Arabian Nubian shield to the north (Teklewold Ayalew, 1997).

The Western Precambrian of Ethiopia is characterised by high grade gneiss and migmatite in the east and west part and low grade metavolcano-sedimentary rocks such as metabasalt, marble, quartzite, talc schist, and chlorite schist, at the centre of the shield (Fig.1.1) with the associations of mafic-ultramafic intrusions and syn-to post-tectonic gabbroic to granitic intrusions (Teklewold Ayalew, 1997; Tadesse Alemu and Tsegaye Abebe, 2007; Blades, 2015). The lithologic boundary between the gneissic and metavolcano-sedimentary terranes is tectonic, as marked by ultramylonitic rocks (Abraham, 1989 as cited in Tesfaye Kebede and Koeberl, 2002). The Western Ethiopia Shield (WES) is one of the largest continuous outcrop tracts in the EAO and it is found between the Arabian-Nubian Shield and Mozambique Belt (Stern, 1994; Johnson et al., 2011; Fritz et al., 2013; Robinson et al., 2014, 2015 as cited in Blades, 2015). The earlier study of Kazmin et al, (1979) as cited in Tadesse Alemu and Tsegaye Abebe, (2007), classify the Western Ethiopian basement from east to west into five lithological units/zones:(i) eastern block of high grade Pre–Pan-African rocks, (ii) ophiolite belt, (iii) dioritic and grano-dioritic and intermediate volcanics, (iv) metavolcano-metasedimentary belt and (v) western block of high grade Pre –Pan- African rocks.

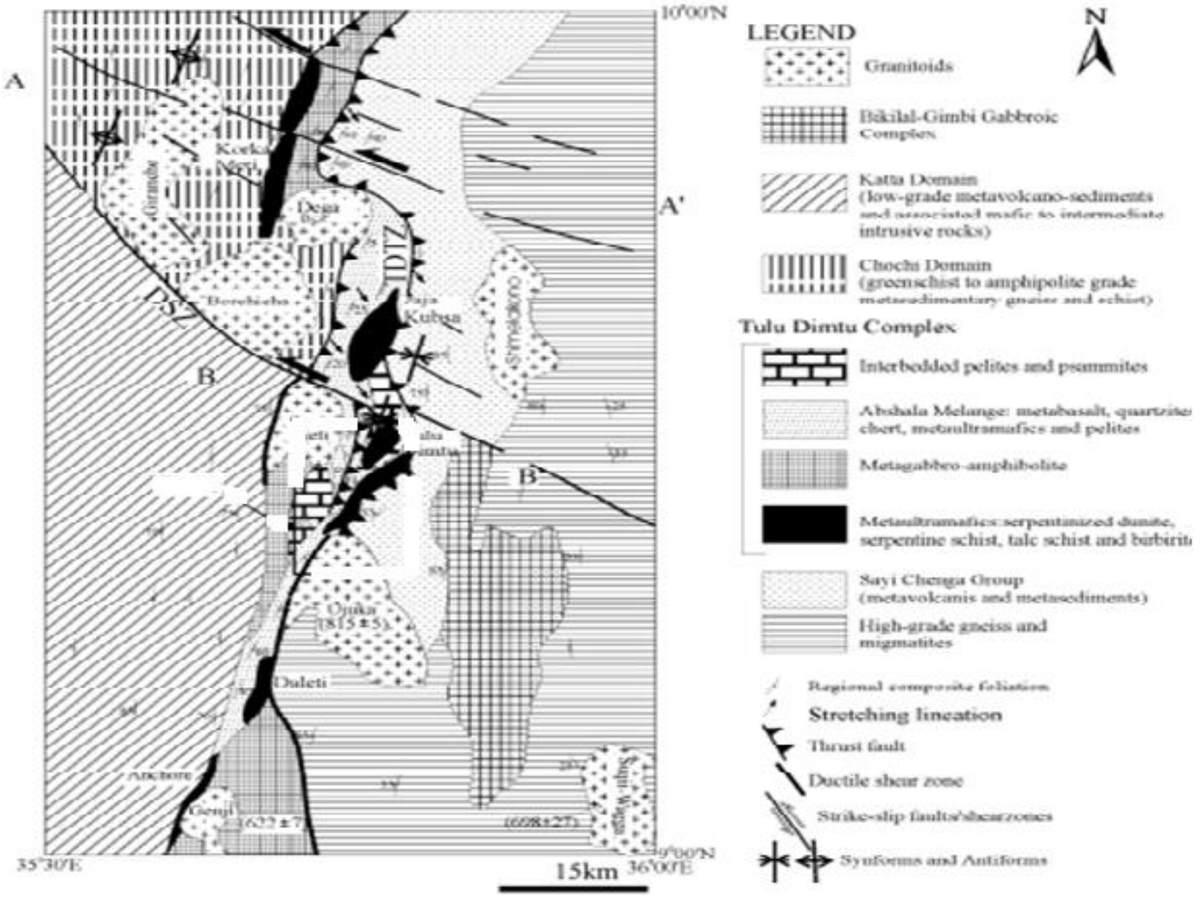

Figure 1.1 Geologic map of Tulu Dimtu Belt and adjacent areas (Tadesse Alemu and Tsegaye Abebe, 2007)

The recent studies divide Western Ethiopian basement into the Gore-Gambella area that comprise Birbir, Baro and Gore domains (Teklewold Ayalew, 1997), and Tulu Dimtu belt that comprise five domains (Fig.2.2) from east to west; Didessa, Kemashi, Dengi, Sirkole and Daka domains (Allen and Gebremedhin Tadesse, 2003). Mengesha Tefera and Berhe (1996), as cited in Teklewold Ayalew (1997) suggested that the litho-tectonic units of the Gore-Gambella include Baro and Geba domains that comprise high grade rocks such as; gneisses and migimatites and Birbir domain that comprise lower grade metamorphic rocks. The Tuludimtu Belt that covered Gimbi-Asosa area consists of a variety of moderate to high grade gneisses and low to moderate grade metasedimentary rocks intruded by deformed and undeformed ultramafic, mafic, intermediate and felsic igneous bodies (Allen and Gebremedhin Tadesse, 2005).

According to Teklewold Ayalew (1997) structural characteristics of western Ethiopia is affected by (D1–D4) deformational events in the case of Gore-Gambella area (Birbir, Baro and

Geba domains) and (D1–D3) in the case of Tulu Dimtu belt (Didessa, Kemashi, Dengi, Sirkole and Daka domains) that is applied only to the volcano-sedimentary lithologic units, and represented the Pan African deformation histories (Allen and Gebremedhin Tadesse, 2005; Tadesse Alemu and Tsegaye Abebe, 2007). The age of the ductile deformation recorded in the gneiss domains is of pre-pan African age and the pan African imprint may be latest ductile and brittle deformation phases (Allen and Gebremedhin Tadesse, 2005).

In Western Ethiopian Shield three syn-tectonic magmatism took place at 850–840 Ma, 790–780 Ma and ca. 660 Ma. Hafnium isotopic analysis from Didesa and Kemashi Domains indicates that the early Cryogenian magmas were originated from juvenile Neoproterozoic mantle sources with little involvement of the pre-Neoproterozoic continental crust (Blades et al., 2015). The deformation and metamorphism of Western Ethiopian basement was take place before intrusion of the post-tectonic 585 ± 8 Ma Ganjii Granite(Blades et al., 2015).

Bila area (study area) is one less studied part of Western Ethiopian Basement in terms of geochemistry, petrography and structural study which is found in Kemashi domain according to division of Allen and Gebremedhin Tadesse (2003). So, this study aims to provide the detailed description and analysis of the petrographic character, lithologic units, structural geology, deformation history and geochemistry of the area.

1.2 Geographic Setting of the Study Area

1.2.1 Location and Accessibility

The study area is located in western Ethiopian basement in the Boji Wereda, west Wollega, Oromia regional state along the road from Addis Ababa-Nekemte-Gimbi-Bila Area, on Kemashi road way, at a distance of approximately 541km from Addis Ababa. The area is located between 1038000-1045000N and 796000-804000E UTM coordinates.

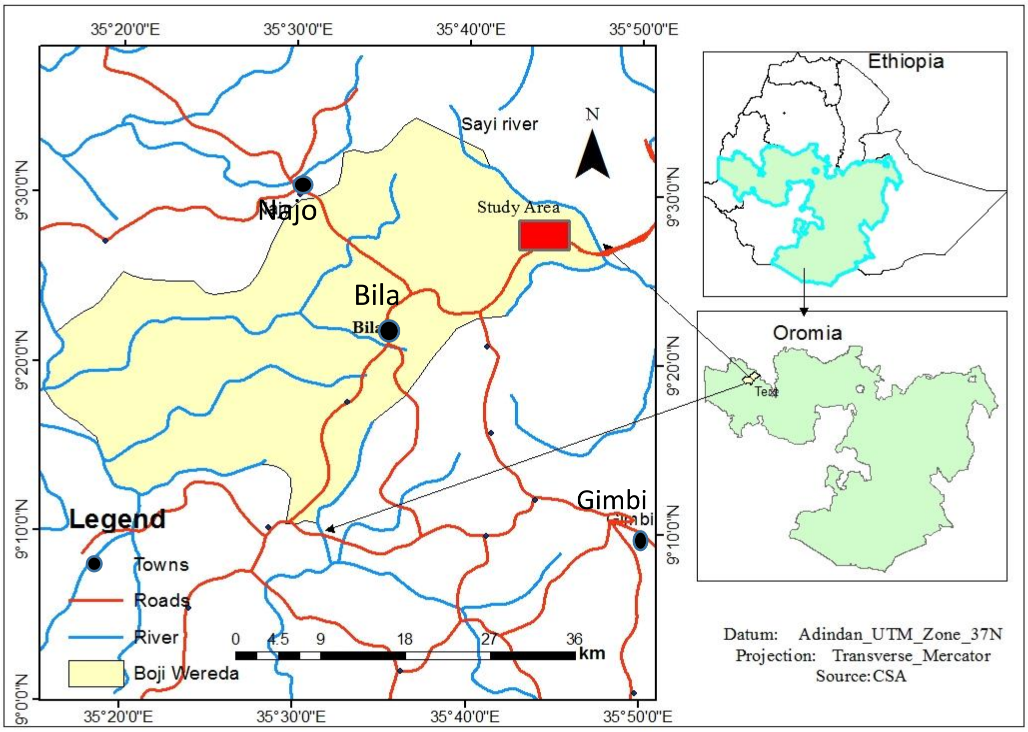

Figure 1.2 Location map of the study area

1.2.2 Physiography of the Study area

The landscape of the study area is characterized by rugged topography like mountain, ridge and flat. The southern and western part is mountainous but the eastern part is slightly flat. The drainage patterns was dendritic drainage system. The elevation is ranging from 1250 to 2000m.

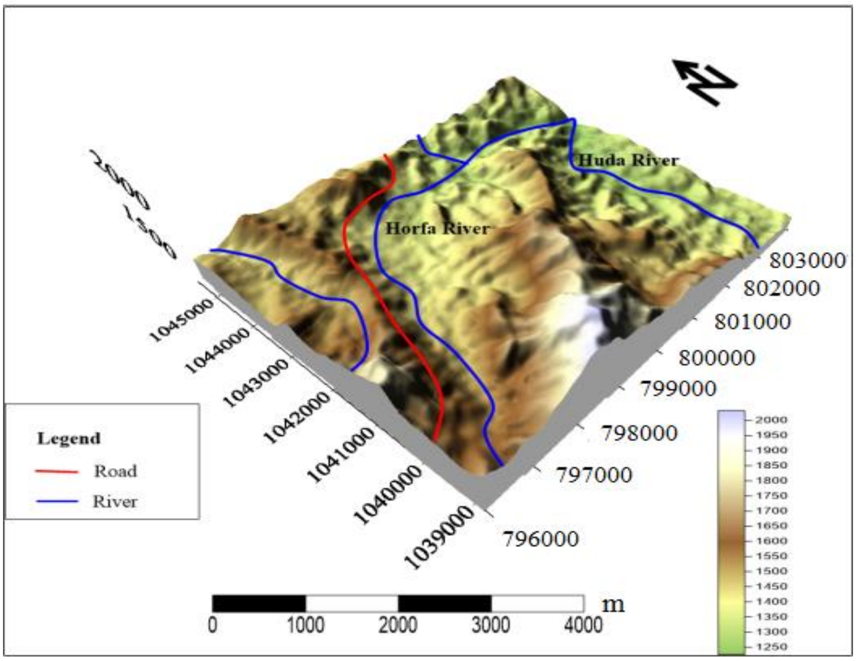

Figure1.3 Physiographic map of Bila area

1.2.3 Climatic Condition and Vegetation

Climate condition of the study area is characterised by moderately humid to semi-arid with average annual temperature of 21.2^{o}C and annual rainfall of 973mm. The area gets high rain from May to October. The study area is covered by grasses and moderately vegetated by different types of forests trees. The most common vegetation covers are savannah grass, bamboo forest, and deciduous trees. Since the geologic exposure of the area is found along the river and the area gets high rainfall during the summer, it is difficult for field work during summer time.

1.2.4 Population and Settlement

The population density in the study area is very low**.** The ethnic group in the area were the Oromo people and their official language is Oromeffa. Their religion is mostly Protestant with very few Orthodox Christian follower. The livelihood of the local people is dependent on farming. The common types of crops cultivated in the area are maize, sorghum, teff, coffee, pepper and the likes.

1.3 Problem Statement

Some previous researchers have worked on regional study on the western part of Ethiopian basement regarding geology, geochemistry and structural geology (Teklewold Ayalew and Johnson, 2002; Tesfaye Kebede and Koeberl, 2002; Allen and Gebremedhin Tadesse, 2003; Tadesse Alemu and Tsegaye Abebe, 2007; Blades, 2013, 2015). However there are many parts of metamorphic terrains of west Ethiopian shield that require detailed study regarding lithologic unit identification, metamorphic grade and facies, deformation history and geochemistry for the better understanding of geological history. So Bila area is part of the west Ethiopian basement that require more study. In the present work an attempt has been made to map the area in detail at scale of 1:30,000 to describe lithologic units, structures, establish the deformation history qand geochemistry of the rocks of the area.

1.4 Significance of the Study

- To give a detailed petrography, structural characteristics and geochemistry of the lithological units in the Bila area for better understanding of geological history.
- This research work will fill the existing gap of detail information in the western Ethiopian basement specifically about Bila Area.

- It contributes some dataset to the ongoing study of basement rocks, deformation history and geochemistry of the western Ethiopia.

1.5 Objectives

1.5.1 General Objective

The main objectives of this study are to describe petrography, structures, deformation history and geochemistry of the basement rocks in the Bila area.

1.5.2 Specific Objectives

- To produce geological map of the area at scale of 1:30,000.
- To describe metamorphic facies and grade of the rocks.
- To describe phases of deformations in relation to regional tectonics.
- To determine tectonic setting and trace the origin of the basement rocks of the area.

1.6 Limitation

- The western Ethiopian basement is largely covered by soil and vegetation, so there is lack of good exposures for mapping and structural geology study.

1.7 Materials and Methods

1.7.1 Materials

The following materials are used in order to meet the objectives of the study: Brunton compass, GPS (Global Positioning System), maximized topo map by 1:30,000, geological hammer, hand lens, diluted HCl, digital camera, sample bag, petrographic microscope, jaw crusher and mill.

1.7.2 Methodology

1.7.2.1 Fieldwork

In order to achieve the general and specific objectives of the thesis, the methods have been used are divided into three stages: the pre-field activity, the field-work and the post-field activity. In the pre-field work review of the literatures on the geology, structures, geochemistry, accessibility and the methods that would be applied on the study area are reviewed from previous works. During the field work, for 15 days collections of 30 representative rock samples for preparation of rocks thin-sections and geochemical data as well as collections of structural data have been done. And also geologic map at the scale of 1:30,000 is prepared. At the stage of post field work petrographic, geochemical and structural data analysis and descriptions have been done.

1.7.2.2 Petrographic analysis

Thirty thin sections were prepared in the mineralogy and petrography laboratory of Geological Survey of Ethiopia (GSE). The prepared thin sections were described using polarized petrographic microscope in the petrology laboratory of school of earth sciences at Addis Ababa University. A detailed petrographic study for mineral assemblages identification, calculate modal proportion, textural descriptions, and the rock naming has been carried out.

1.7.2.3 Structural data analysis

All the structural geology data that are found in the study area including: orientation of foliations, fold axis, fold axial planes, joints, faults and veins are collected during field work. These structural elements are plotted and analysed using the stereo-plot software.

1.7.2.4 Geochemical analysis

Six selected rock samples were crushed to less than 2mm, and the split samples were pulverized to about -200 mesh size at the laboratory of Geological Survey of Ethiopia (GSE). The pulverised sample were submitted to ALS geochemical laboratory PLC, Addis Ababa for preparation. Then the pulverized samples were shipped to ALS Services of Ireland country for complete whole rock analysis.

1.8 Previous Works in the Western Ethiopian Shield

The Precambrian basement of western Ethiopia (WE) is the largest Precambrian block in Ethiopia, which is extending north ward from 6^0 N for about 650 km (Tadesse Alemu and Tsegaye Abebe, 2007). Some geological works have been done regionally on Western Ethiopian Shield for the last decades regarding geology, geochemistry and tectonic evolution. According to Kazmin et al. (1979, as cited in Tesfaye Kebede, 1999) geology of Precambrian terrain of WE is considered to contain lithological units common to both the Arabian-Nubian Shield (ANS) in the north and the Mozambique Belt in the south. The WES consists of a variety of moderate to high grade gneisses and migmatite, ophiolitic rocks and low to moderate grade metasedimentary and metavolcanic rocks intruded by deformed and undeformed ultramafic,

mafic, intermediate and felsic igneous bodies (Allen and Gebremedhin Tadesse, 2003; Tadesse Alemu and Tsegaye Abebe, 2007; Teklewold Ayalew and Johnson, 2002).

Geotectonic evolution and tectonic subdivision studies have been carried out on WES. According to (Kazmin et al.1978, as cited in Teklewold Ayalew and Johnson, 2002) the geotectonic evolution of the WES has been interpreted in terms of early rifting and associated sedimentation, followed by subduction and island-arc formation, arc-accretion and finally, continent-continent collision. The later studies of tectonic subdivisions of Tulu Dimtu complex have been described by (Allen and Gebremedhin Tadesse, 2003) and that of Gore-Gambella area have been described by (Teklewold Ayalew and Johnson, 2002). According to these studies Tulu Dimtu Belt is subdivided into five litho-tectonic domains; the Didesa, Kemashi, Dengi, Sirkole and Daka Domains, that is formed during the amalgamation of western Gondwana before the final closure of the Mozambique Ocean. And also that of Gore-Gambella area is divided in three litho-tectonic domains; Birbir, Baro and Geba domains.

Some studies have been also conducted on geochemistry and geochronology of Western Ethiopia by Tesfaye Kebede and Koeberl, (2002); Gebremedhin Tadesse and Allen, (2005) on the Ganjii monzogranite, Homa gneissic granite, Tuppii granite, Tullu Kapii quartz syenite and Tulu Dimtu ophiolite. The positive Nd (625) values (+4 to+4.5) and the low initial 87Sr/86 Sr ratio (average =0.7025) suggest derivation of the source magma from sub-continental lithospheric mantle with insignificant pre-Pan-African crustal involvement (Tesfaye Kebede and Koeberl, 2002).

Limited studies also carried out on the structural studies of the western basement. According to several authors (Tadesse Alemu and Tsegaye Abebe, 2007; Allen and Gebremedhin Tadesse, 2005 and Teklewold Ayalew and Johnson, 2002) WEB is exposed as a NNE- trending fold and thrust belt, which can be traced for the entire length of western Ethiopia and continue north and south along the Pan-African Barka-Tulu Dimtu suture.

Even though different studies have been conducted on west Ethiopian Belt from different perspective, no detailed study of geochemistry, detail lithologic unit identification and structures has been done on the region. So this study aimed to contribute to the existing gap on detail lithologic identification, deformation history and geochemistry of the rocks of Bila area.

CHAPTER TWO

Review of Regional Geological Setting

2.1 East African Orogeny

East African Orogen (EAO) is the site where a complex history of intra-oceanic and continental margin, magmatic, metamorphic activity and tectonothermal events taken place (Stern, 1994). The orogenesis was originally interpreted by Stern (1994) which is the result of collision between two Neoproterozoic continental masses, East Gondwana (India–Australia–Antarctica) and West Gondwana (Africa–South America). According to Grenne et al. (2003, as cited in Blades et al., 2013) East African Orogen started from the Neoproterozoic subductions of the Mozambique Ocean, which separated India from African continent and was deformed and amalgamated during the late Neoproterozoic-Cambrian assembly of Gondwana. The tectonic evolution of EAO (Fig.2.1) involves; (1) rifting, (2) sea-floor spreading, (3) continental collision between West and East Gondwana forming the East African Orogen, closuring of the Mozambique Ocean, granitic magmatism and post-amalgamation volcanic sedimentary deposition from 650-600Ma; (4) further crustal shortening, orogenic collapse and extension leading to the break-up of Gondwana at 600 to 540 Ma (Stern, 1994: Kroner and Stern, 2005). Many of the rocks in the Orogen formed in volcanic arcs during the Neoproterozoic subduction of the Mozambique Ocean (Meert, 2003; Collins and Pisarevsky, 2005; Meert and Lieberman, 2008, Fritz et al., 2013; Johnson et al., 2011 as cited in Blades et al ,2015).

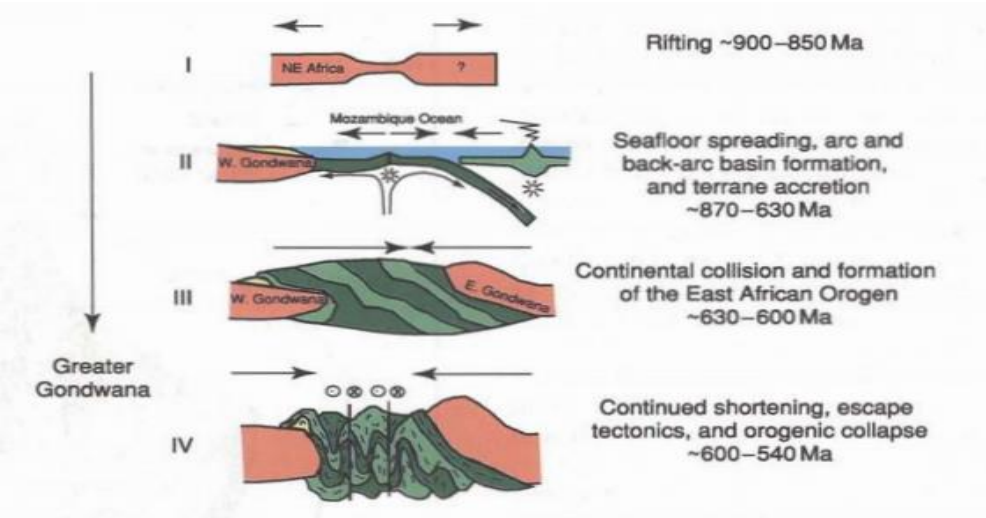

Fig.2.1 Evolution of the Arabian-Nubian Shield (Kroner and Stern, 2005)

East African Orogeny (EAO) is subdivided into two terrains based on the lithological and metamorphic differences (Blade et al, 2015); the Arabian-Nubian Shield and the Mozambique Belt(MB). The Arabian Nubian Shield (Johnson et al., 2011 as cited in Blade et al., 2015), is dominated by low grade volcano-sedimentary rocks with association of plutons and ophiolitic remnants (Kröner et al., 1991; Stern, 1994, Abdelsalam and Stern,1996; Shackleton, 1996; Allen and Tadesse, 2003; Cox et al., 2012; Robinson et al., 2014 as cited in Blade et al., 2015). The Arabian-Nubian Shield predominantly consists of Neoproterozoic supracrustal and magmatic assemblages, many of juvenile origin, structural and metamorphic histories that are similar to those in Phanerozoic age collisions and accretions belts. The Mozambique Belt (MB), which is a tract of largely older continental crust that was characterised by the deformed and metamorphosed during the Neoproterozoic/Cambrian (Meert, 2003; Yibas et al., 2003, Woldemichael and Kimura, 2008; Woldemichael et al., 2010 as cited in Blade et al., 2015). This studies also revealed that the Mozambique Belt contains polydeformed high-grade metamorphic assemblages, that exposing middle to lower crustal levels.

2.2 The Ethiopian Basement

The Precambrian rocks of Ethiopia is exposed around the Eastern, Western, Southern and Northern parts of the country (Kazmin et al., 1978 and Mengesha Tefera et al., 1996). The exposure of Ethiopian basement comprises variety of volcano-sedimentary and plutonic rocks metamorphosed to varying degrees from green schist to amphibolite-facies and locally granulite-facies condition (Kazmin, 1971 as cited in Asrat et al., 2001). The earlier studies classify Precambrian rocks of Ethiopia into three main complexes that have been identified in the country (Kazmin ,1971 ; 1975 as cited in Kazmin, 1978), the Lower, the Middle and the Upper Complexes. The lower complex includes various high grade gneisses and migmatites found in the south and south west (Konso, Alghe, Awata and Yavelo gneisses). The middle complex is represented by rocks such as psammitic and pelitic metasediments (biotite and quartzmuscovite schists, meta-arkoses, quartzite) with subordinate marbles, calc-silicates and amphibole schists which has been exposed in Sidamo, Hareghe and Western Ethiopia (Kazmin et al.,1978). The upper complex is composed of low grade rocks such as amphibolite, chlorite-actinolite schist, metavolcanics, graphitic schist, phyllite, metasandstone and meta conglomerate (Beyth, 1972; Garland, 1980; Fiori et al., 1988 as cited in Asrat et al., 2001). According to Kazmin et al. (1978) the lower complex is archaean in age. However based on the recent geo-chronological, thermochronaological, geochemical and lithotectonic data, this classification of three stratigraphic units are oversimplified and the maximum age constrained from pre- and syn-tectonic intrusive rocks are not more than 1100ma (Asrat et al., 2001).

2.3 Lithology and Stratigraphy of Western Ethiopian Shield

The Precambrian geology of western Ethiopian terrain consists of volcano-sedimentary terrain, gneissic terranes and ophiolitic rocks which are similar to Neoproterozoic rocks of the ANS and rocks of the MB (Kazmin et al., 1978; 1979; de Wit and Senbeto Chewaka, 1981; Teklewold Ayalew et al., 1990 as cited in Teklewold Ayalew and Johnson, 2002). The lithological components found in this region includes; high grade rocks; ophiolite belt; dioritic (granodioritic) batholiths and associated intermediate volcanics; a metavolcano-sedimentary rocks (Kazmin et al., 1978; 1979).

The current studies have been divide tectonic evolution of the WES (Fig.2.2) into Gore-Gambella area which comprise Birbir, Baro and Geba domains (Teklewold Ayalew, 1997), and Tulu Dimtu belt which includes (Aba Sena-Gimbi-Inango-Ayra transects) and comprises five domains from east to west; Didessa, Kemashi, Dengi, Sirkole and Daka domains (Allen and Gebremedhin Tadesse, 2003). This classification is primarily based on grade of metamorphism and also lithological similarities within the same domain (Teklewold Ayalew and Peccerillo, 1998). Divisions of Domains of WES made by (Teklewold Ayalew, 1990: 1997; Allen and Gebremedhin Tadesse, 2003) are described as follows;

2.3.1 Birbir Domain

The Birbir domain consists metasedimentary and metavolcanic rocks including mafic to felsic intrusive and extrusive rocks (Ayalew et al, 1990). The metasedimentary rocks encompasses metagreywacke, pelite, volcanoclastic and carbonate rocks (Ayalew et al, 1990). Foliation of the Birbir domain was result from syn-tectonic recrystallization during early shearing that may related to formation of early folding (Teklewold Ayalew, 1997). According to Teklewold Ayalew, (1997) structures within Birbir domain have the orientation of north-south striking foliations that dip steeply toward the west and the stretching lineations defined by deformed clasts, minerals and mineral aggregates, which was plunge < 20° to the north and south within the domain.

2.3.2 Geba Domain

Geba domain encompasses rocks such as quartzofeldspathic gneisses, medium grained biotite and hornblende-biotite gneisses (Teklewold Ayalew, 1997). Gneisses in this domain is characterised by migmatitic and contain numerous subconcordant lenses of granitic and pecmatitic materials (Ayalew et al, 1990). The structures of Geba domain is characterised by open D2 folding of the gneissic layering (S1) around gently plunging of NNE-trending axes and foliations that dips toward the west direction (Ayalew et al, 1990).

2.3.3 Baro Domain

Lithologic units in the Baro domain includes garnet-sillimanite gneiss, calc-silicate gneiss with subordinate garnet-amphibolite and magnetite-bearing quartzite (Ayalew et al, 1990). Teklewold Ayalew, (1997) suggests that the Baro domain contains planar structures with the orientations of northerly strike and moderate dips to the east and west direction whereas the orientation of linear features in this domain is plunge gently to north or south.

2.3.4 Didesa domain

Didesa domain is characterised by moderate-grade para- and ortho-gneiss, intruded by Neoproterozoic intrusive rocks like poly deformed gabbroic and granitoids bodies and post-kinematic mafic and felsic plutons (Allen and Gebremedhin Tadesse, 2003). Para-gneisses in this domain includes biotite-amphibole gneiss, garnet-biotite gneiss and quartzo-feldspathic gneiss, and ortho-gneisses are consists banded mafic gneiss containing ultramafic bands and derived from a layered mafic intrusive body (Tadesse Alemu and Tsegaye Abebe, 2007). Most of lithologic units found in the Didesa domain shows strongly foliated and undergone intense folding with abundant refolded folds indicating poly phase folding (Allen and Gebremedhin Tadesse, 2003. Tectonic contact marked by the N–S trending Chugi Shear Zone separate this domain with the adjacent Kemashi Domain to the west (Allen and Gebremedhin Tadesse, 2003).

2.3.5 Kemashi domain

Kemashi domain is located to the west of Didesa domain in the west Ethiopian shield. This domain encompasses lithological units such as; low grade metasedimentary rocks like pelitic to psammitic schist, intercalated with chert, graphitic phyllite and marble, and ultramafic–mafic metavolcanic rocks such as serpentinite, talc-chlorite–tremolite schist, metabasalt, talc schist, talc-carbonate schist and pyroxenite (Allen and Gebremedhin Tadesse, 2003). According to

Allen and Gebremedhin Tadesse (2003), rocks within this Domain are highly deformed and sheared. Recumbent, tight to open, westerly-verging, small-scale F1 folds commonly fold bedding of metasedimentary units are common (Allen and Gebremedhin Tadesse, 2003: Tadesse Alemu and Tsegaye Abebe, 2007). Contact between the Kemashi Domain and adjacent terranes are tectonic contact of N–S orientation of the Beleke Shear Zone (Allen and Gebremedhin Tadesse, 2003).

2.3.6 Dengi domain

This Domain is located to the west of the Kemashi Domain. Dengi domain consists a deformed and metamorphosed volcano-sedimentary sequences such as metabasalts, metaandesites, metarhyolites, phyllite, garnet mica schists, marbles, metagabbros, amphibolite and metagranitoids (Allen and Gebremedhin Tadesse, 2003). The rocks of this area were metamorphosed under epidote-amphibolite facies metamorphic conditions (Allen and Gebremedhin Tadesse, 2003). The gneisses and the volcano-sedimentary succession are in tectonic contact across both the N–S Gember Shear Zone. Within this Domain the foliation trend from N–S to NW–SE is associated with the sinistral NW trending Chochi Shear Zone (Allen and Gebremedhin Tadesse, 2003).

2.3.7 Sirkole domain

Sirkole Domain is located to the north-western part of the Tulu Dimtu belt and it extends to Sudan. According to Allen and Gebremedhin Tadesse (2003) the rock units that occupies Sirkole domain includes; moderate-grade polydeformed gneisses, low- to moderate-grade metasedimentary rocks and mafic to felsic metavolcanic rocks with intruded by deformed and undeformed granitoid plutons (Allen and Gebremedhin Tadesse, 2003). The Grade of metamorphism in this area is characterised by amphibolite facies assemblages occur in both the gneiss and the volcano-sedimentary successions (Allen and Gebremedhin Tadesse, 2003). Allen and Gebremedhin Tadesse (2003) suggests that volcano-sedimentary succession in Sirkole domain is folded and strongly cleaved with a N–S striking, easterly dipping schistosity, and a mineral stretching lineation plunging gently eastwards.

2.3.8 Daka domain

This domain occupies the south-western corner of the Tulu Dimtu belt, and extends into Sudan. Allen and Gebremedhin Tadesse (2003) suggests that Daka domain consists of lithological units characterised by high grade rocks such as; moderate-high grade polydeformed gneisses and intruded by syn-kinematic granitoids. The gneissic rocks of Daka Domain are subdivided into three lithological units (Tesfaye Kebede and Koeberl, 1999). Two of the units are correlated with the two gneissic units of the Sirkole Domain, i.e. the Tosho Gneiss, and the Yangu Granitoid Gneiss. The third gneissic unit in the Daka Domain is a banded ortho-pyroxene-bearing granulite facies units. Daka daomain was dextral NE–SW trending shear zone, theYangu Shear Zone, cuts the northwestern part of this domain north of the Daka River Thrust, an area mainly occupied by the Yangu Granitoid Gneiss.

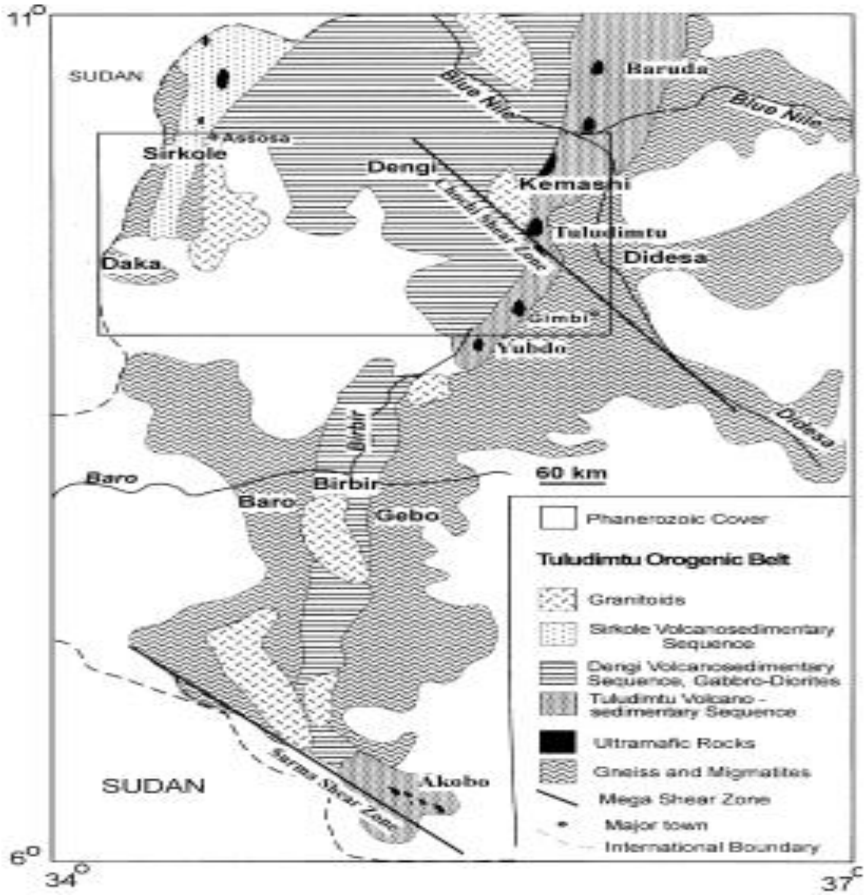

Figure 2.2 Geological map of the Tuludimtu Belt in western Ethiopia (Allen and Gebremedhin Tadesse, 2003)

2.4 Structural Evolution of Western Ethiopian Shield

Tulu Dimtu Belt (TDB) is exposed in the west Ethiopian shield as a NNE- trending fold and thrust belt at western Ethiopia shield (Allen and Gebremedhin Tadesse, 2003; Tadesse Alemu and Tsegaye Abebe, 2007). The structural evolution of WES (Tulu Dimtu Belt) is being presented by D1–D3, which is applied only to the volcano sedimentary units, and represented the Pan African deformation sequence, but most of the ductile deformation recorded in the gneiss domains is of pre-Pan African age and that the Pan African imprint may be represented only by the very latest ductile and brittle deformation phases (Allen and Gebremedhin Tadesse, 2003).

D1 is associated with the formation of tight to isoclinal, recumbent F1 folds (Allen and Gebremedhin Tadesse, 2003). Easterly dipping N–S shear zones such as the Beleke and Chugi Shear Zones (Allen and Gebremedhin Tadesse, 2003) and Tulu Dimtu shear zone (Tadesse Alemu and Tsegaye Abebe, 2007) are associated with D1 deformation events (Fig 2.3 a). D2 is characterised by open upright F2 folds with fold axes plunging gently to the NNW, which fold the S1 axial surfaces (Allen and Gebremedhin Tadesse, 2003; Tadesse Alemu and Tsegaye Abebe, 2007). This deformation event is also associated with the development of the NW–SE Chochi and NE–SW Yangu Shear Zones (Allen and Gebremedhin Tadesse, 2003). Chochi synform and Tulu Dimtu antiform (Fig.2.3 b) are recognized as D2 deformation phases (Tadesse Alemu and Tsegaye Abebe, 2007). D3 deformation event (Fig 2.3c) of Tulu Dimtu Belt is characterised by N-, NNE-, NW- trending brittle-ductile strike slip fault/ shear zone (Tadesse Alemu and Tsegaye Abebe, 2007). The major example that shows the D3 deformation event in the Tulu Dimtu Belt is Didesa shear zone which is the boundary between the Chochi and Katta domains (Tadesse Alemu and Tsegaye Abebe, 2007). Sinistral offset of the Dengi, Kemashi, Didesa, Daka and Sirkole Domains may be associated with this D3 deformation history (Allen and Gebremedhin Tadesse, 2003).

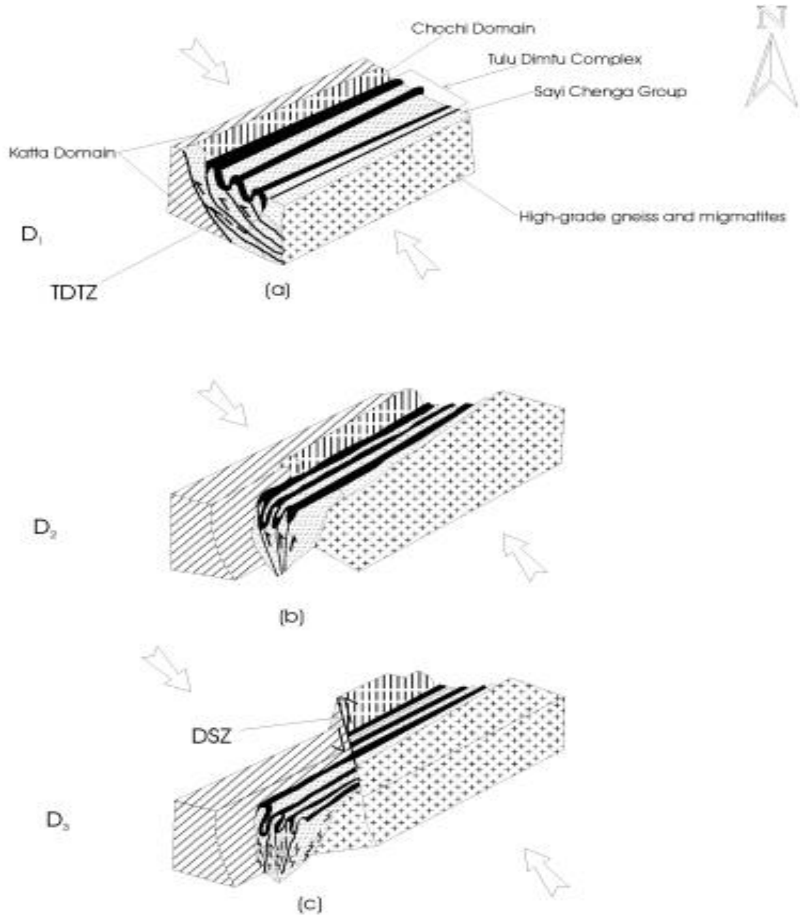

Figure 2.3 Structural evolution of Pan African Tulu Dimtu Belt according to Tadesse Alemu and Tsegaye Abebe, (2007), a) early deformation (D1), TDTZ (Tulu Dimtu thrust fault/ shear zone). b) D2 deformation, which is resulted in deforming the initially sub-horizontal, D1structures about more upright folds, c) D3 represent extensive shortening, which resulted in formation of N- and NNE- trending ductile shear zone and NW sinistral Didessa shear zone (DSZ).

WES (Gore-Gambella) recorded four regional deformation events D1-D4, (Teklewold Ayalew and Johnson, 2002). The first deformation event, D1 (Fig. 2.4a), resulted in the formation of a sub-horizontal gneissosity within the gneissic terranes which was subsequently folded by D2 (Fig.2.4 b). D2 (E-W shortening) is present in all domains, formed following east-west shortening of the region (Teklewold Ayalew and Johnson, 2002). This deformational event is ubiquitous throughout WES. Mylonites, the result of intense D3 shearing (Fig 2.4.c), occurs throughout the Birbir domain. The Birbir shear zone, which is NNE-striking is one example of D3 deformational event. D4 (Fig 2.4 d) occurred much later (post Pan-African) and resulted in the formation of large northwest-southeast oriented brittle structures (Teklewold Ayalew and Johnson, 2002).

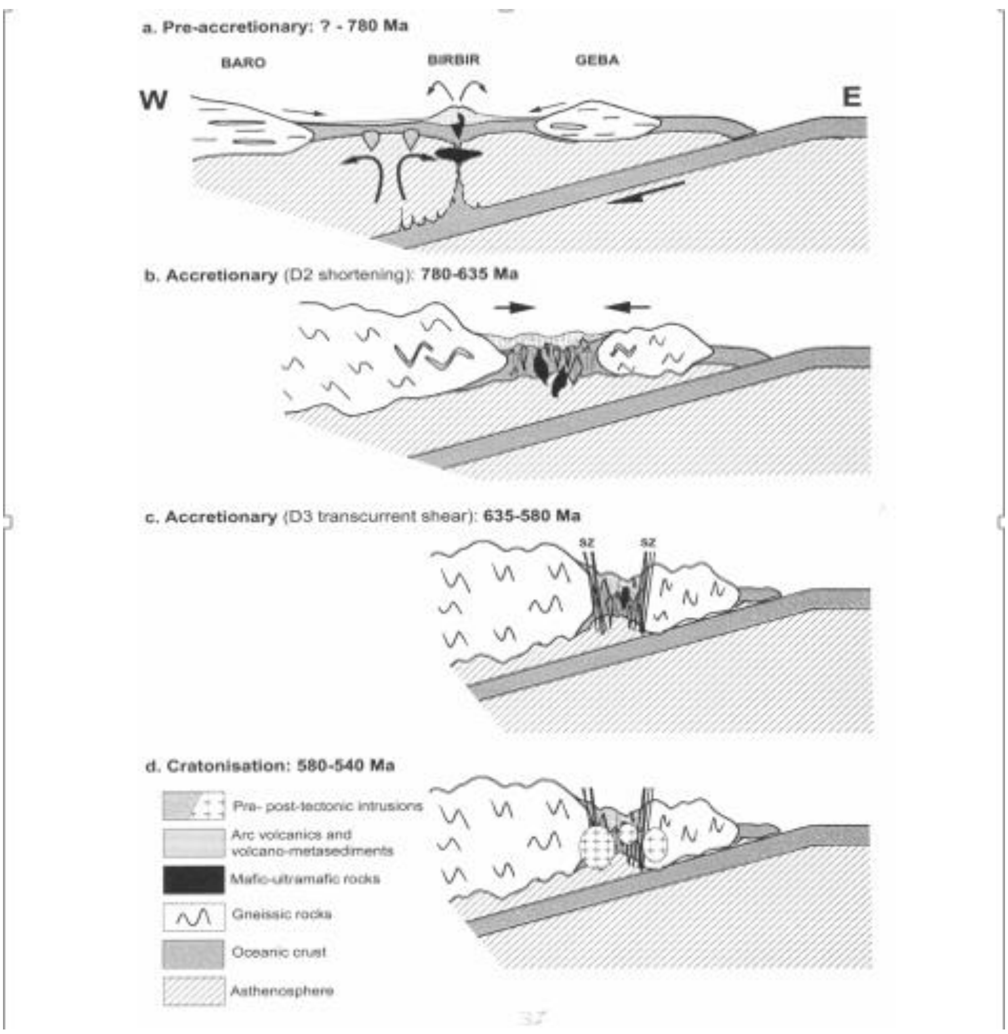

Figure 2.4 Tectonic evolution of western Ethiopia in the late Proterozoic (Teklewold Ayalew and Johnson, 2002).

CHAPTER THREE

Lithology, Petrography and Metamorphism of Bila area

3.1 Lithologic Units of the Study area

Geology of the Bila area encompasses three rock groups: - metasedimentary, metavolcanic and metaultramafic rocks (Fig.3.1). The metasedimentary group consists of slate, marble, phyllite, quartzite and graphite schist and occupy most part of the study area. The metavolcanic group includes: metabasalt and chlorite schist. While, the metaultramafic one consists of serpentinite, talc schist and actinolite-tremolite schist and they cover north-western and southern part of the study area (Fig.3.1). Ten mappable lithologic units (Fig.3.1) are identified and described based on their textural fabric and mineralogical composition. These are:

1) Slate
2) Phyllite
3) Marble
4) Graphite schist
5) Quartzite
6) Metabasalt
7) Chlorite schist
8) Talc schist
9) Actinolite tremolite schist
10) Serpentinite

For the detailed identification of mineral assemblages of Bila rocks petrographic investigations of 30 representative thin sections were studied under polarised light microscope. Simple counting technique has been used in the estimation of the modal proportion of the minerals in the rock and then rock is named based on the amount of the proportion of the minerals. Lithologic and petrographic descriptions of the rock units of the study area have been described together in this chapter.

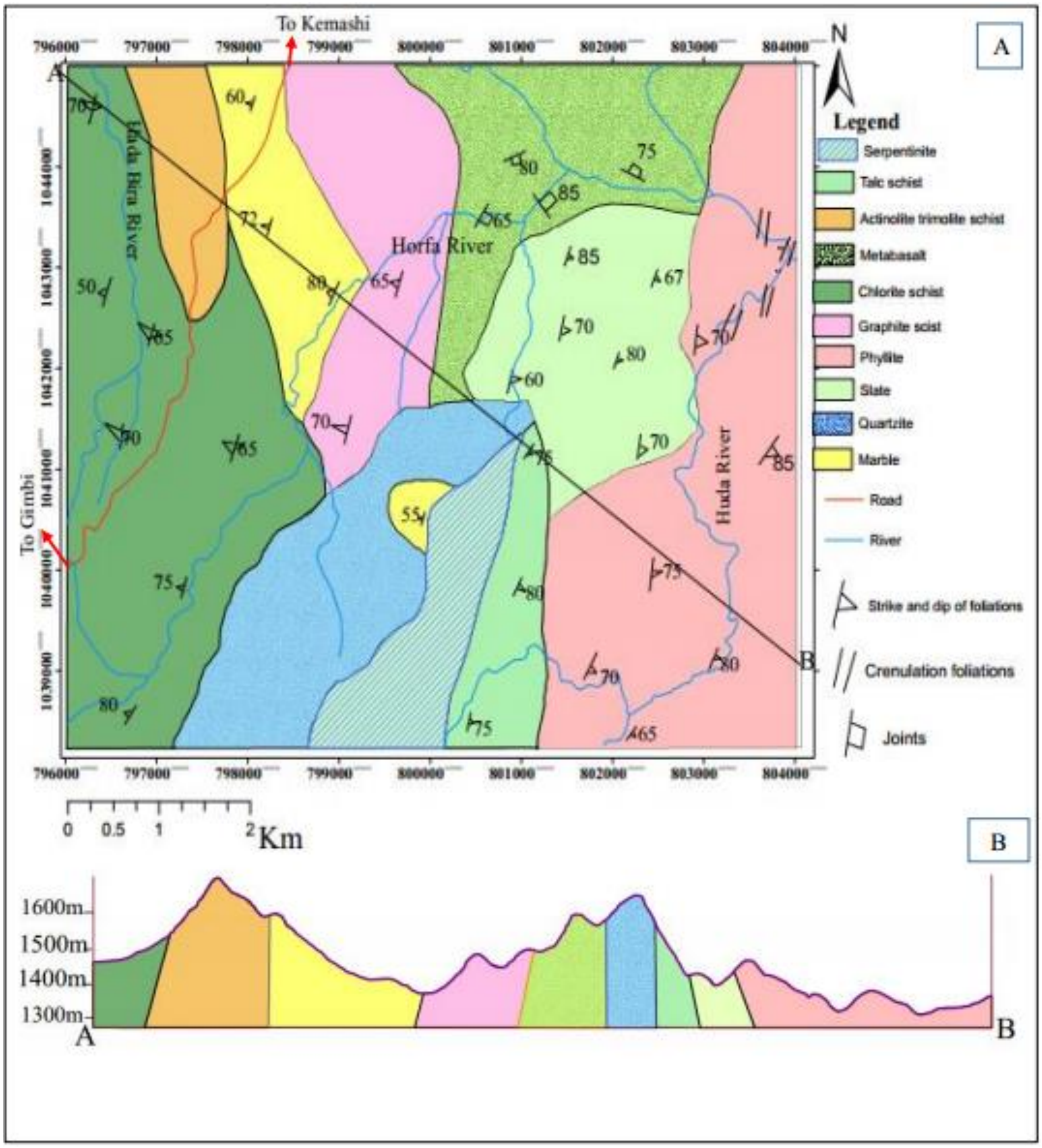

Figure 3.1 Geologic map (A) and Geologic cross section (B) of Bila area.

3.1.1 Serpentinite unit

The exposures of the serpentinite unit is found at the southern part of the study area. This rock unit is exposed at quarry site around King and by road cut at Daga Marrata. The exposures of this rock unit is dark green but brown when weathered, weakly foliated, fibrous and fine to medium grained. Most of the serpentinite outcrops are affected by weathering. The representative rock samples and photo pictures (Fig.3.2A and C) were collected from the quarry site along Dongoro-Kemashi road at Daga Marrata.

Microscopic investigation indicate that the rock is composed of 75% serpentine, 15% magnesite, 7% opaque (ilmenite or magnetite) and 3% chlorite. This thin section show simple foliation defined by serpentine and opaque. Highly altered magnesite and serpentine are common in these rock thin sections.

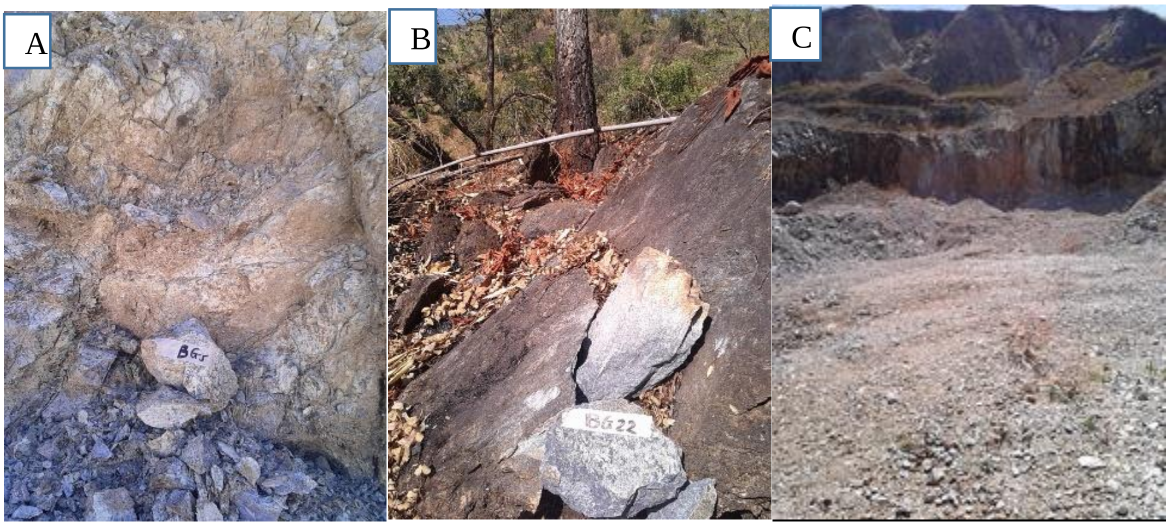

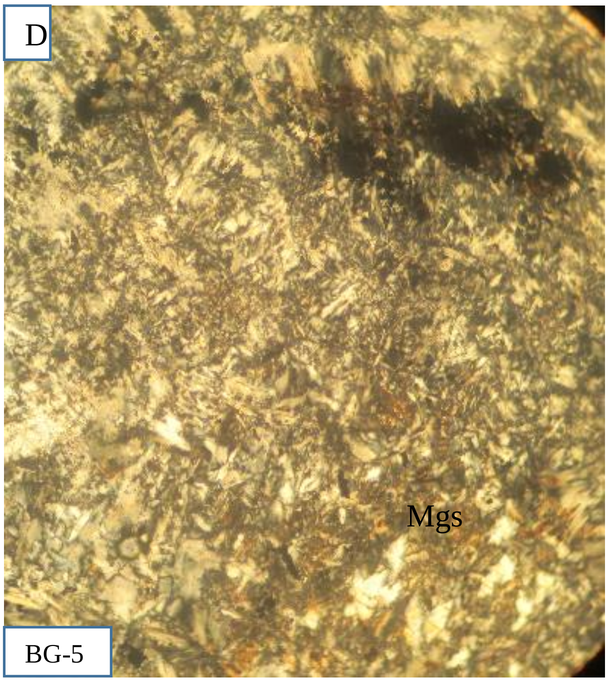

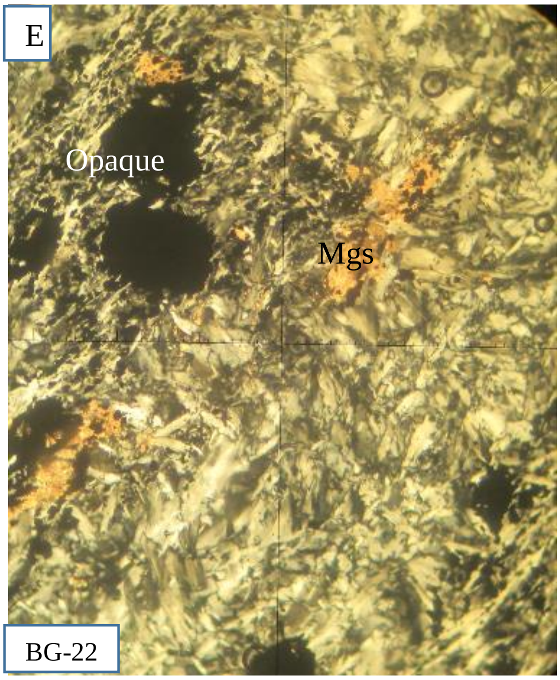

Figure 3.2 Field and microscopic photographs of serpentinite outcrops. A) Weathered outcrops of serpentinite unit. B) Slightly foliated, fibrous and contains asbestos. C) Quarry site of serpentinite outcrop. D) Altered serpentinite and magnesite. B) Over grew of opaque on serpentine grains.

3.1.2 Talc schist

This rock unit is exposed at the eastern part of the study area with small thickness as compared with other rock unit of the study area (Fig.3.1). The exposure of talc schist unit is strongly foliated, brown to whitish, very fine grained and schistose. The foliations of this unit is mostly striking 025˚ to 045˚ and steeply to vertical dipping 70˚ to 90˚ SE.

From the petrographic analysis the rock is composed of 60% talc, 20% magnesite, 15% actinolite and 5% opaque (Fig.3.3D and E). Talc, magnesite and opaque minerals show well developed parallel alignment and they define strong foliation for this thin section. This thin section display schistose texture.

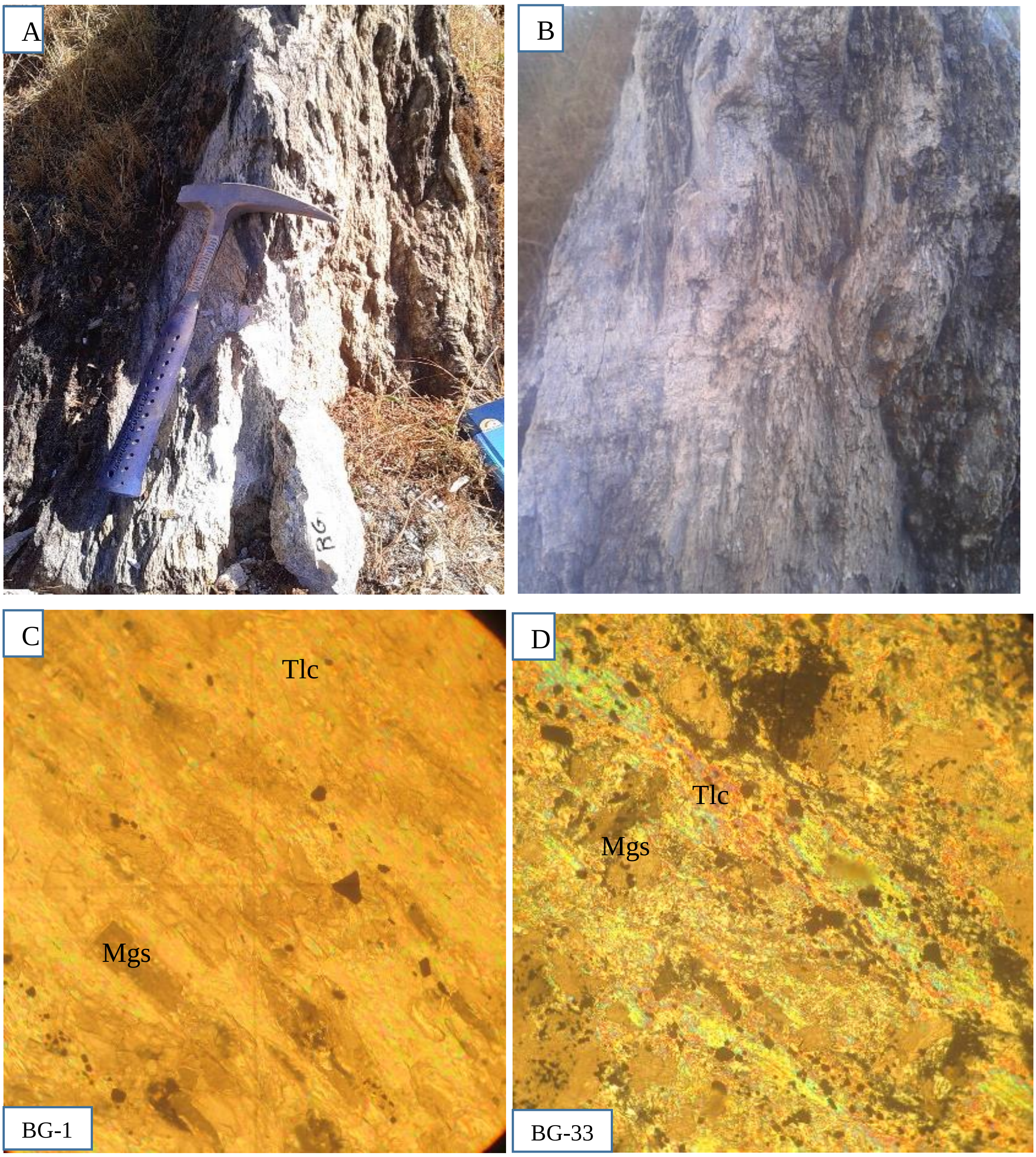

Figure 3.3 Field and microscopic photographs of talc schist outcrops. A) Whitish colour and strongly foliated (N-1041136, E-0800776). B) Strongly foliated and schistose (N-1040938, E-0801186). C) Most of this field of view is covered by talc. D) Opaque rich at the upper part of the field of view.

3.1.3 Actinolite-tremolite schist

This rock unit is exposed at the western part of the study area (Fig.3.1). It is moderately to strongly weathered, greenish but yellow when weathered, course-grained and foliated. The hand specimen of this rock unit contains visible elongated large grains of actinolite.

The microscopic observation of this unit indicates that the rock unit is dominated by actinolite, tremolite, magnesite and chlorite. Based on the proportions of these minerals this unit is classified as chlorite-actinolite schist and actinolite-tremolite schist.

I. Chlorite-Actinolite schist

Compositionally this thin section contains 55% actinolite, 35% chlorite and 10% opaque (Fig.3.4). Actinolite, chlorite and opaque minerals show well developed parallel alignment and they were the result of strong foliation in this rock thin section (Fig.3.4C).

II. Actinolite-tremolite schist

This rock thin section contains 75% actinolite, 12% talc, 10% magnesite and 3% opaque. Actinolite in this section shows needle shape, elongated grains and acicular texture (Fig.3.4D). Parallel alignment of actinolite and talc grains defines foliation of the thin section. Alteration and recrystallization of actinolite grains in this thin section is common.

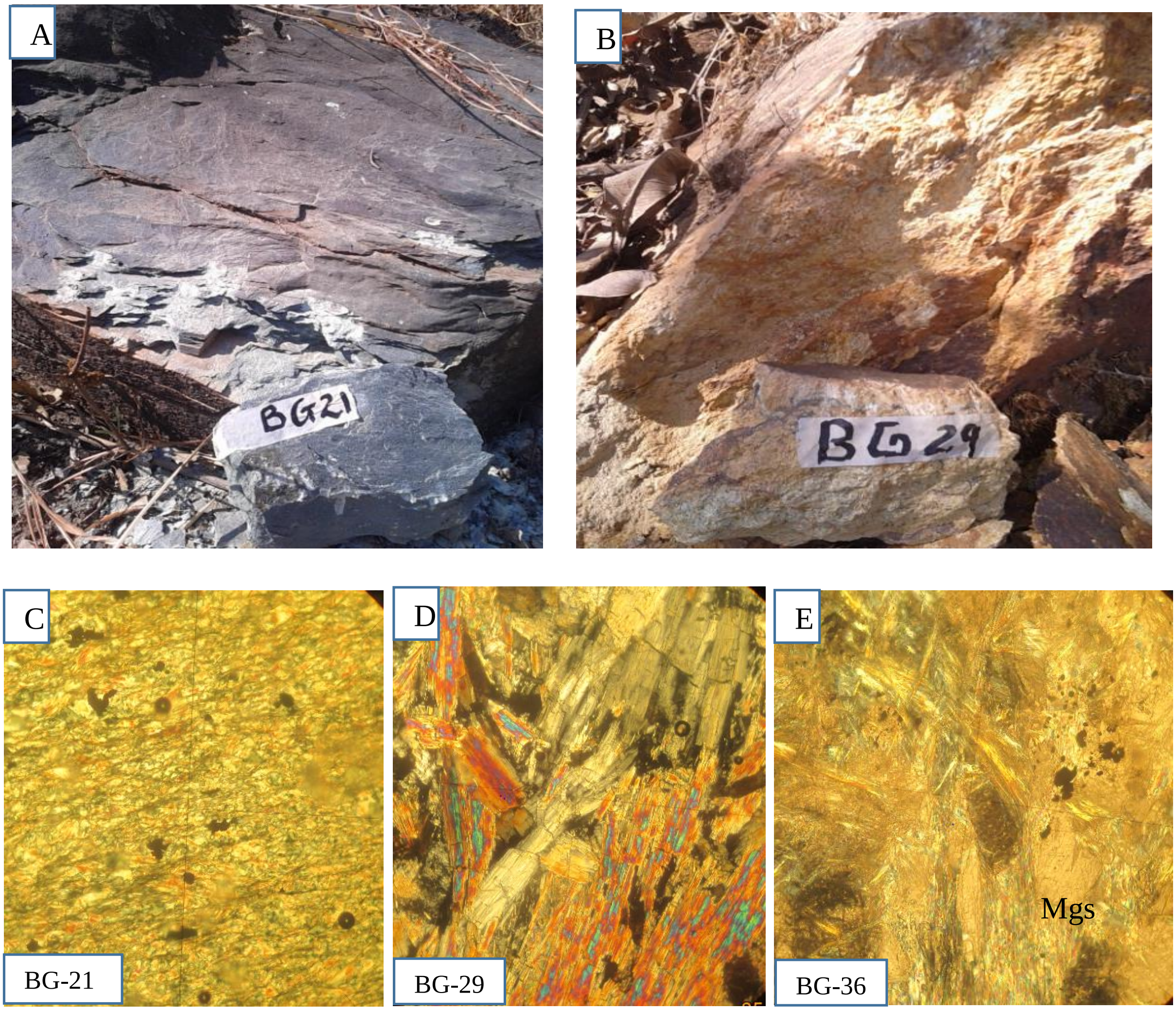

Figure 3.4 Field and microphotographs of actinolite tremolite schist outcrops. A) Fine grained and foliated. B) Weathered outcrops (location; E-0797161, N-1044453). C) Fine grained thin section. D) Sugarcane like shape of elongated actinolite grains. E) Needle shape grains of actinolite in the thin section.

3.1.4 Metabasalt unit

This lithologic unit is exposed at the northern part of the study area mostly around the river cut (Fig.3.1). The outcrops of this unit exhibit fine grained, grey green to dark and mostly massive. It is the most affected lithologic unit by brittle deformations among the rock units exposed at the study area. During the field investigation two variety of metabasalt is identified. One is fine grained, dark grey and foliated (Fig.3.5A). The second one is characterised by grey green, fine to medium grained, massive and affected by three set of joint systems. This one is exposed around Horfa river and Aba Gutu stream (Fig.3.5B and C).

Five thin sections are prepared from metabasalt unit for petrographic analysis. Two thin sections from foliated and three thin sections from massive metabasalt. The analysis revealed that the rock unit contains minerals such as plagioclase, chlorite, epidote, quartz, muscovite, calcite, sphene and opaque with the relict of olivine and pyroxene. Even if the all thin sections contain approximately similar mineralogical proportions they exhibit difference in texture and fabrics. The petrographic analysis of this rock unit is discussed as follows:

I. Foliated metabasalt

The dominant mineralogical compositions of this rock is 40% plagioclase (albite), 15% chlorite, 13% epidote, 10% quartz, 10% calcite, 5% muscovite, 5% opaque (magnetite) and 2% sphene (Fig.3.5D and E). Quartz, calcite, muscovite (sericite) and opaque minerals show parallel alignment as a result the section show foliation. Veins and recrystallized of quartz grains are common in this thin section. Sphene and opaque in this rock were show randomly distribution. Plagioclase show alteration to calcite and sericite.

II. Massive metabasalt

This rock is composed of approximately 40% plagioclase (albite), 20% chlorite, 20% pyroxene, 10 % epidote, 5% sphene, 3% quartz, 1% olivine and 1% opaque (Fig.3.5 F,G, H and I). The matrix of the thin section is defined by minerals such as epidote, chlorite, quartz, sphene and opaque but, plagioclase, pyroxene and sanidine are present as a ground mass and phenocrist. Epidote and plagioclase show alteration in the most of these rock thin sections. Interlocking of plagioclase grains with polysynthetic character as well as quartz veins are seen in these thin sections. Plagioclase show alteration to calcite and sericite.

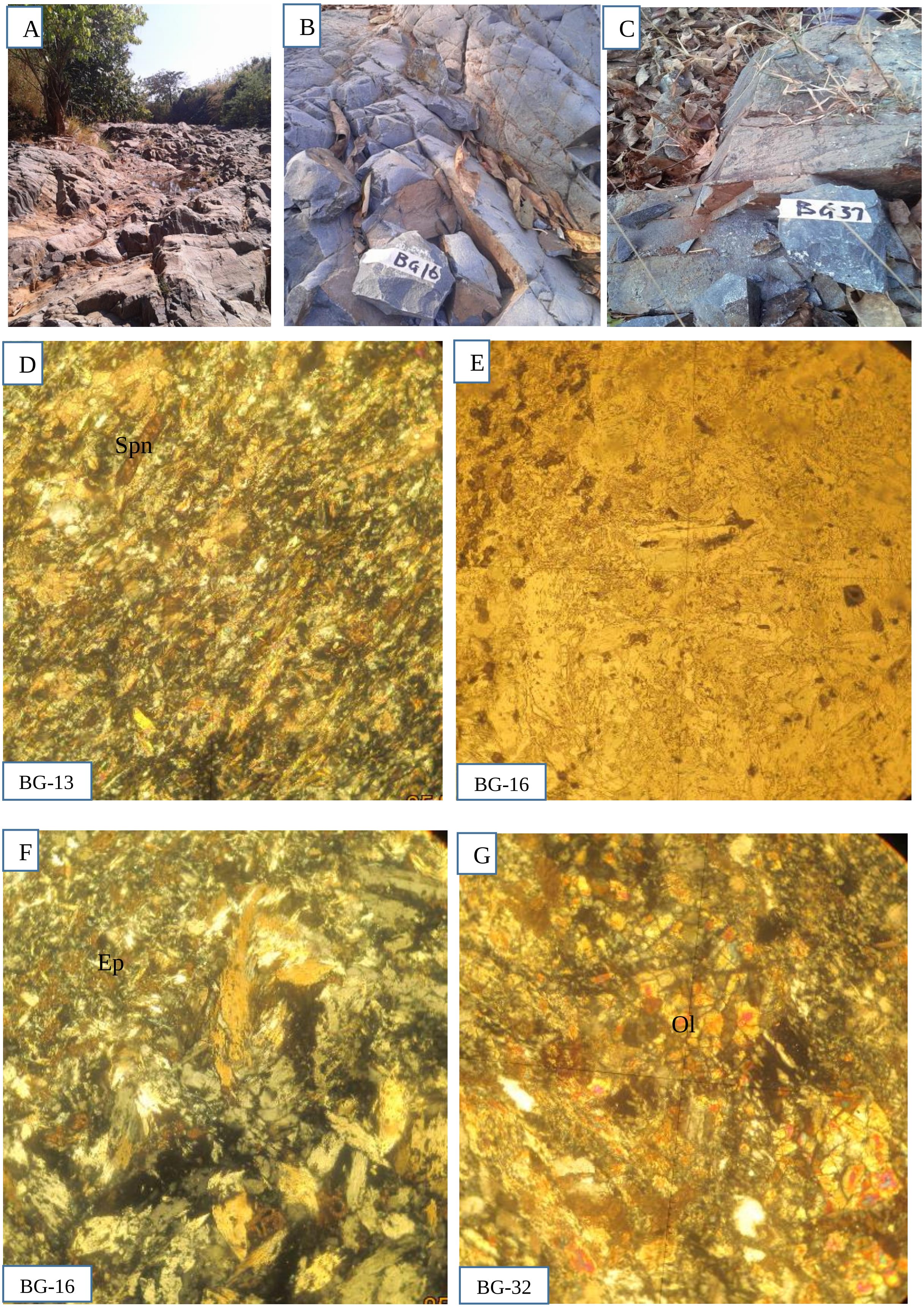

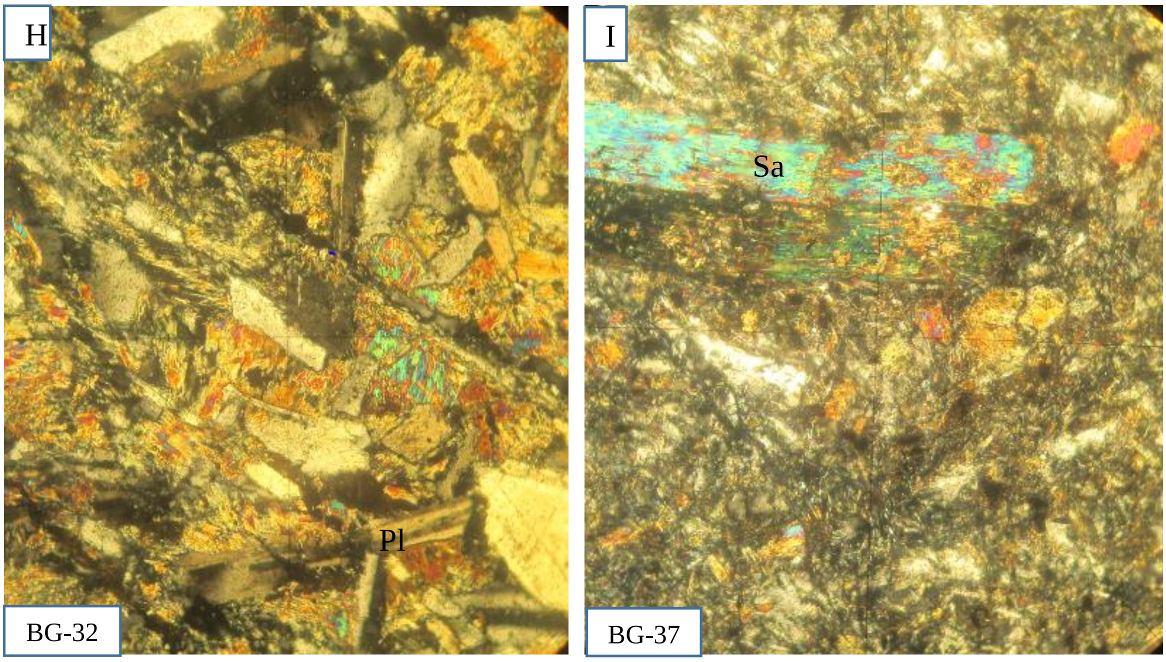

Figure 3.5 Field and microscopic photographs of metabasalt outcrops. A) Outcrops of massive metabasalt along the river cut (N-1042815, E-0801120). B) Massive metabasalt (N-1038889, E-081439). C) Out crops of massive metabasalts affected by multiple joint sets. D) Randomly distributed sphene grains. E) Parallel alignment of sphene grains at the left part of fiel. F) Parallel alignment of calcite grains at the left part of field of view. G) Relict of olivine grains. H) Interlocking of plagioclase grains. I) Sanidine phenocryst.

3.1.5 Chlorite schist

Exposures of this unit occupied the western part of the study area around Horde and Hada Bira river. This unit is characterised by fine to medium grained, foliated, dark grey to greenish and it is pyritised. The pyrite in this rock unit can be identified by the naked eye.

Petrographic analysis indicate that chlorite schist exposed in the study area is dominated by chlorite and epidote but there are also other minerals such as muscovite, plagioclase, quartz, opaque and calcite in small proportions (Fig.3.6D, E, F and H). The modal proportions of these minerals are approximately 50% chlorite, 20% epidote, 10% calcite, 8% quartz, 5% plagioclase, 3% muscovite, 5% biotite and 2% opaque. The well-developed parallel alignment of chlorite, biotite, quartz, epidote, muscovite and opaque display strong foliation as a result they produced schistose texture in the thin sections. From the petrographic analysis of this unit, one thin section shows the high content of chlorite (Fig.3.6I). This thin section contains 80% chlorite, 15% opaque (pyrite) and 5% actinolite. Most of the opaque in this thin section show euhedral shape. Foliation in this thin section is defined by chlorite and actinolite.

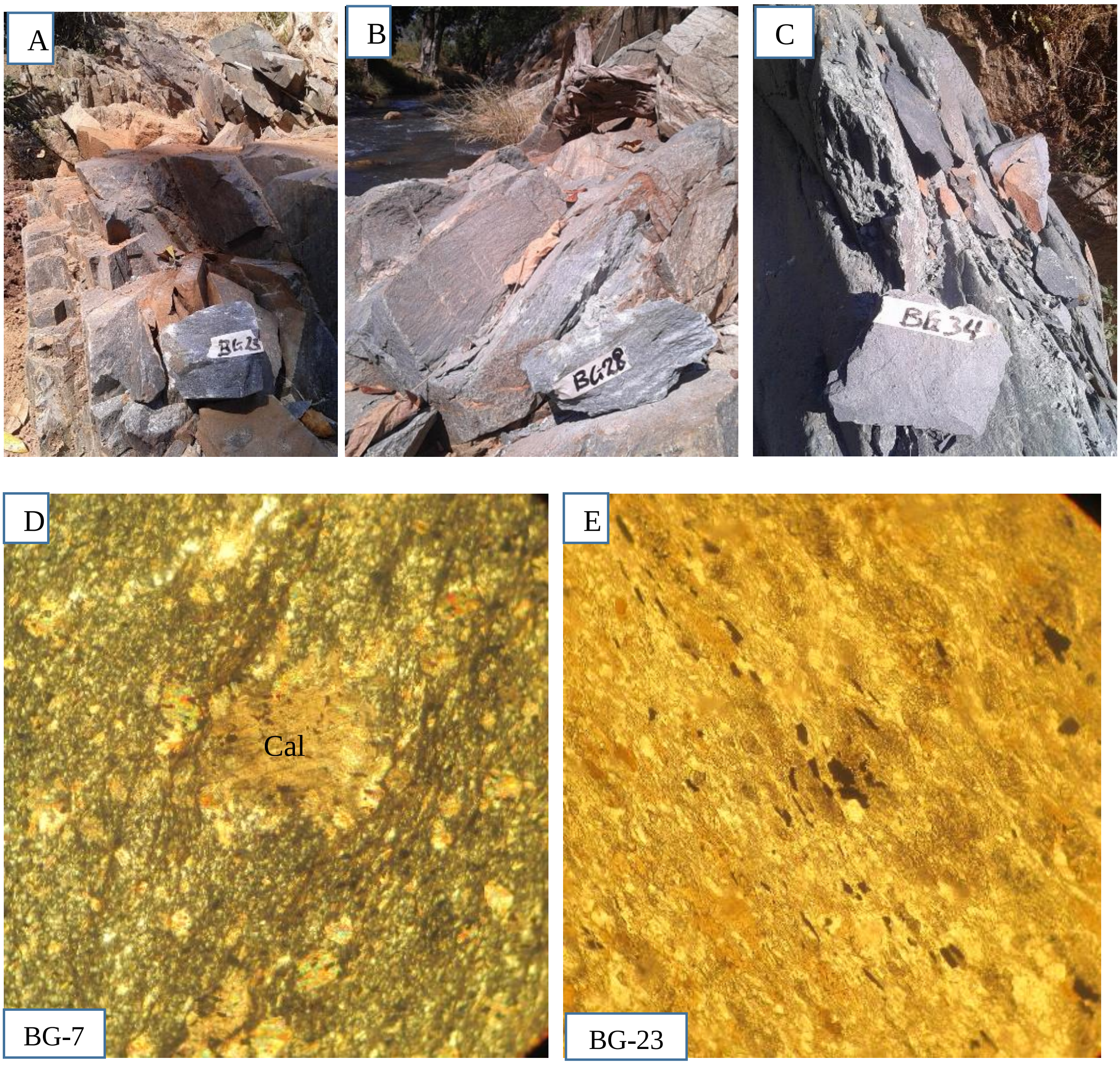

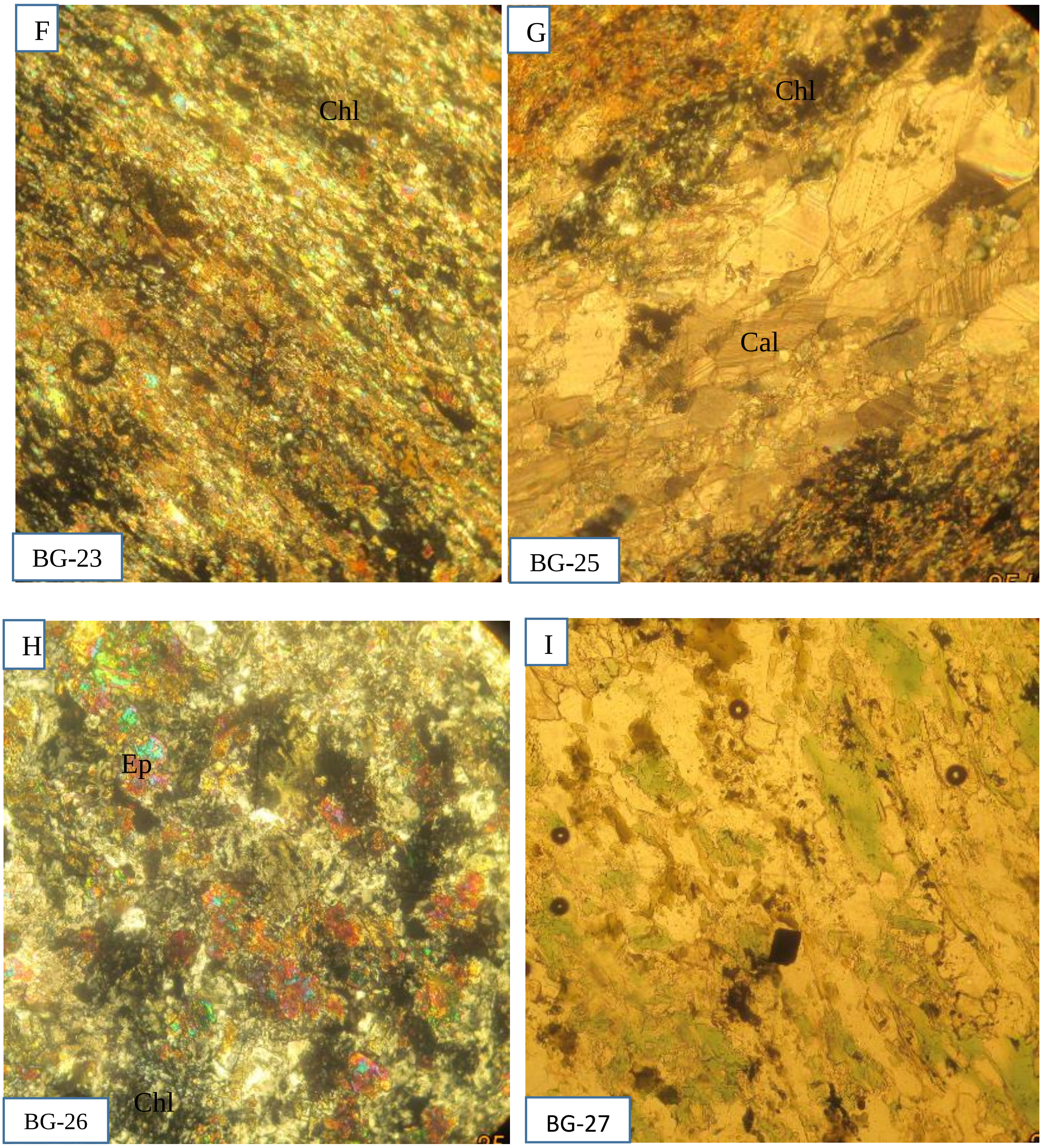
F
Chl
BG-23
G
Chl
Cal
BG-25
H
Ep
Chl
BG-26
I
BG-27

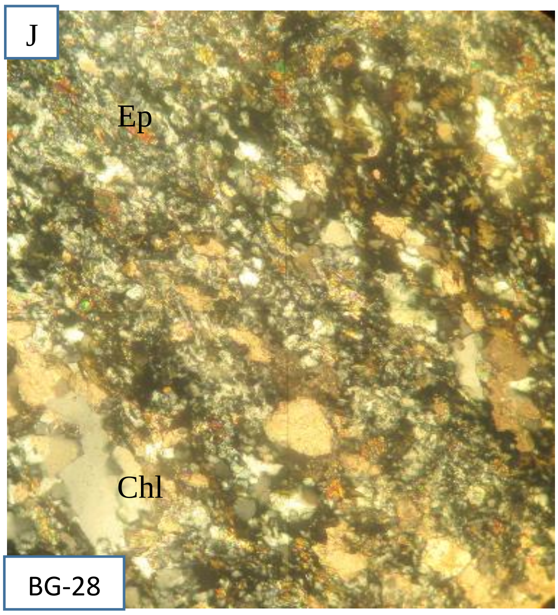

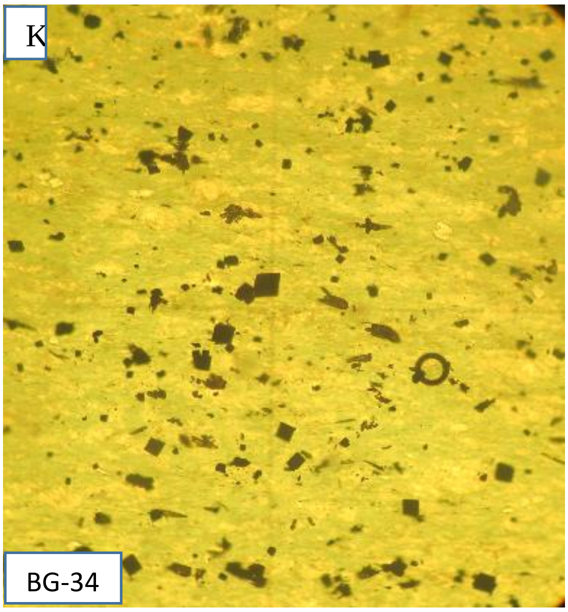

Figure 3.6 Field and microphotograph of chlorite schist outcrops. A) Grey green chlorite schist (N-10938274, E-0799701), B) Foliated and dark grey of chlorite schist. C) Pyritised chlorite schist (N-1038240, E-0803189). D) Calcte grain at the center of field of view. E) Parallel alignment of opaque grains. F) Strongly parallel alignment of epidote, biotite, chlorite and muscovite. G) Development of calcite vein. H) High interference colour of epidote. I) Foliation defined by chlorite. J) Well develop alignment of calcite, quartz, chlorite and micas in the section. K) Dominated by chlorite.

3.1.6 Graphite schist

This unit is exposed at the north western part of the study area around Boke mountain and along the Horfa river (Fig. 3.1). The graphite schist exposed in this area show weakly to moderately weathered, dark grey, slaty cleavage, very fine grained and strongly foliated. The foliation in this unit is mostly striking 030˚ to 045˚ and steeply dipping 60˚ to 75˚ NW.

Thin section of this rock unit contains 55% graphite, 25% quartz, 13% muscovite (sericite) and 7% biotite. Quartz, graphite, muscovite (sericite), opaque and biotite show strong parallel alignment and they define strong foliation as a result the thin section show schistose texture. Quartz and graphite display xenoblastic texture, muscovite (sericite) display tiny platy and biotite display flaky. Quartz vein is common in this thin section.

The other thin section prepared is graphite-mica schist (Fig.3.7 F and G). The major mineral constituent of this section is 35% biotite, 30% opaque (graphite), 20% most probable andalusite, 10% quartz, 3% muscovite and 2% plagioclase. The dominant matrix minerals are biotite, muscovite and quartz. However, andalusite present as inclusion in the thin section.

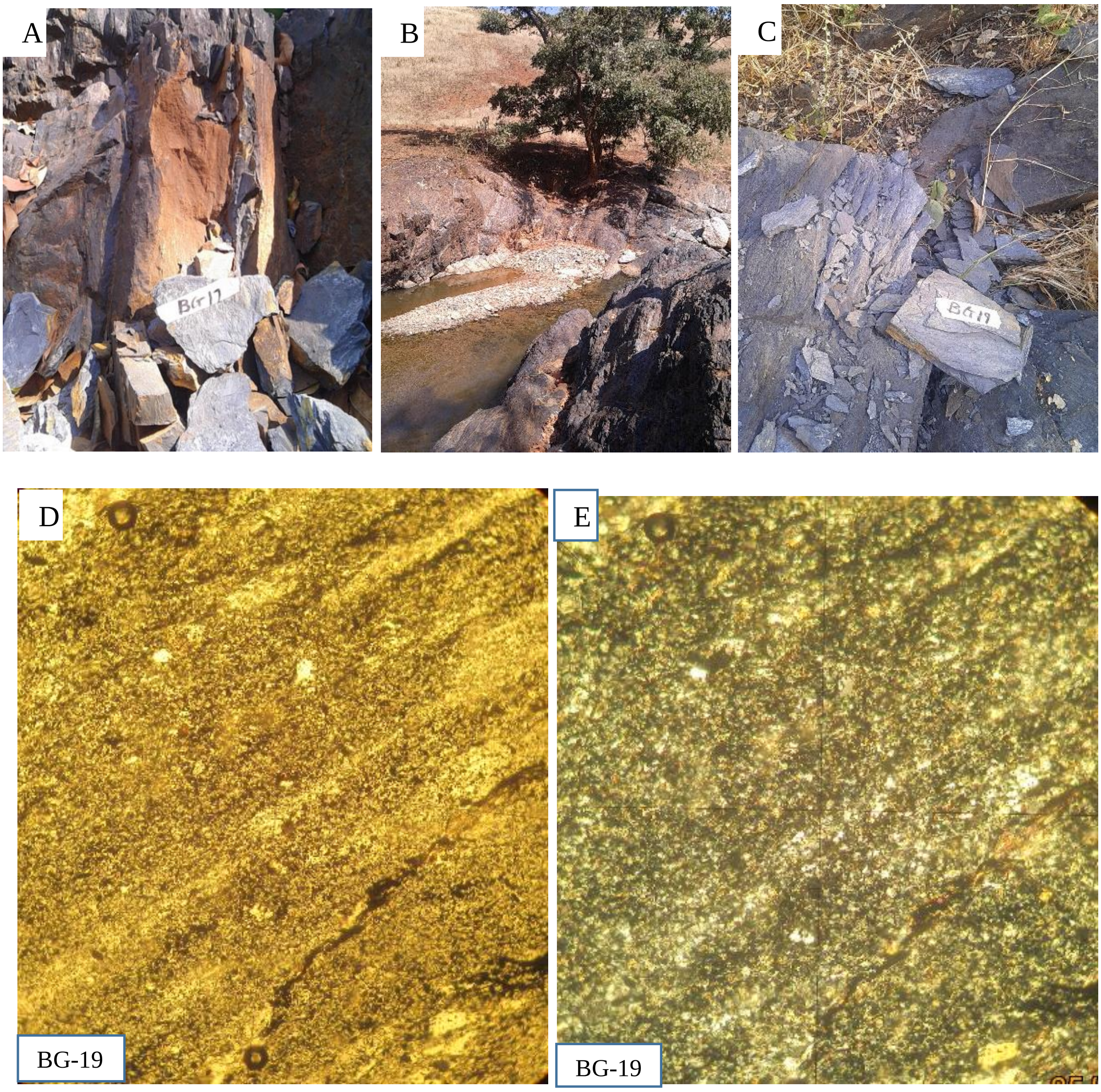

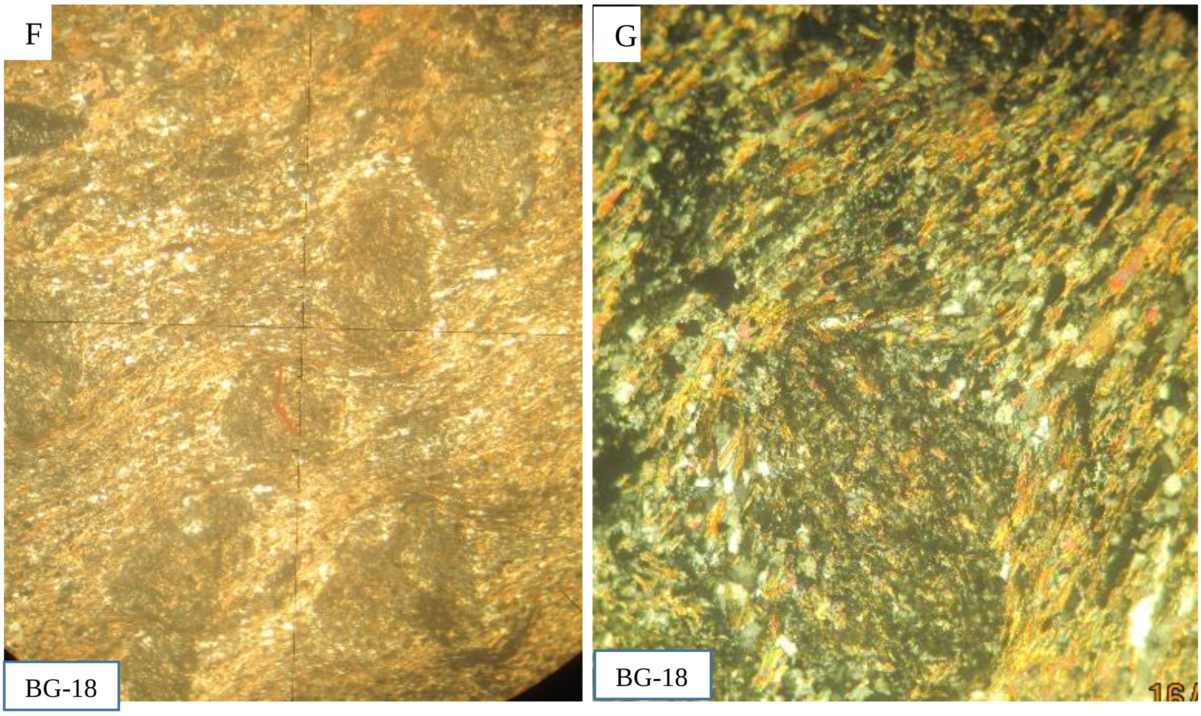

Figure 3.7 Outcrop and microscopic photographs of graphite schist and graphite-mica schist. A) Moderately weathered (N-1043520, E-0800175). B) Graphite schist outcrop exposed at the river cut. C) Photo picture of graphite unit which is fresh and highly foliated (N-1041064, E-0798991). D) Microphotographs of graphite schist under PPL. E) Microphotographs of graphite schist under XPL. F) The alignment of andalusite porphyroblasts in biotite schist. G) Graphite-mica schist under PPL.

3.1.7 Phyllite unit

Phyllite unit is the lithologic unit covered most of the eastern part of the mapped area (Fig.3.1). The exposures of this rock unit is mostly found along the river cut such as Huda river, Horfa river and Aba Arari stream. This lithologic unit is the most affected rock unit by brittle and ductile geologic structures among the other lithologic units of the study area. Ductile structures such as foliations, lineations and folds whereas brittle structures such as joints and faults are experienced by this unit. The mesoscopic crenulation foliation and lustrous sheen behaviour are also encountered by this rock unit. It is also showing banding of the primary bedding. The foliation of this unit is mostly striking 025˚ to 045˚ and steeply dipping 65˚ to 85˚ towards the east and south east direction.

Petrographic analysis revealed that the phyllite unit is composed of 30% chlorite, 20% muscovite (sericite), 15% quartz, 15 % opaque (Fe-oxide), 12% calcite, 5% plagioclase and 3% biotite (Fig.3.8 E and H). Quartz, chlorite, calcite, opaque, biotite and muscovite (sericite) show well develop parallel alignment and they define strong foliation of this thin section as a result they also produced schistose texture. Muscovite, calcite, chlorite, biotite and opaque recognised in the section as the matrix, but both quartz and plagioclase occurs as inclusion and matrix. Alteration of feldspar to sericite were common.

The micro folding formed by mica is observed in this rock (Fig.3.8E and G). This micro folding exhibit presence of S1 and S2 rock fabric of crenulation cleavage. Including the micro folding the thin section also shows pressure shadow which may trace tectonic event of the area. Development of pressure shadow revealed that the grains were form before foliation developed. In other way, over grew of opaque on S1 foliation of the section indicate post-tectonic event, this means opaque grains are developed after foliation. The calcite vein is developed parallel to the S1 foliation in this rock thin section (Fig. 3.8H).

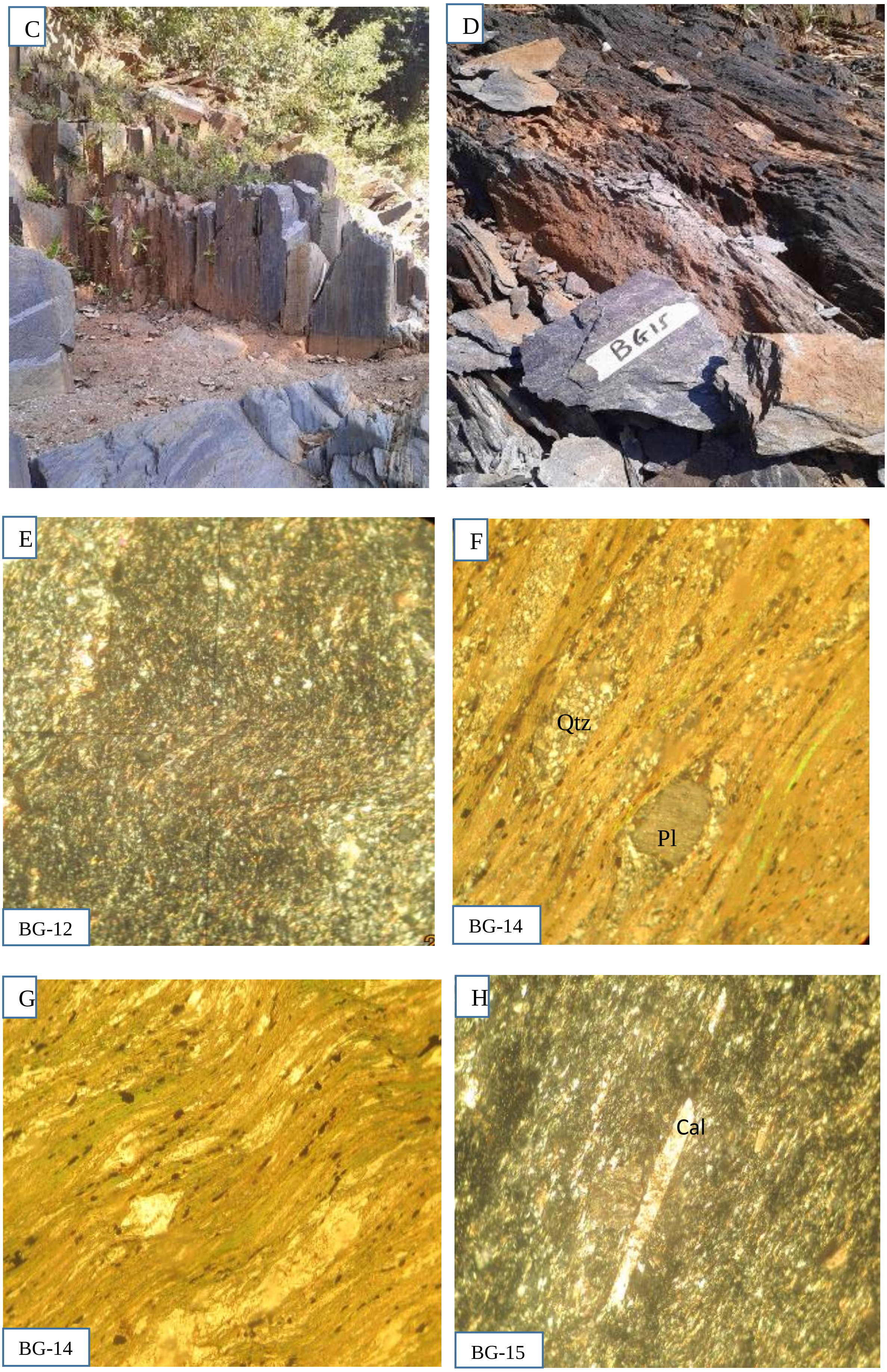
C
D
BG15
E
BG-12
F
Qtz
Pl
BG-14
G
BG-14
H
Cal
BG-15

Figure 3.8 Field and microscopic photographs of phyllite outcrops. A) Phyllite unit which is grey green, fine grained and moderately foliated (N-1041556, E-0802880). B) Field photo of phyllite unit which shows green and strongly foliated (N-1042753, E-0803617). C) Highly foliated and steeply dipping outcrop of phyllite unit. D) Field photo of phyllite outcrops which show crenulation cleavage (N-1043113, E-0803925). E) Microfolding that show S1 and S2 crenulation cleavage. F) Pressure shadow at the bottom of the field of view. G) Microfolding and quartz porphroblast. H) Calcite vein formed parallel to phyllitic layer.

3.1.8 Slate unit

This lithologic unit is located at the central part of the study area (Fig.3.1). Based on the field description two varieties of slate unit are exposed in the study area. One is highly foliated, dark grey to black, fine grained, fresh and shows slaty cleavage (Fig.3.9A and B). The other exposure of slate unit exhibit fine grained, foliated, brown as a result of weathering, slaty cleavage and moderately to strongly weathered (Fig.3.9C). Most of the exposures of this lithological unit is affected by weathering. The foliations of this unit is mostly striking 020° to 050° and steeply dipping 60° to 85° towards the east and south east direction.

Petrographic description revealed that the slate unit in the study area is compositionally dominated by the minerals like quartz, sericite, chlorite, opaque and calcite. Based on the proportions of these mineralogy, slate unit of the area is categorised as muscovite (sericite) - quartz - chlorite slate and sericite slate.

I. Muscovite (sericite) – Quartz - Chlorite Slate

This rock is composed of 30% chlorite, 25% quartz, 15% muscovite (sericite), 15% opaque (Fe-oxide), 10% K-feldspar and 5% calcite. The well develop parallel alignment of quartz, chlorite, calcite, opaque and muscovite (sericite) in this thin section show strong foliation (Fig.3.9 D). The development of bedding defined by chlorite and quartz parallel to foliation is recognised in the thin section. Quartz grains in this thin section show undulose extinction.

II. Sericite Slate

This thin section contains 50% muscovite (sericite), 15% chlorite, 15% quartz, 10% opaque (Fe-oxide), 5% calcite and 5% biotite (Fig.3.9 E). Muscovite(sericite), chlorite, quartz,biotite and opaque show strong parallel alignment and they define strong foliation in the thin section. Feldspar shows alteration to sericite. Quartz vein parallel to the S1 foliation is also common in this rock.

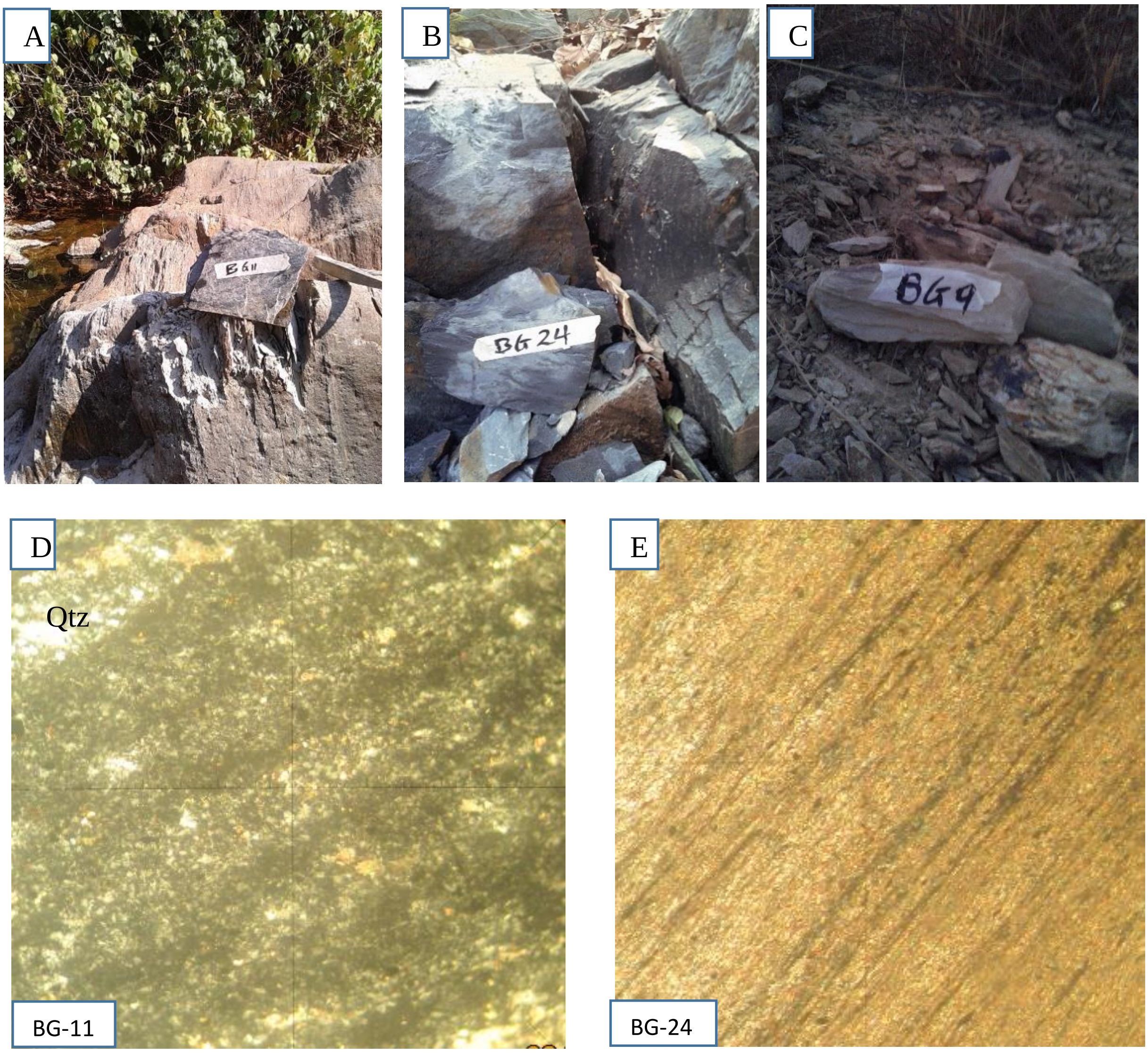

Figure 3.9 Field and microphotographs of slate unit outcrops. A (N-1041295, E-0802506) and B (N-1039850, E-0798750) fresh outcrops of slate. C) Strongly weathered slate outcrop. D) Show bedding and cleavage domains. E) Strong foliation defined by mica.

3.1.9 Quartzite unit

The quartzite outcrops are exposed around Gidano King mountain with the intercalations of monomineralic quartz veins. The outcrops of this rock unit is characterised by fine grained, weakly weathered, reddish to brown and moderately foliated. Field investigations shows two variety of quartzite unit: the first one is brown colour which is moderately foliated (Fig.3.10A) and the other one is weakly weathered, reddish and massive (Fig.3.10B).

Two thin sections are prepared from this unit for petrographic analysis. The analysis shows that more than 80% of this rock unit is occupied by quartz and the rests are occupied by 15% opaque (Fe- oxide) and 5% biotite. All of the minerals in this thin section displays xenoblastic texture.

Quartz, biotite and opaque minerals show sub parallel alignment and they define moderate foliations of the thin sections. Grains of quartz phases in this thin section show recrystallization, flattening, alteration and elongate fabric as a result of deformation. The stained grains of quartz show variety of colours under the microscope.

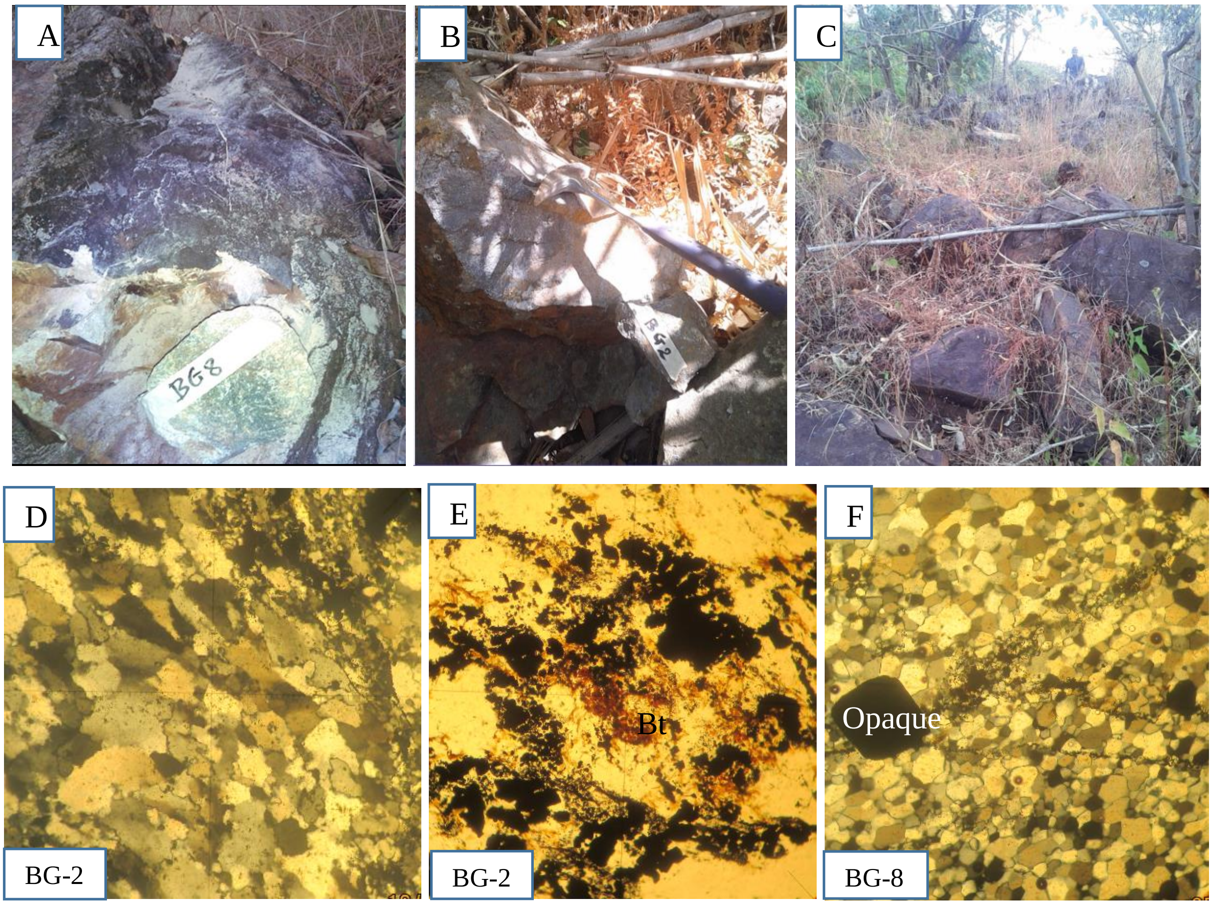

Figure 3.10 Field and microphotographs of quartzite outcrops. A) Massive and reddish (N-1042954, E- 0801342). B) Foliated and brownish (location; N-104079834, E-0800202. C) Quartzite outcrops (location; N- 103933226, E-0799263). D) Flattening of quartz grains. E) Biotite at the centre of field of view. F) Over growth of opaque over the quartz grains.

3.1.10 Marble unit

Three varieties of the marble unit are exposed in the mapped area. The first one is grey colour, foliated and undeformed (Fig.3.11A). It exposed around Gidano King mountain near the road of Dongoro-Kemashi. The second one is characterised by fine grained, massive and shows pure sugary white calcite grains (Fig.3.11B). This one is exposed at the central and northern part of the study area. The last one is impure colour, affected by poly phase deformation and cut by deformed mafic dike of 15-20cm thickness (Fig.3.11C). It exposed around the western part of the study area by the stream cut. The foliation of marble unit at this area is mostly striking 030° to 055° and steeply dipping 60° to 90° W.

From this lithologic unit three thin sections are prepared. Even if they are different in colour and encountered different degree of deformations thin sections of the rock unit contains approximately similar modal proportions of minerals. More than 90% of this rock is calcite (Fig.3.11D, E and F). The rests are 5% opaque, 2% quartz, 2% muscovite and 1% chlorite. Textural characteristics of calcite mineral in this thin section is xenoblastic. Sub parallel alignment of calcite mineral grains define weak to moderate foliation in the some thin sections (Fig.3.11E).

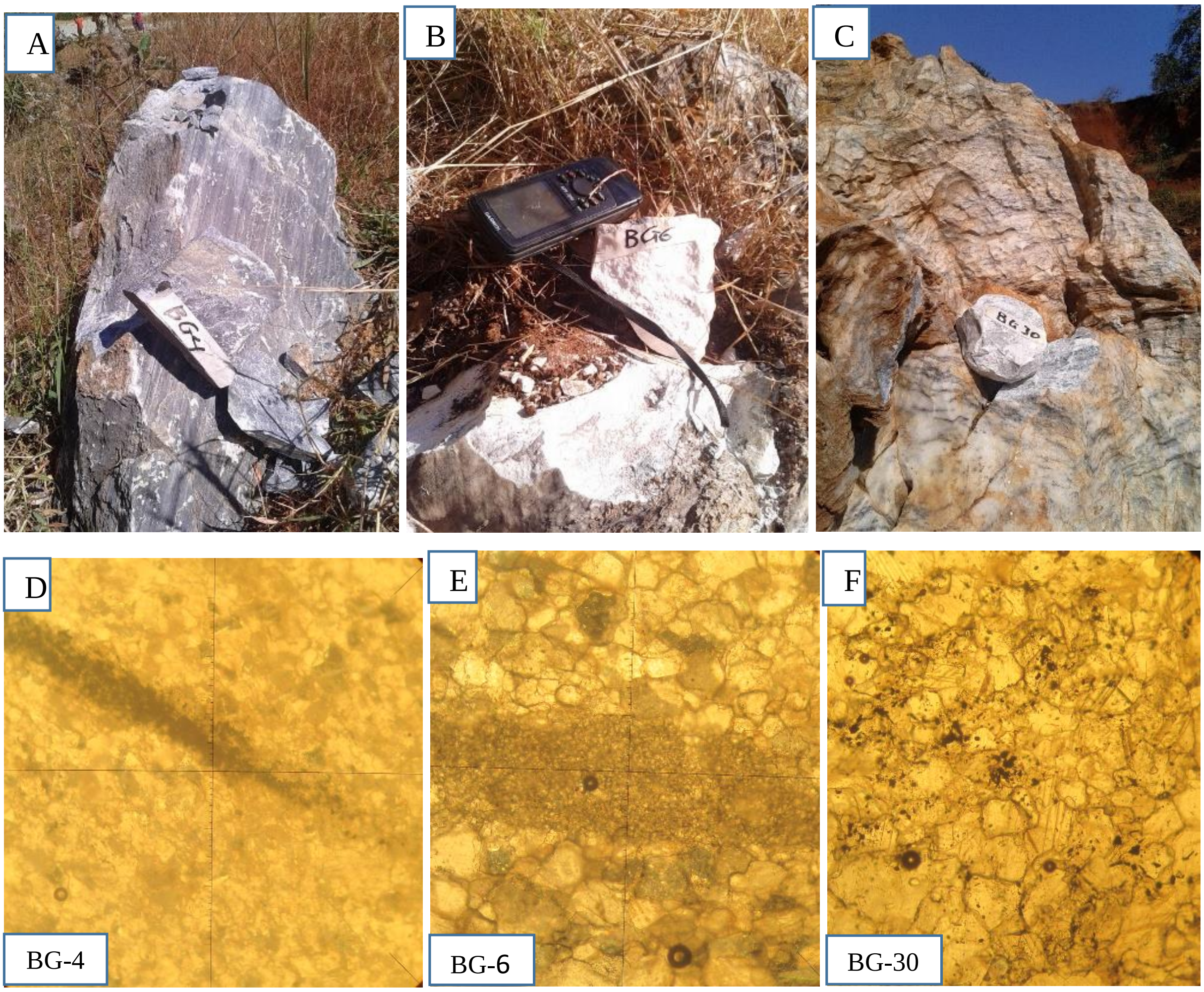

Figure 3.11 Field and microphotographs of marble outcrops. A) Foliated and grey (N-1040549, E-0799913). B) Show sugary calcite grains (N-1042313, E-0801534). C) Strongly deformed

marble outcrop (N-1044973, E-0798103). D) Fine grained and foliated. E) Inter locking of smaller grains of calcite at the centre of the field of view. F) Opaque rich plate.

3.2 Metamorphism

Field study and petrographic analysis revealed that all the rocks in the study area were highly metamorphosed. Evidence of metamorphism such as textural, grain size and recrystallization in the rocks of the area were recorded with relict of some minerals from the pre-existing rock types. The metasedimentary rocks are retained primary bedding and composed of mineral assemblages such as chlorite, mica, sericite, quartz and feldspar which show their origin may be came from pelitic rocks or clay rich rock materials. The presence of such mineral assemblages in the metasedimentary rocks of the study area indicate that the area were affected by low grade metamorphism of green schist facies. Additionally, the abundance of mineral assemblages such as quartz, sericitized plagioclase, chlorite, epidote, actinolite, feldspar, opaque, calcite, talc and some relict of pyroxene and olivine in metaultramafic and metavolcanic rocks indicate that the area is experienced low grade green schist facies metamorphism.

The Mineral assemblages of various rock units from the study area are described as follows:

a. Slate
   I. **Chl** + **Qtz** **+** **Ser** + Cal + K-feldspar + Bt + Opaque
   II. **Ser** + **Chl** + Qtz +Cal + Bt + Opaque

b. Phyllite

   Qtz **+** **Ser** **+Chl** **+** Cal + Opaque + Pl (alb) + Bt

c. Marble

   Cal + Opaque + Qtz + Ms

d. Quartzite

   Qtz + Op + Bt

e. Graphite schist

   Gr + **Qtz** + Ser

f. Chlorite schist

Chl + **Ep** + Cal +Ms + Qtz+ Opaque + Pl + Bt

**Chl + ** Act + Opaque

g. Metabasalt

I. **Pl + Chl + Ep** + Cal **+** Ms + Qtz + Opaque + Spn

II. **Pl** + **Chl** + Pyx + Ep + Cal + Qtz + Ms + Opaque + Ol + Spn

h. Talc Schist

Tlc + Mgs + Act + Opaque

i. Actinolite schist

I. **Act +** Chl **+** Opaque

I. **Act**+ Mgs + Tlc + Opaque

j. Serpentinite

I. **Srp +** Mgs **+** Opaque + Chl

CHAPTER FOUR

Structures and Deformation History of Bila Area

4.1 Introduction

Rocks of the study area recorded both early deformation (ductile structures) and later deformational phases (brittle structures). Ductile structures obtained in the study area includes folds, foliations and lineations whereas brittle deformations recorded includes veins, faults and joints. Ductile deformation more affected metasedimentary rocks of the area, whereas brittle deformation affected both metavolcanic and metasedimentary rocks. Both ductile and brittle deformational phases are not similarly distributed in the entire study area. However, there is an increase in structural complexity and intensity of ductile deformational phases from eastern to western part of the study area. The phyllite and marble rock units mostly experienced the ductile deformation while, metabasalt and some other metasedimentary rocks were highly affected by the brittle deformation.

Field work and petrographic analysis revealed that the rocks of Bila under gone poly phased deformation history. Based on analysing the geometry of the rocks and their attitudes in the field and petrographic analysis, at least three deformational phases are recorded in the area. D1 and D2 phases are mostly attributed to the ductile deformational phases but, post D2 deformational phase may be attributed to the brittle deformational phase during which the faults, veins, dikes and joints were developed. Each structures observed in the study area and their deformation history are discussed in this chapter in detail.

4.2 Earlier (D1) Structures

A) Fold

Fold is the most common structure in the metamorphic rocks of Bila. During the field investigation different types of mesoscopic F1 folds were identified. These mesoscopic folds ranges in size from centimetre to very few meters. Folds such as similar fold (Fig.4.1A), parasitic fold (Fig.4.1B and F), ptygmatic fold (Fig.4.1G, H and I) and plunging fold (Fig.4.1E) are encountered at the area. The axial planes of these folds are parallel to the S1 foliation (parallel to regional foliation). Stereographic projection also shows that most of the axial planes of these folds were striking to NE-SW and dipping SE (Fig.4.2). The axial planes of most of the minor parasitic folds are almost parallel to the axial planes of the larger folds in which they are associated. Folds in the study area are observed mostly in the phyllite and marble outcrops. Parasitic, ptygmatic and similar folds were highly distributed at the eastern part of the study area where the phyllite unit was dominant. Antiform and synform folds are common in the marble outcrops.

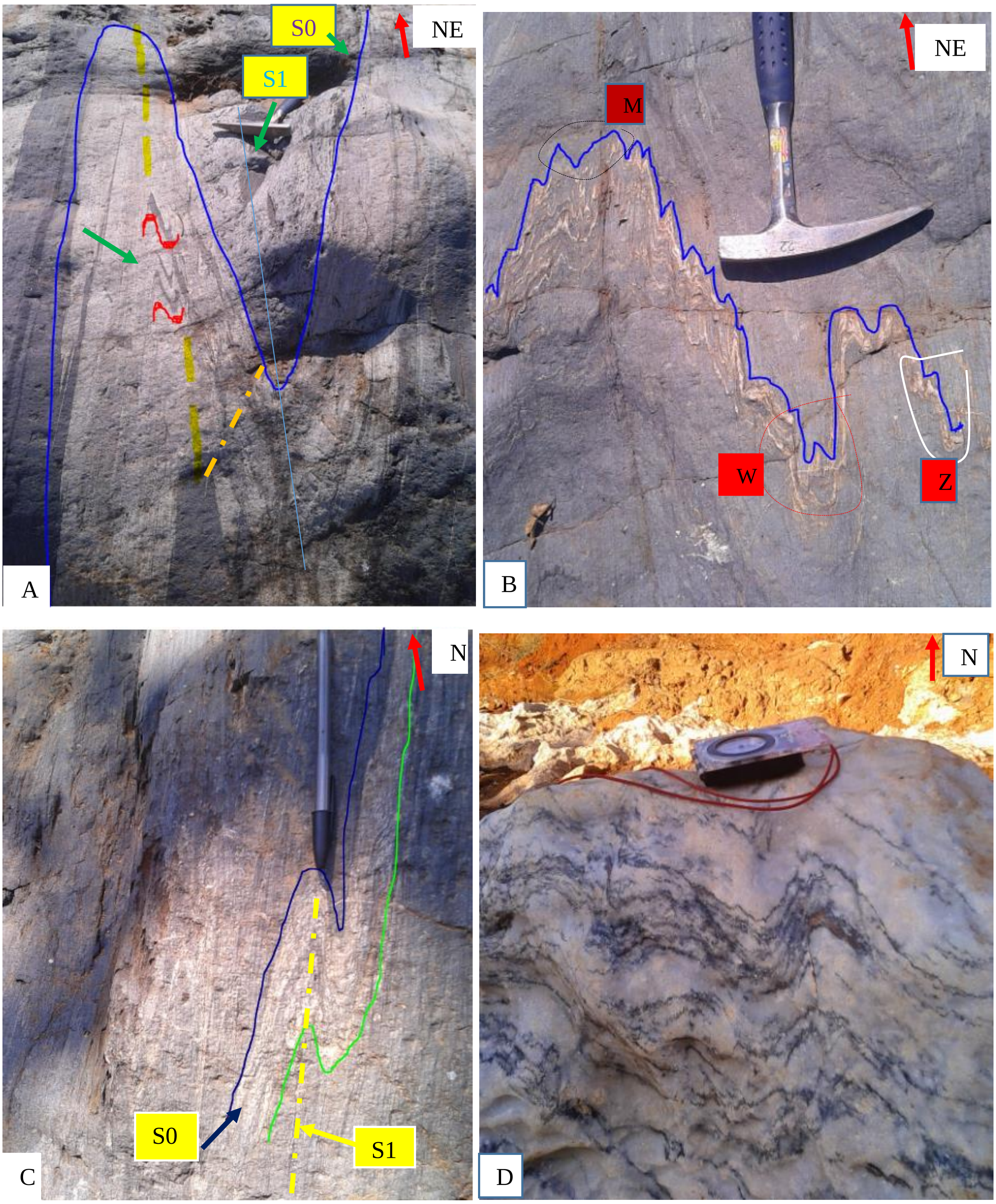

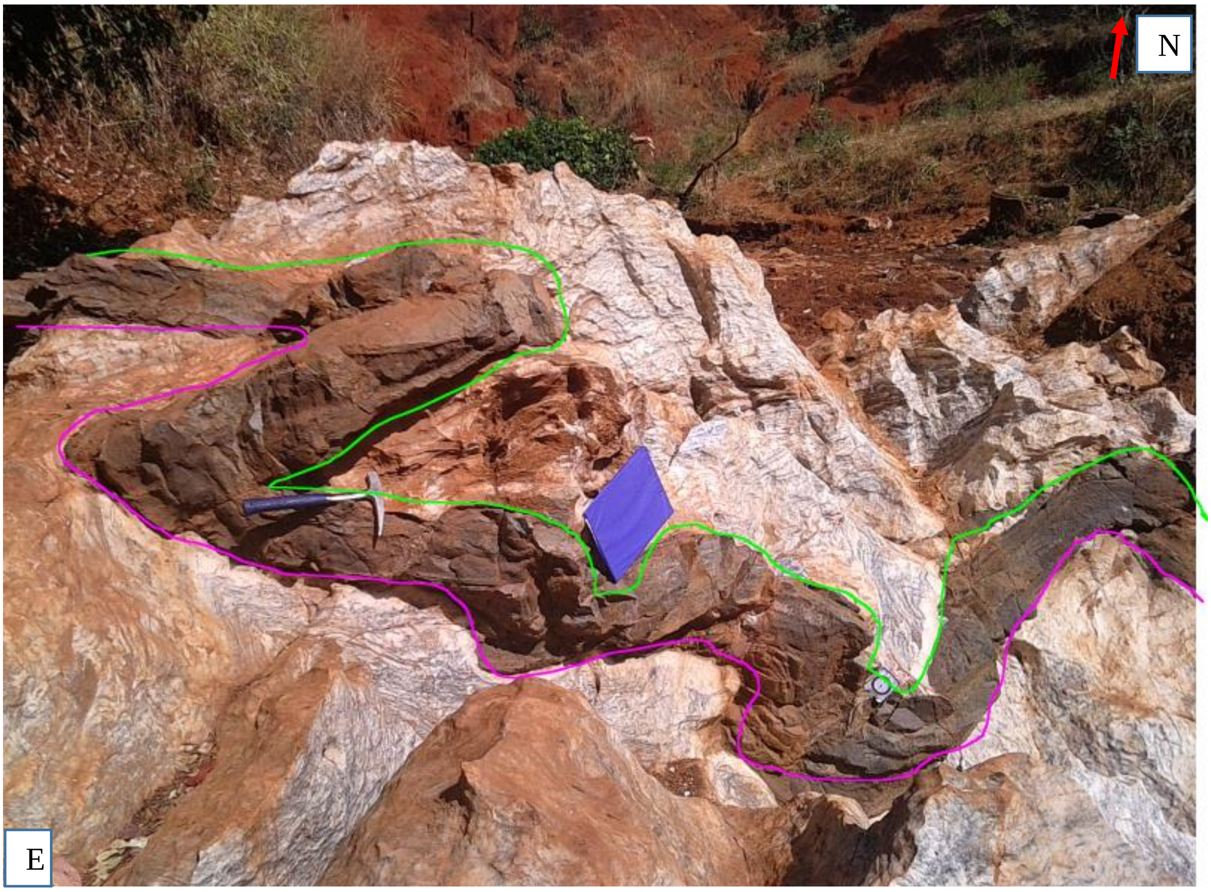
N
E

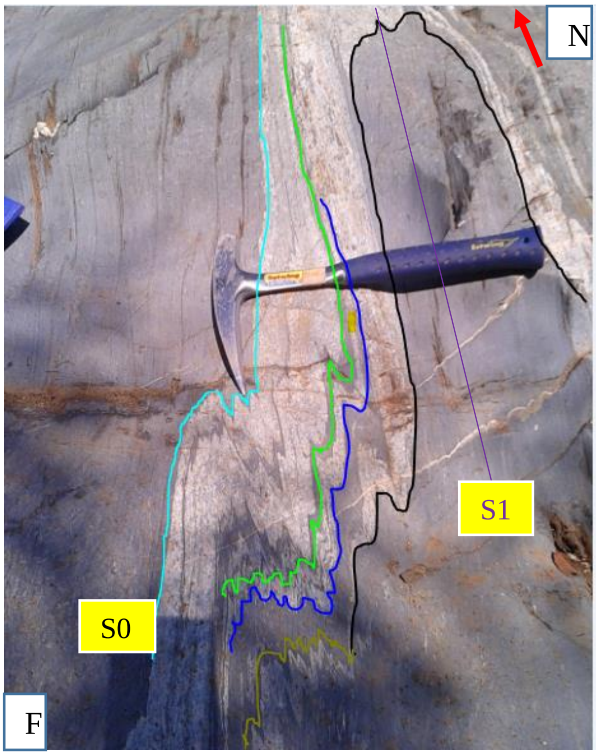
N
S1
S0
F


N
G

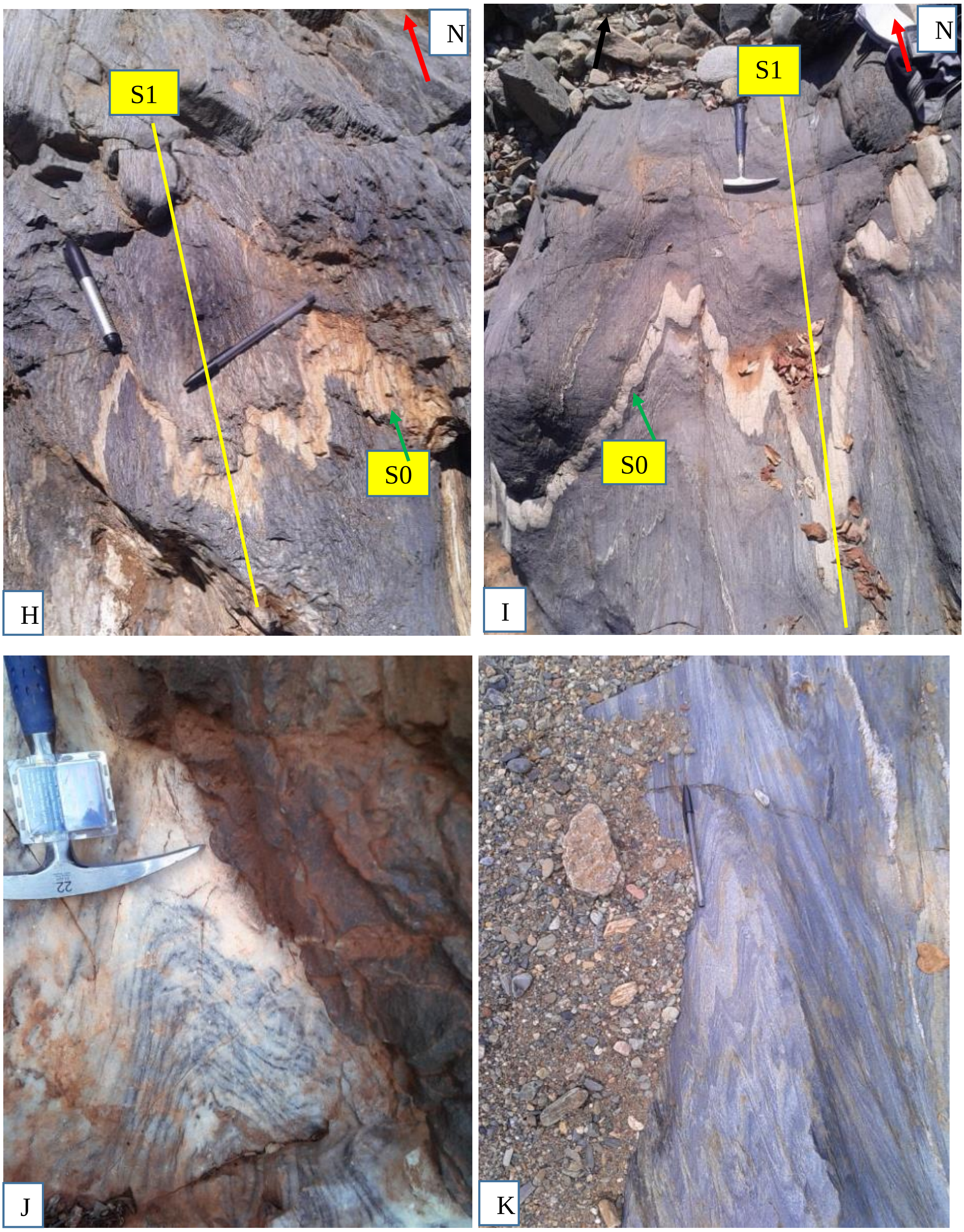

Figure 4.1 Field photographs of different types of folds. A) A mesoscopic similar fold that contains many minor similar folds in the hinges and limbs of the larger fold. Axial plane of this fold is striking N30˚E and dipping 50˚towards SE and with vertical plunging of fold axis. This fold is formed by primary layer (S0) present in phyllite unit. Generally this picture shows S0 and S1 foliations. Photo taken from the top view from Huda river, at E-0802958, N-1041263. B) M, W and Z shape of minor parasitic fold in a phyllite outcrops (location; N-1042312, E-

0803163). Photo taken from the top view. C) Fold formed by individual primary layer (S0) of phyllite unit (location; N-1042802, E-0803681). The axial plane of this fold was striking N10˚E and dipping 75˚ E. Photo taken from the top view. D) Mesoscopic folding of multiple layer of black and white layer of antiform and synform folding of marble unit (location; N-1044652, E-078335). E) Plunging folds formed by dike in marble unit (location; N-1044973, E- 0798103). F) Parasitic folds developed in the limb of larger fold of phyllite layer and fracture filled by quartz vein. In this case the axial plane of the smaller folds are closely parallel to the axial plane of major folds in which they are associated. Picture taken from Huda river from the top view. G) Ptygmatic fold formed by a single layer in phyllite unit (location; N-1043113, E-0803925). The axial plane of this fold is parallel to S1 foliation. H) The ptygmatic fold in the phyllite outcrops (location; N-1042753, E-0803617) and C (N-1042558, E-0803197). J) Antiform folding in marble unit. Hammer is used for scale. K) Mesoscopic small scale folding in the phyllite unit. A pen is used for scale.

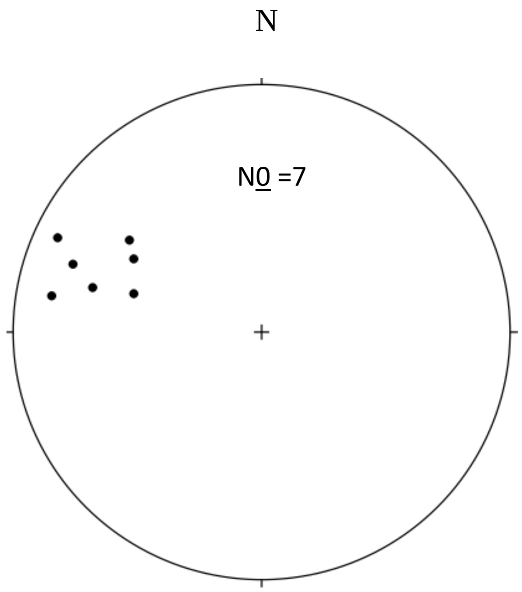

Figure 4.2 Equal area stereo-plot *of pole to axial planes of F1 fold.*

B) Foliations (S1)

S1 foliation is the most common structure, which affected most of the rocks of the area. In Bila area this foliation is defined by slaty cleavage, phyllitic crenulation cleavage and alignment of elongate minerals. Spaced and continuous cleavages are the most common S1foliations in the Bila area. The intensity of rocks affected by foliations are controlled by the type of the rock and degree of metamorphism/deformation occurred during their formation. This S1 foliations are mostly developed in the metasedimentary and metaultramafic (talc schist) rock groups.

Petrographic analysis also show the presence of well aligned minerals such as chlorite, mica, feldspar, actinolite and talc which were define the development of strong S1foliations in the most rocks of the area (Fig.4.3C and D). Foliation (S1) in the area is mostly striking NNE to NE with gently to vertical dipping WNW and SE as shown in the stereographic projection (Fig.4.4). Most of the time the (S1) foliation in this area was parallel to the axial plane of F1 folding in the area.

*Figure 4.3 Field and microphotographs of S1 foliations. A**)** Field photographs of highly foliated talc schist (location; N-1041833, E-0801707). Photos taken looking toward the north. B)*

Banding (primary bedding) in phyllite unit. C) Strong foliation in slate. D) Well develop parallel alignment of minerals in the thin section.

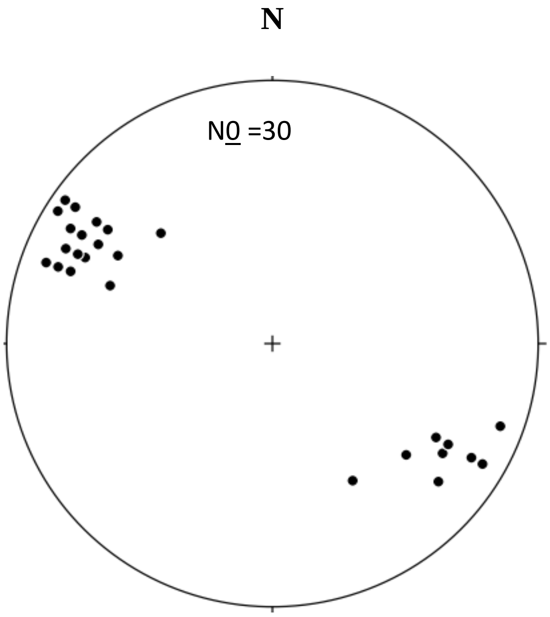

Figure 4.4 Equal area stereo-plots of the S1 foliation.

4.3 D2 deformational Phases

A) S2 Foliation

Field investigation and petrographic analysis suggests the development of crenulation foliation in the study area. Mesoscopic crenulation foliation that show S2 foliations observed from this area during the field investigation (Fig.4.5A and B). Additionally micro-folding from petrographic analysis exhibit S2 crenulation foliation, which are defined by minerals such as chlorite and mica (Fig. 4.5 C and D). S2 crenulated foliation is experienced only in the phyllite rock unit of the Bila area as a result of D2 deformational phases of originally aligned minerals in the rocks.

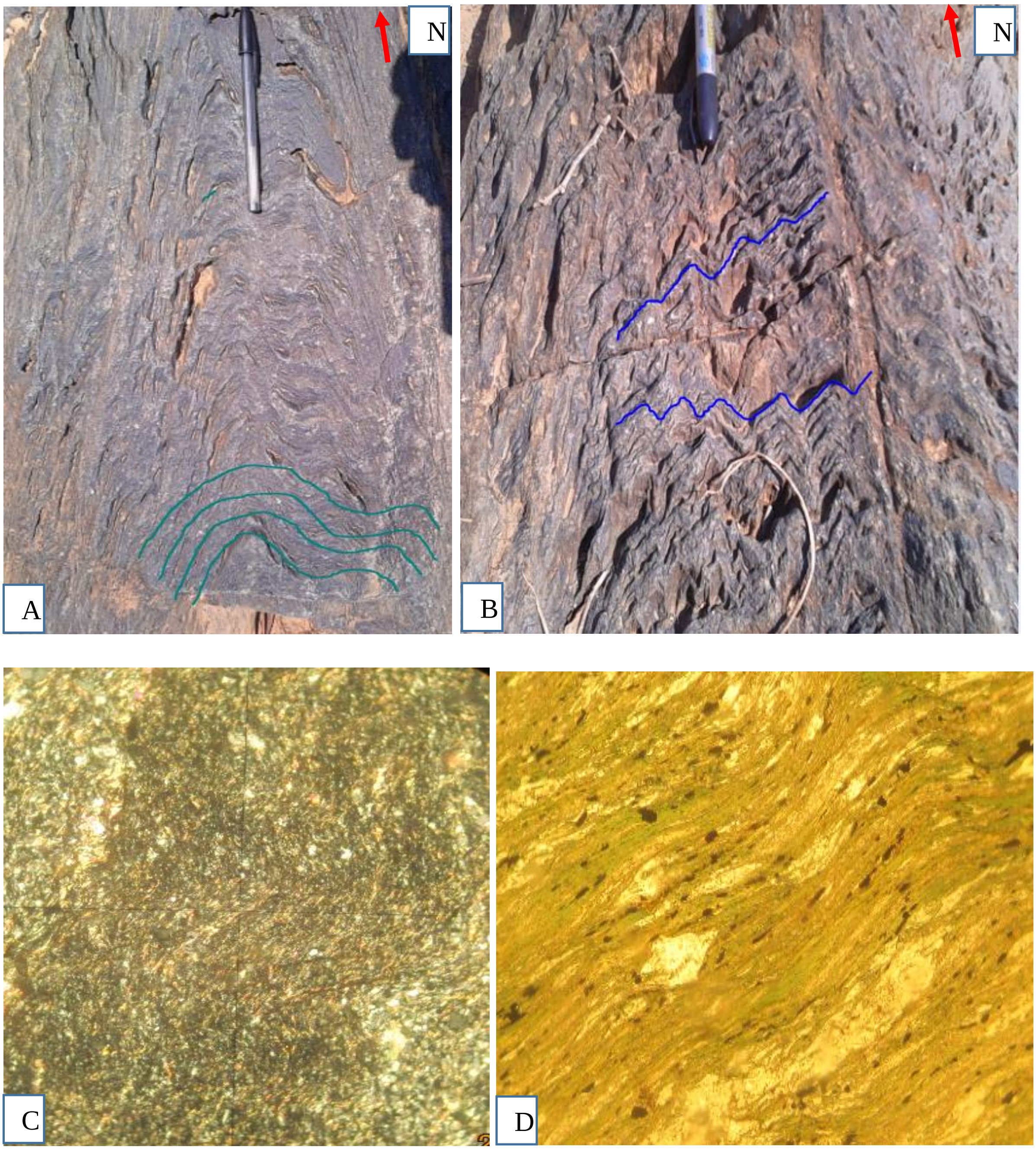

Figure 4.5 Field and microphotographs of S2 foliations. A) Asymmetrical crenulation cleavage in phyllite outcrop. Photo taken from top view at N-1043110, E-083923. B) Angular asymmetrical crenulation cleavage in the phyllite unit (location; N- 1043113, E-0803930). Photo taken from top view around where Huda and Horfa river cut each other. C and D) Micro folding that show S1 and S2 foliations.

B) Crenulation lineation (L2)

The linear structures observed in the study area mainly included fold axes and crenulation lineation. The crenulation lineation in this case is very clear in hand specimen and outcrops. It is a penetrative lineation. Crenulation lineation in this area is formed by mica and chlorite in the phyllite rock unit.

Figure 4.6 Field photograph of crenulation lineation in the phyllite unit. Photo taken from Huda river at N-1042753, E-0803617.

C) F2 fold

The F2 folds are not abundant as such other structures in the outcrops of the study area. But, the open recumbent fold formed by the refolding of the pre-existing axial plane of the F1 fold is obtained in the study area (Fig.4.7).

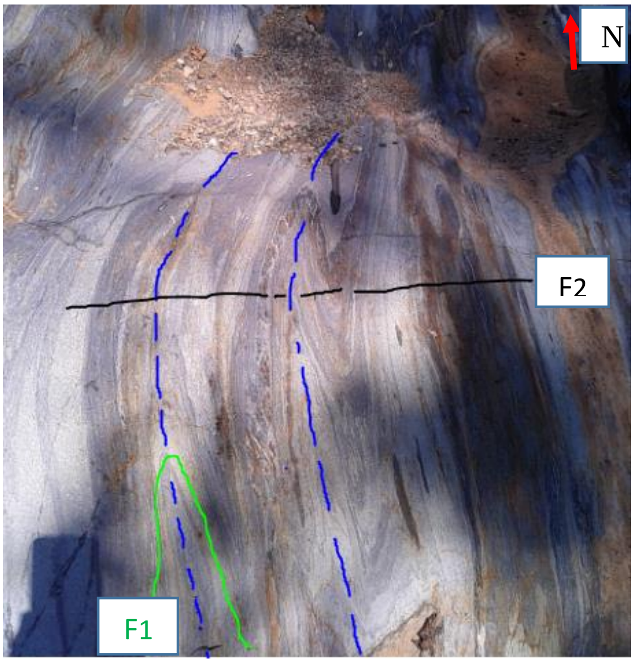

Figure 4.7 F2 recumbent fold in the phyllite outcrops. A pen is used for scale.

4.4 Post D2 structures

A) Fault

Fault is another the most common structure in the metamorphic rocks of the study area. The mesoscopic dextral strike-slip faults of NE and NW trending were recognized in the study area (Fig.4.8A-F). Evidence of fault comes from the motion of marker layer in the phyllite outcrops. Among different lithologic unit in the Bila area the phyllite unit is mostly affected by it. Concentration of this structure is exposed around Dobo and Huda river.

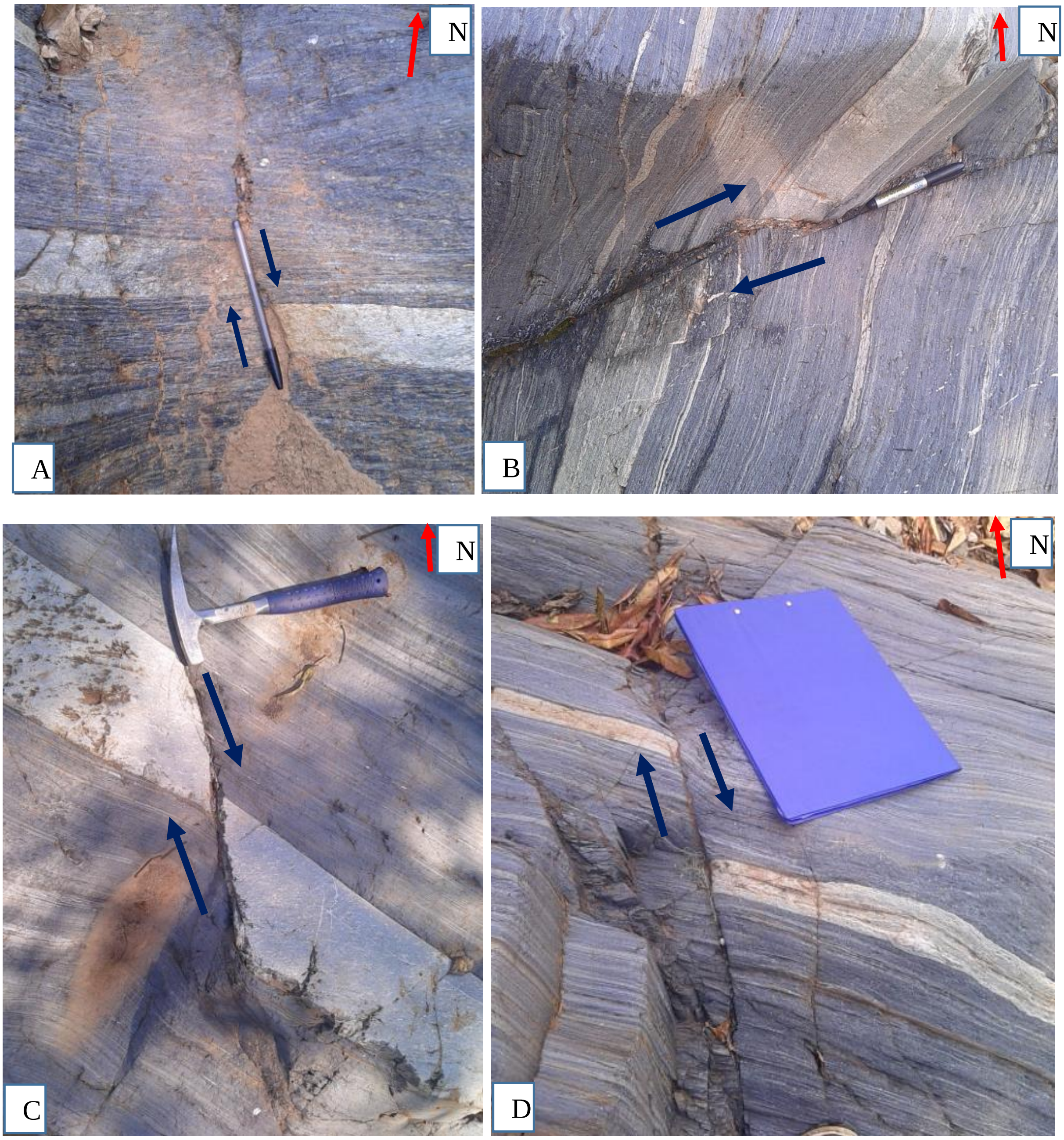
N
A
N
B
N
C
N
D

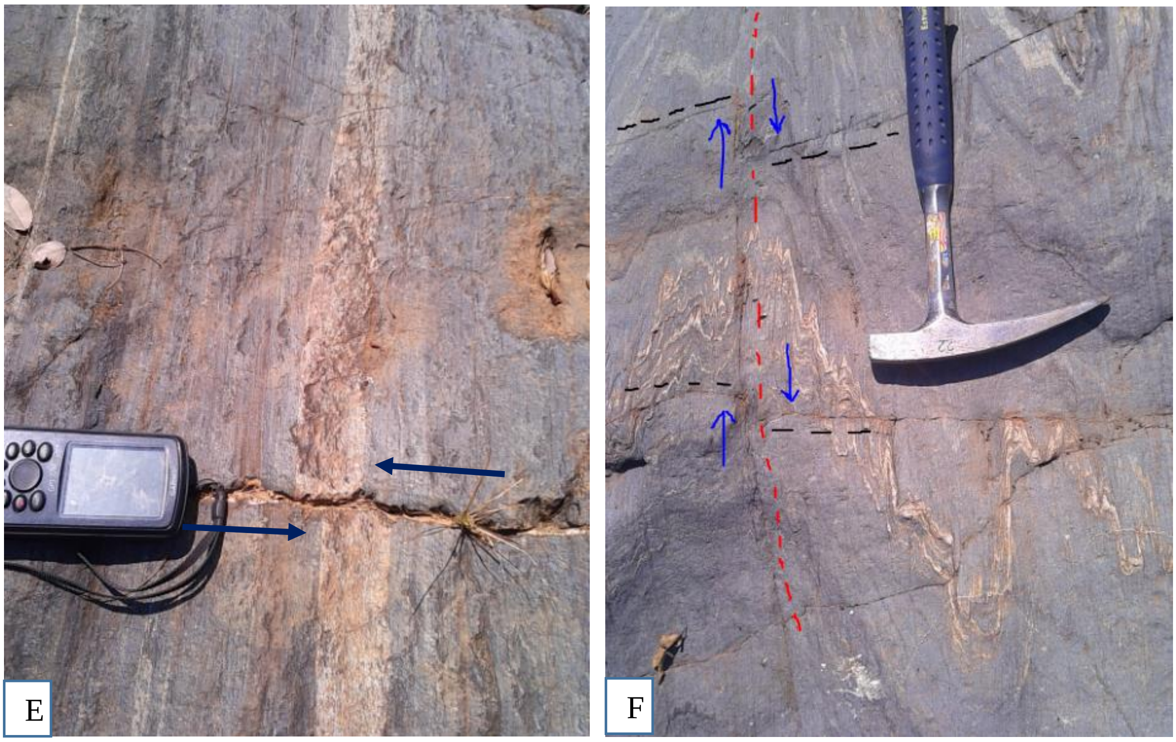

Figure 4.8 Field photo pictures of the mesoscopic faults in the Bila area. A) Dextral strike slip fault, a pen is used for scale. This fault was striking 330° and dipping 75° toward the NE. Photo taken from Huda river at N-1042313E- 0803176. B) Mesoscopic dextral strike slip fault in phyllite outcrop. Photo taken from Horfa river at N-1042314, E-083159. This fault was striking N40°E and dipping 55° towards SE. C) Dextral strike slip fault, hammer is used for scale (location, N-1043203, E-0803922). This fault was striking 310° and dipping 70° towards NE. D) Dextral strike slip fault which is striking 340° and dipping 45° towards the SW at N-1043464, E-080350. E) Small scale dextral strike slip fault in the phyllite outcrop. GPS is used for scale. F) Minor dextral strike slip fault in the phyllite unit.

B) **Joint**

Joint is another common brittle structural feature identified in the metamorphic rocks of Bila with variable in opening style and geometry (Fig.4.9A-E). Joints of the area were mostly trending N, NE and SE with sub vertical to vertical dipping. It is formed as a result of later deformation. Some of the joints and fractures are filled by quartz or calcite veins as observed in the field.

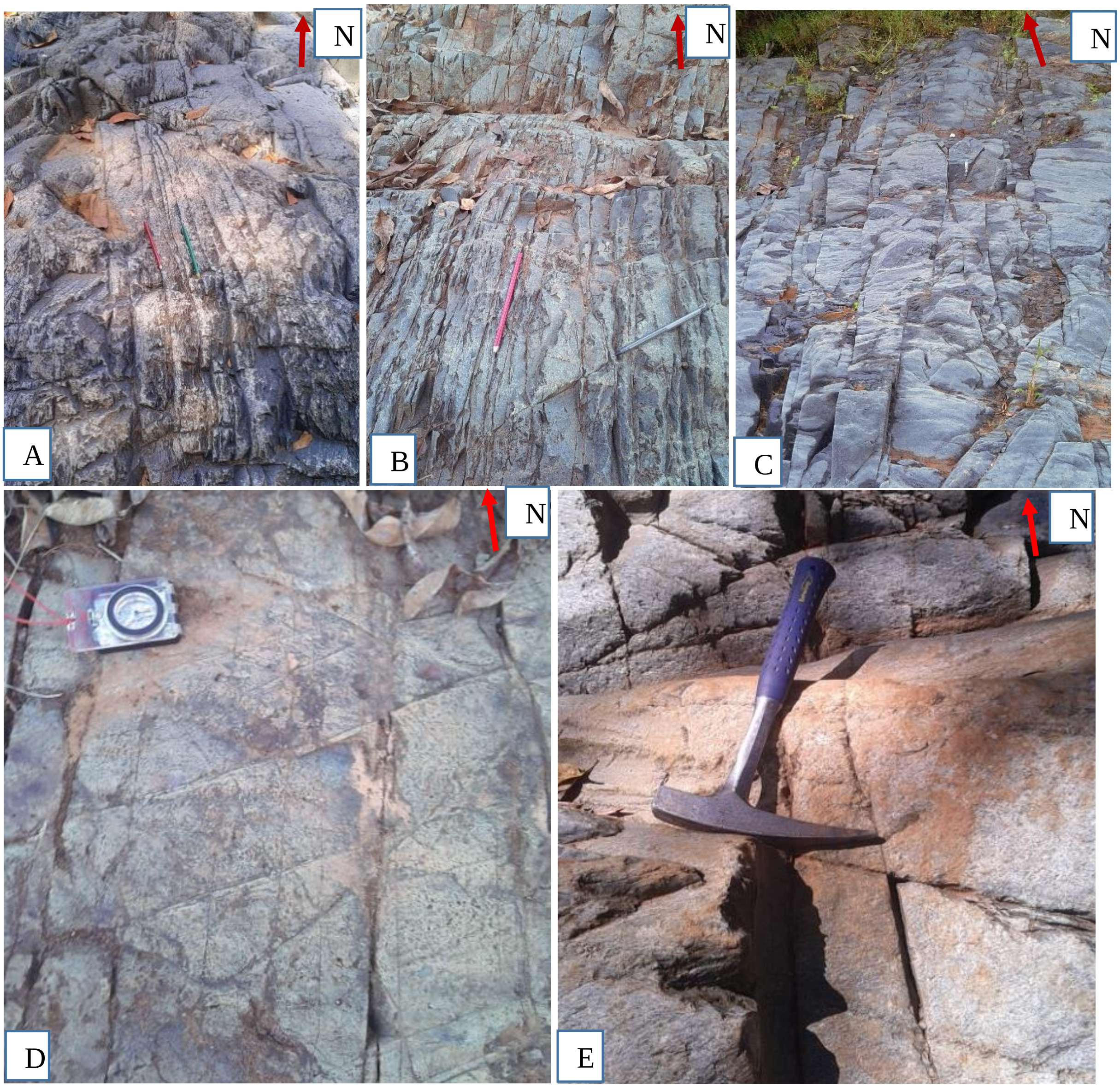

Figure 4.9 Field pictures of different orientations of joints in the Bila rocks. A) Field photographs of one set of joint in the metabasalt (location N-1043300, E- 0796684). Pencil is used for scale. B) Two set of joint in metabasalt (location N-10434330, E- 08000935), C) Development of joint across (almost perpendicular) to S1 foliation. D) Rhombohedral shape of joint in the metabasalt (location; N – 1043626, E- 0801140). E) Systematic two sets of joint in the phyllite outcrops that show rhombohedral shape (location; N-1042534, E-0798877).

C) Vein

Both syntaxial (Fig.4.10A) and antitaxial vein (Fig.4.10B) types are obtained during field work and from petrographic analysis. The most common veins in the study area were calcite and quartz veins. Both vein types obtained in the metavolcanic and metasedimentary rocks of the study area as the mesoscopic or microscopic scale.

Figure 4.10 Field photographs of veins. A) Syntaxial quartz vein in the quartzite unit which has the orientation 300˚ and 45˚SW. B) Antitaxial quartz vein in phyllite.

D) Dike

Field study revealed that the presence of mafic dike in the Bila rocks. This mafic dikes were classified into undeformed and deformed. The undeformed one is parallel to S1 foliation of the area (Fig.4.11A and B). Degree of deformation of this dike is increasing from east to west part of the area. Among the lithologic unit of the study area, the marble unit is highly affected by it.

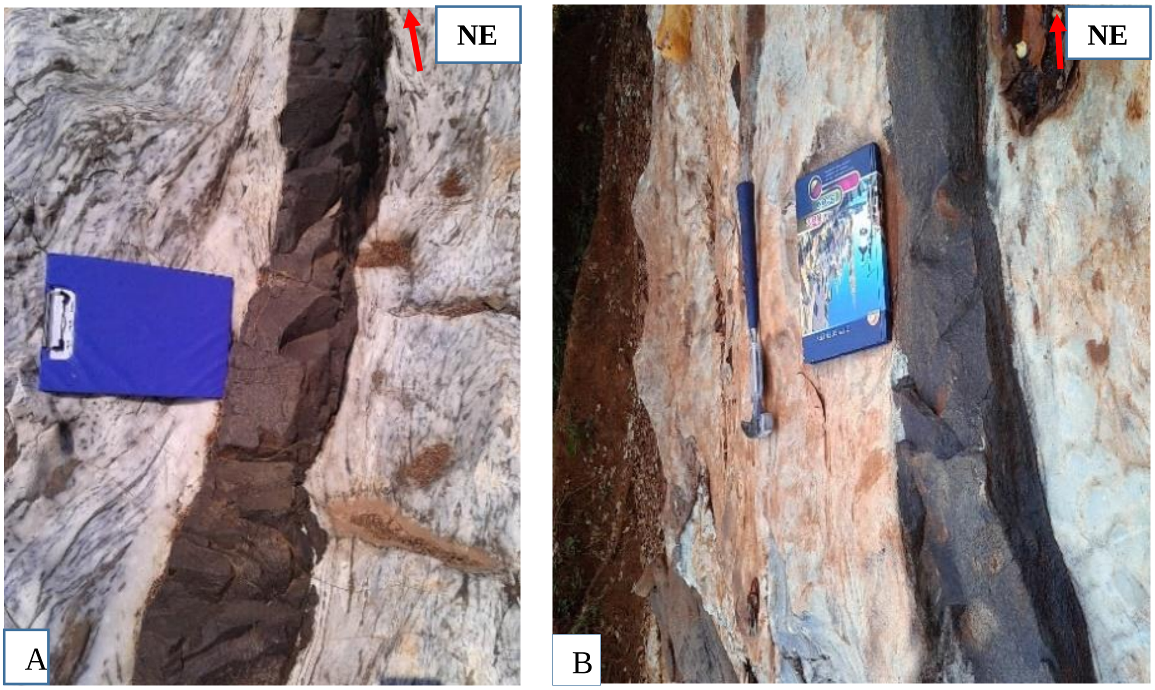

Figure 4.11 Field pictures of mafic dike in marble rock unit. A) Unfolded (undeformed) mafic dike in the deformed marble, photo taken from Daga Boka at N-1042170, E-0798557. In this case the dike is parallel to the S1 foliation of the rock unit. Orientation of this dike was striking N30˚E and dipping 65˚SE. B) Mafic dike in the undeformed marble unit (location; N-1044652, E- 078335).

4.5 Correlation with the Regional Structures

A. D1 deformational phases

Foliation (S1) of the Bila area is correlated with the regional S1 foliation of trending NNE to SSW and variably dipping SE (Tadesse Alemu and Tsegaye Abebe, 2007).

Fold (F1**)** of the study area is regionally correlated with D1 structural folds which are associated with the formation of tight to isoclinal, which fold bedding (S0) of the rocks in the Tulu Dimtu belt (Allen and Gebremedhin Tadesse, 2003).

B. D2 deformational phases

S2 foliation in the study area is regionally correlated with weakly to strongly developed crenulation cleavage (S2) axial planar to the D2 folds of Tulu Dimtu belt (Tadesse Alemu and Tsegaye Abebe, 2007).

F2 recumbent fold is obtained at the Bila area but F2 folds which are correlated with D2 folds of tight to open upright folds of the Chochi antiform and the Tulu Dimtu synform (Tadesse Alemu and Tsegaye Abebe, 2007) are not exposed at the study area.

C. D3 deformational phases

The D3 structural phases of the Bila area is regionally correlated with the D3 deformational phases which are represented by brittle-ductile reactivation of N, NNE and NW trending strike slip faults in the Tulu Dimtu belt (Allen and Gebremedhin Tadesse, 2003; Tadesse Alemu and Tsegaye Abebe, 2007). Even though most structures are studied regionally there is no information about the deformation history of joints and veins whether they are Precambrian or later events.

CHAPTER FIVE

Whole Rock Geochemistry of Bila Metavolcanics

5.1 Analytical Methods

6 fresh samples from metavolcanic rocks were selected for geochemical analysis. The samples are five from metabasalt (BG-13, BG-16, BG-23, BG-32 and BG-3) and one sample from chlorite schist (BG-7). The selected rock samples were crushed to less than 2mm, and the split samples were pulverized to about -200 mesh size at the laboratory of Geological Survey of Ethiopia (GSE). The pulverised sample were submitted to ALS geochemical laboratory PLC, Addis Ababa for preparation.

Geochemical data used in this work is obtained through the combined methods of inductively coupled plasma mass spectroscopy (ICP-MS) and inductively coupled plasma-atomic emission spectrometry (ICP-AES) of geochemical methods. Six pulverised rock samples were analysed for major, trace and rare earth elements.

ICP-AES is used to analyse major elements in their oxide forms including SiO_2, Al_2O_3, Fe_2O_3, CaO, MgO, Na_2O, K_2O, Cr_2O_3, TiO_2, MnO, P_2O_5, SrO, BaO and LOI. The thirty gram (30g) of pulverised rock samples are dissolved and mixed with water and the sample solution was transformed into an aerosol by a nebuliser. After dissolved with water, the sample is then, topped off with dilute HCl and the solution containing the sample is analysed using inductively coupled plasma-atomic emission spectrometry (ICP-AES).

ICP-MS method is a complete whole rock element package which uses 30g of pulverised sample. It involves lithium borate fusion of the sample prior to acid dissolution and provides the most quantitative analysis approach for a broad suite of trace elements. The thirty gram (30g) of pulverised rock samples added to lithium metaborate flux (0.9g). Then it is mixed well and fused in a furnace at 1000°C for 30 minute. The melt is then cooled for 15 minutes and diluted in 100 mL of 4% HNO_3 or 2% HCl solution so that mineral species including those that are highly refractory are solubilized. The solution is then analysed by inductively coupled plasma mass spectrometry for all REE and trace elements. The result is listed in Table 5.1.

The objective of analysing and interpreting geochemical data in this study is to understand the origin and tectonic setting of metavolcanic rocks of Bila. Harker variation diagrams of MgO versus major oxides, Zr variation diagrams with selected trace elements, chondritic normalized rare earth element (REE) abundance pattern, multi-element variation diagram, Zr-Y-Nb and Th- Ta- Hf triangular discrimination diagrams are plotted for Bila metavolcanic rocks.

Samples	Metavolcanic Rocks					
	BG-7	BG-13	BG-16	BG-23	BG-32	BG-37
SiO_2	60.1	50	49.4	59.6	52.7	54.3
Al_2O_3	12.35	14.55	14.35	15.3	13	15.6
Fe_2O_3	7.91	9.12	11.2	8.4	12.55	9.61
CaO	1.68	7.53	10.75	4.78	7.13	6.06
MgO	4.94	5.25	7.33	3.14	7.88	4.56
Na_2O	2.26	2.65	3.14	2.89	2	4.97
K2O	1.01	1.16	0.16	1.84	0.05	0.4
Cr_2O_3	0.03	0.01	0.05	0.02	0.03	0.01
TiO2	1.02	1.33	1.57	1.29	1.27	1.72
MnO	0.11	0.15	0.18	0.13	0.29	0.17
P_2O_5	0.23	0.19	0.16	0.32	0.08	0.25
SrO	0.03	0.05	0.03	0.04	0.01	0.03
BaO	0.05	0.03	0.01	0.07	<0.01	0.02
LOI	4.82	7.94	2.13	3.62	3.52	2.18
Total	**99.54**	**99.96**	**100.46**	**101.44**	**100.51**	**99.88**
C	0.48	1.34	0.1	0.61	0.03	0.11
S	0.05	0.15	0.19	0.11	0.24	0.01
Ba	477	281	80.2	667	27.7	199
Ce	38.1	28.5	19.9	51.2	6.6	38.5
Cr	210	70	340	120	230	50
Cs	1.52	0.57	0.08	1.35	0.03	1.47
Dy	4.89	5.52	5.13	5.42	5.51	6.08
Er	2.62	3.14	3.17	2.93	3.57	3.61
Eu	1.01	1.6	1.53	1.63	1.08	1.69
Ga	17.2	17.3	18.6	21	15	17.8
Gd	4.44	5.61	5.08	6.06	4.38	6.42
Ge	<5	<5	<5	<5	<5	<5
Hf	3.3	3.6	3	5.2	2	4.6
Ho	0.86	1.18	1.04	1.07	1.26	1.19
La	15.9	12.8	8.7	24.2	2.7	17.8
Lu	0.39	0.4	0.35	0.42	0.53	0.49
Nb	12.5	6.8	6.9	20.5	1.7	13.5
Nd	21.5	17.9	13.8	27.7	6.8	22.3
Pr	4.92	3.69	2.76	6.35	1.16	4.65
Rb	24.9	37.4	1.8	42.6	0.8	13.4
Sm	4.48	4.65	3.64	6.02	2.59	4.93
Sn	1	2	2	2	1	2
Sr	215	414	221	279	131.5	232
Ta	1.2	0.6	0.3	1.2	0.1	0.8
Tb	0.71	0.9	0.82	0.92	0.84	0.91
Th	3.34	2.36	0.82	3.41	0.21	2.88

Tm	0.41	0.51	0.44	0.51	0.55	0.56
U	1.32	0.86	0.28	1.2	0.05	0.91
V	178	175	264	126	306	204
W	45	23	1	1	1	1
Y	24.4	29.2	27.2	28.6	28.9	31.1
Yb	2.56	2.96	2.82	2.88	3.52	3.27
Zr	137	159	110	193	64	183
As	20.5	25.2	5.2	0.7	8.7	14.5
Bi	0.11	0.05	0.01	0.04	0.07	0.01
Hg	<0.005	<0.005	<0.005	<0.005	<0.005	<0.005
In	0.027	0.021	0.012	0.026	0.015	0.017
Re	<0.001	0.001	<0.001	0.005	0.001	<0.001
Sb	0.17	0.11	0.24	0.18	0.21	0.59
Se	0.6	0.4	<0.2	0.5	0.7	0.4
Te	0.05	0.02	0.01	0.01	0.05	<0.01
Tl	0.04	<0.02	<0.02	0.12	<0.02	0.26
Ag	<0.5	<0.5	<0.5	<0.5	<0.5	<0.5
Cd	<0.5	<0.5	<0.5	<0.5	<0.5	<0.5
Co	30	38	42	17	47	27
Cu	56	54	106	33	128	82
Li	20	10	10	20	10	10
Mo	<1	1	<1	9	<1	<1
Ni	110	36	62	58	100	48
Pb	12	<2	<2	<2	5	4
Sc	21	26	42	18	47	28
Zn	109	80	126	101	196	95

Table 5.1 Major, trace and REE element analytical results of the metavolcanic rocks collected from the Bila area.

5.2 Major Element Geochemistry

Bila metavolcanic rocks show significant variation in concentrations of major oxides geochemistry (Table 5.1). This metavolcanic rocks show 49.4-60.1wt% of SiO_2. Almost all of the samples collected from the area shows high content of Fe_2O_3 ranging from 7.99-12.55 wt. % that reflects the abundance of opaque minerals such as magnetite and ilmenite as described in petrographic analysis (see chapter 3). The metavolcanic rocks of this area also show 2-

4.97wt% of Na_2O and 1.68-10.75wt% of CaO (Table 5.1) which may be related to the involvement of plagioclase and epidote in the rocks of the area respectively (Jakes and White, 1972 as cited in Hassan and Bakheit, 2010). The Al_2O_3 contents of the rocks of Bila area varies from 12.35-15.6wt%.

Harker variation diagram is described by using the relationships between concentration of MgO versus all major oxides wt. % (Fig. 5.1 A-L) to describe the origin and behaviour of magma. Some major oxides such as CaO, Al_2O_3, Fe_2O_5, Cr_2O_3 and MnO (Fig.5.1C, E, F, G, I) show increasing trend with increasing MgO and other major oxides such as SiO_2, K_2O, P_2O_5, BaO, SrO and TiO_2 show negative correlation with MgO. The positive and negative correlation of major oxides with MgO may indicate the fractionations of basic magma during its origin (Fig. 5.1). However, MgO versus Na_2O (Fig5.1A) show scattered pattern suggesting later alterations due to the high mobility of Na (Gebremedhin Tadesse and Allen, 2005). MgO versus CaO plot (Fig.5.1C) shows a positive pattern showing simultaneous removal of these two oxides from the parent magma, most probably accomplished by fractionation of clinopyroxene (Gebremedhin Tadesse and Allen, 2005). Harker variation diagrams of MgO versus SiO_2 (Fig.5.D) show negative trend in the Bila metavolcanic rocks. This may suggests the involvement of olivine and pyroxene in the fractionation of the parent magma (Gebremedhin Tadesse and Allen, 2005). Finally the MgO versus P_2O_5 trend (Fig.5.1H) shows strongly negative linear pattern, which may indicate involvement of apatite in the magma fractionation process of Bila metavolcanic rocks (Gebremedhin Tadesse and Allen, 2005).

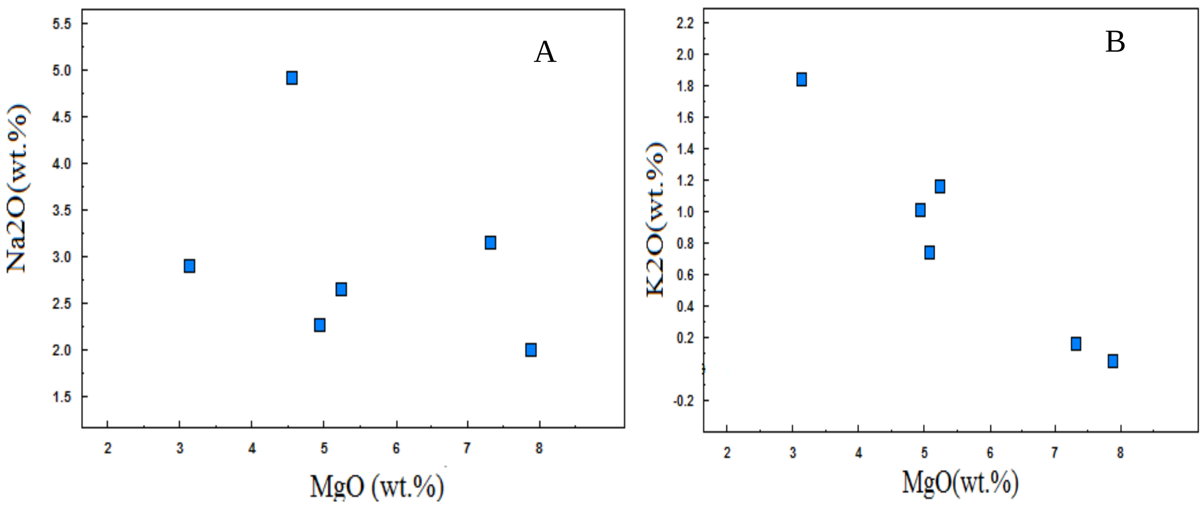

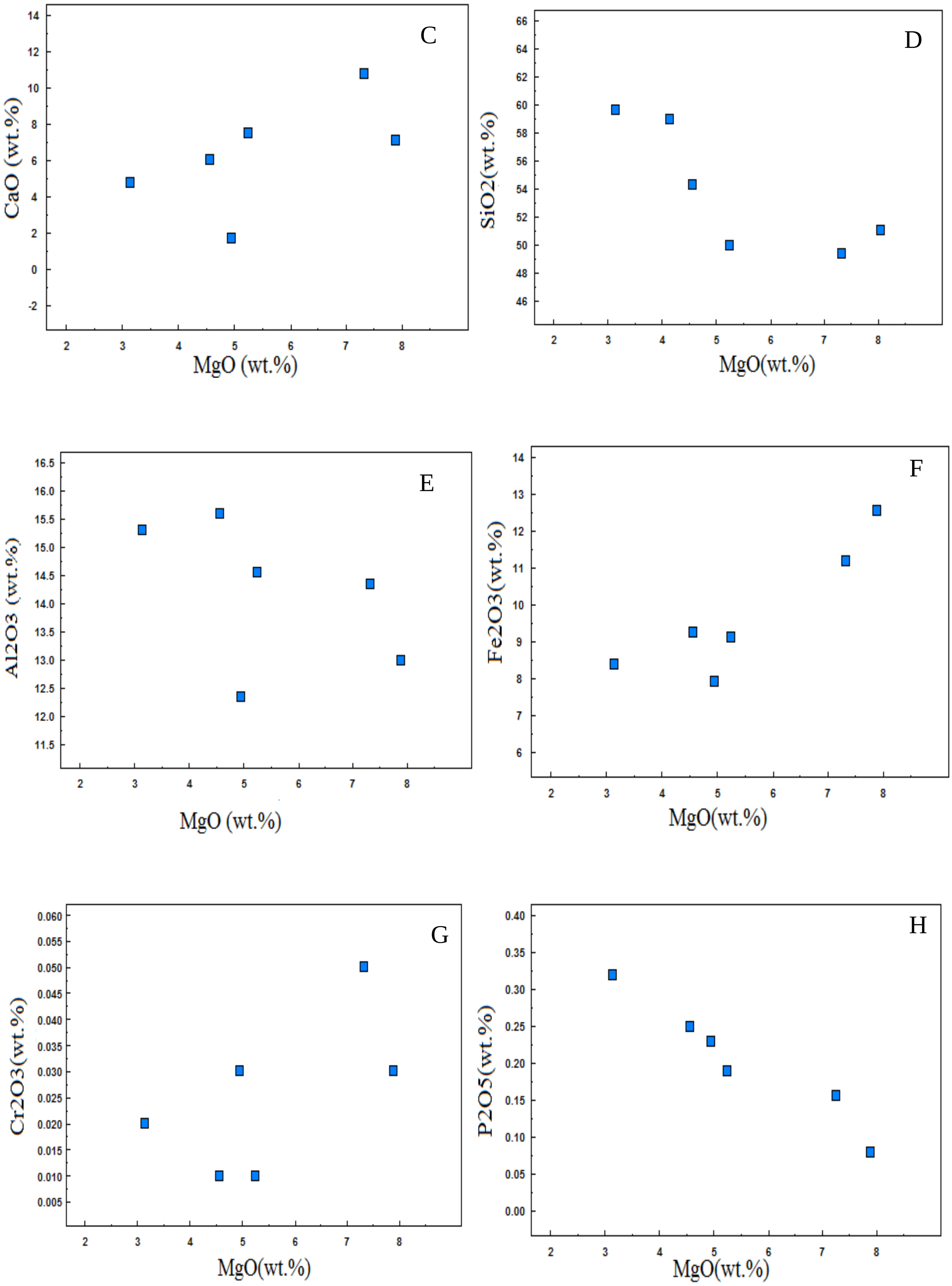
C
CaO (wt.%)
MgO (wt.%)
D
SiO2(wt.%)
MgO(wt.%)
E
Al2O3 (wt.%)
MgO (wt.%)
F
Fe2O3(wt.%)
MgO(wt.%)
G
Cr2O3(wt.%)
MgO(wt.%)
H
P2O5(wt.%)
MgO(wt.%)

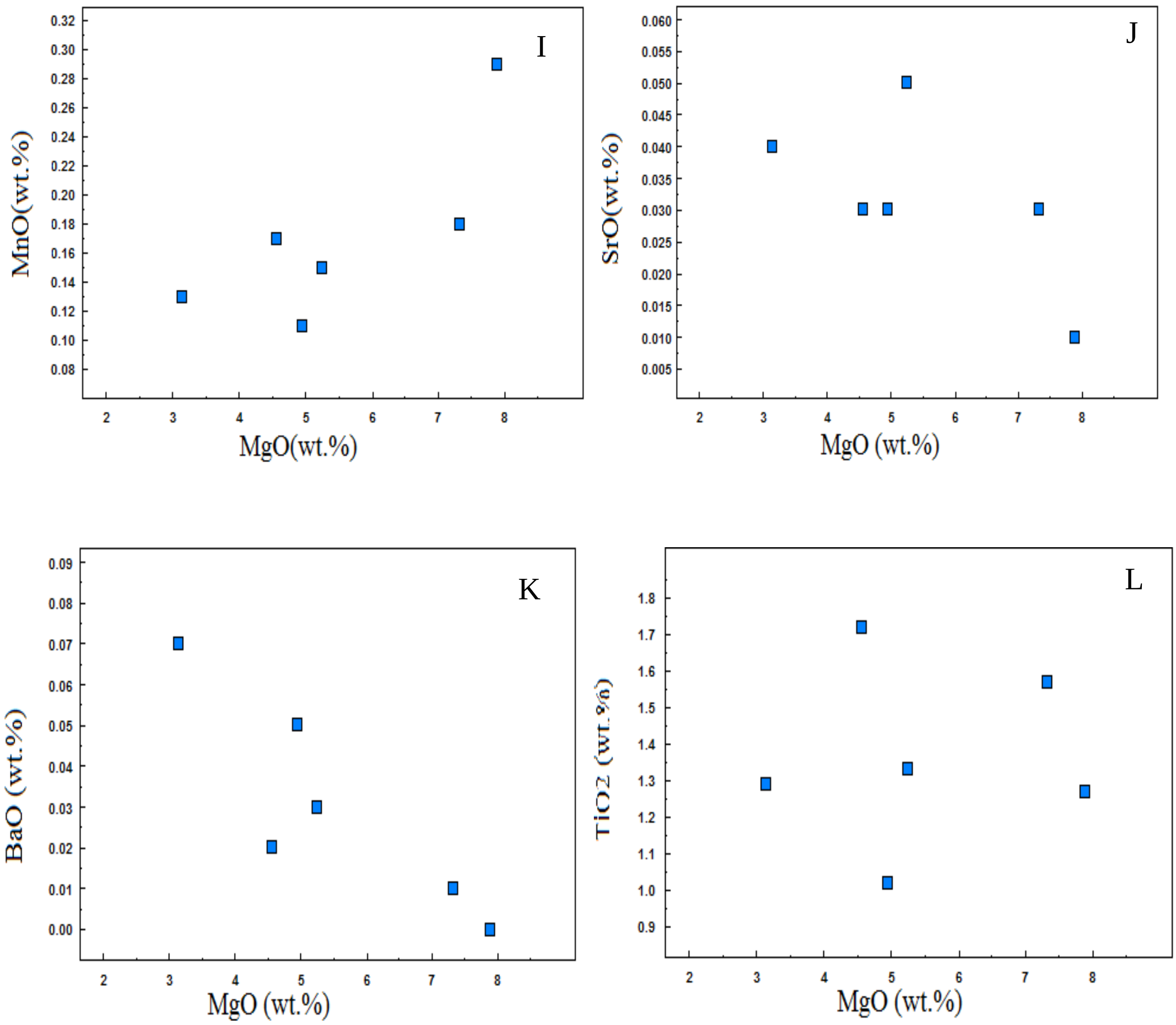

Figure 5.1 Harker variation diagrams of MgO wt. % versus major oxides wt. % for selected rock samples from study area.

5.3 MgO versus Trace Elements Variation Diagrams

MgO versus selected trace elements plots show variation between trace elements and MgO (Fig.5.2A-L). Most of the incompatible trace elements form a negative correlation with MgO. Trace elements such as Th, Hf, Nb, Ga, Rb and Zr are showing negative trend with MgO. However compatible trace elements like Co, Ni, V, Cr and Sc are showing positive trend with MgO. The positive and negative patterns of the compatible and incompatible elements with MgO may reflects the differentiation and fractionation of Mg and Fe bearing minerals such as olivine and pyroxene. The Mg and Fe are the accommodating elements for the compatible trace elements like Ni and Co. The Ni (Fig.5.2H) and Cr (Fig.5.2J) contents have positive correlation with MgO and negative correlation with Th (Fig.5.2A) indicating fractionation of the parental magma (Tadesse Yihunie et al., 2006).

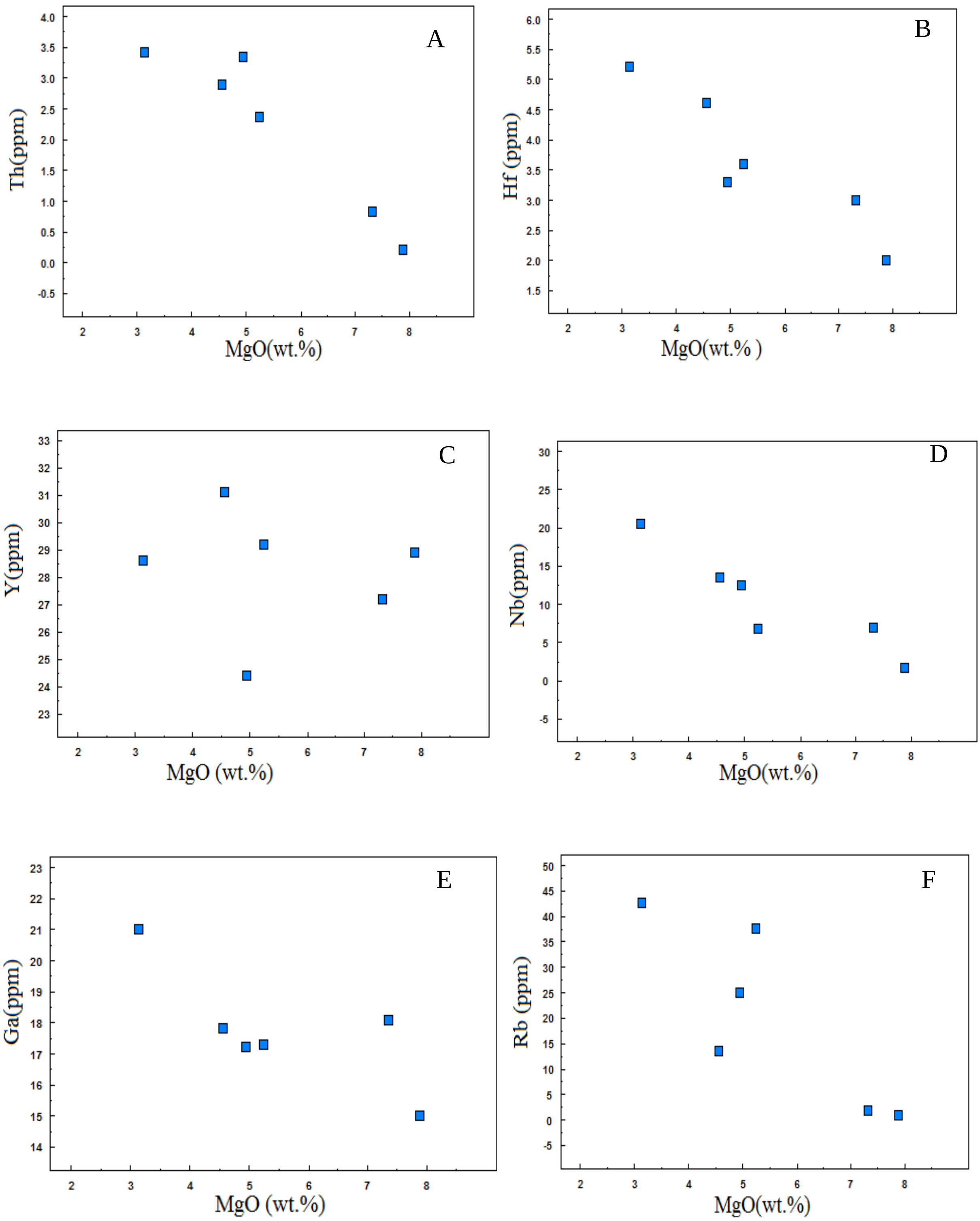
A
Th(ppm)
MgO(wt.%)
B
Hf (ppm)
MgO(wt.%)
C
Y(ppm)
MgO (wt.%)
D
Nb(ppm)
MgO(wt.%)
E
Ga(ppm)
MgO (wt.%)
F
Rb (ppm)
MgO(wt.%)

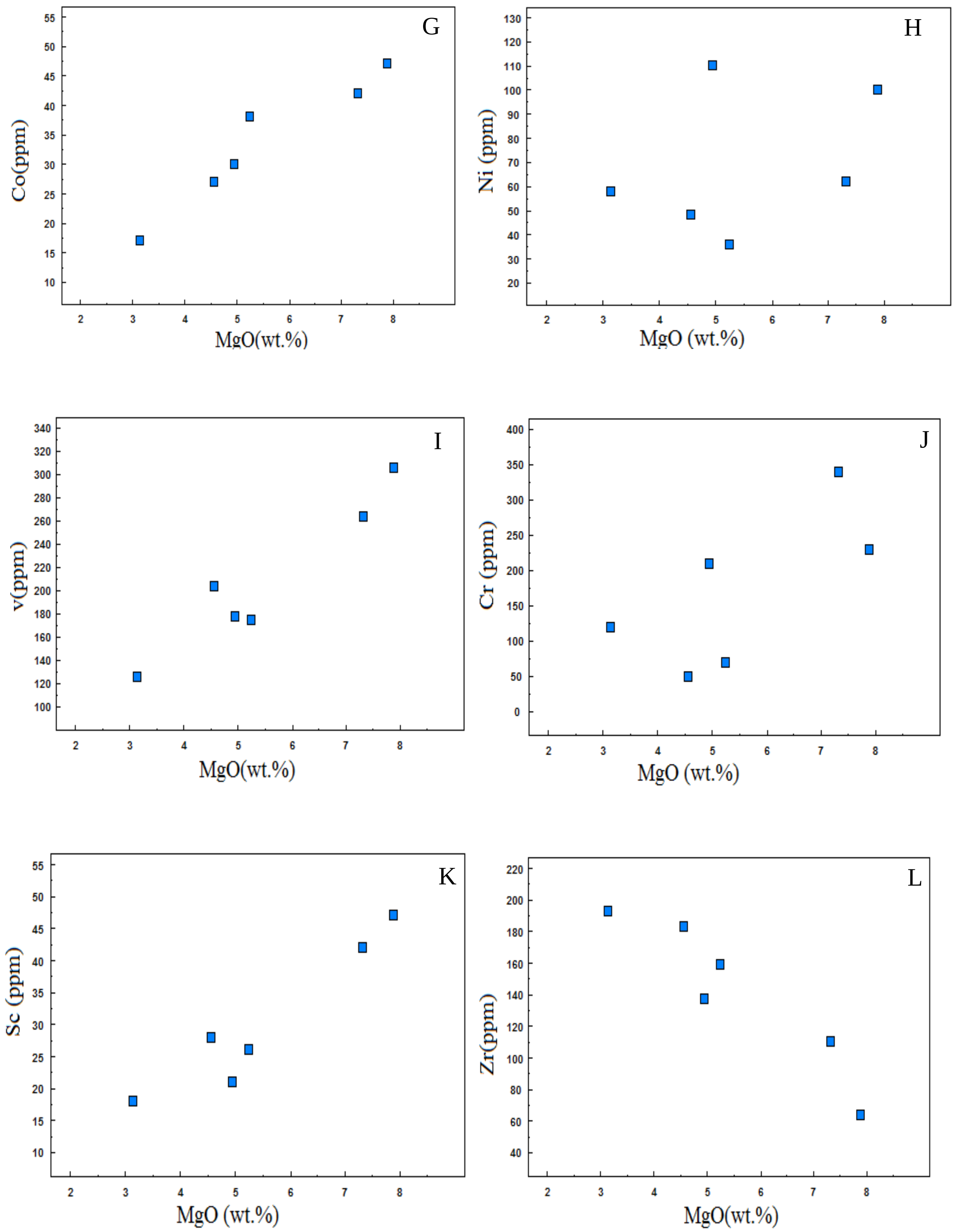

Figure 5.2 MgO versus selected trace elements variation diagrams for Bila metavolcanic rocks.

5.4 Zr Variation Diagrams for Trace Elements

Harker variation diagram is also plotted as a function of Zr versus selected trace elements, to understand their characteristics and to establish their relative mobility (Fig.5.3A-J). Green

(1980) as cited in Alene et al. (2000) suggested that Zr is the most incompatible element that cannot readily substitute in major mineral lattice. Based on this idea Zr is used to construct Harker variation diagram with selected trace elements such as Nb, Rb, Y, Hf, Th, Cr, Co, Sc and Ga for Bila metavolcanic rocks (Fig.5.3). Zr variation diagram patterns show a positive correlation with Nb, Rb, Y, Hf, Th, U and Ga, but it show negative correlation with Co and Sc. According to Alene et al. (2000) if Zr variation diagrams show continuous trend with trace element such as Nb, Rb, Y, Hf, Th, U, Cr, Co, Sc and Ga, it may suggest that the rocks were derived from a common source and those show negative correlation may suggests that they are concentrated in early fractionating ferromagnesian minerals. By similar condition, there are Zr variation diagram of Bila metavolcanic rocks showing continuous trend which may also reveal that most of these rocks were cogenetic suite. And also trace elements such as Co and Sc show negative correlation for both Bila metavolcanic and metaultramafic rocks, which may also suggest that they may concentrated in early fractionating ferromagnesian minerals of the rocks of study area.

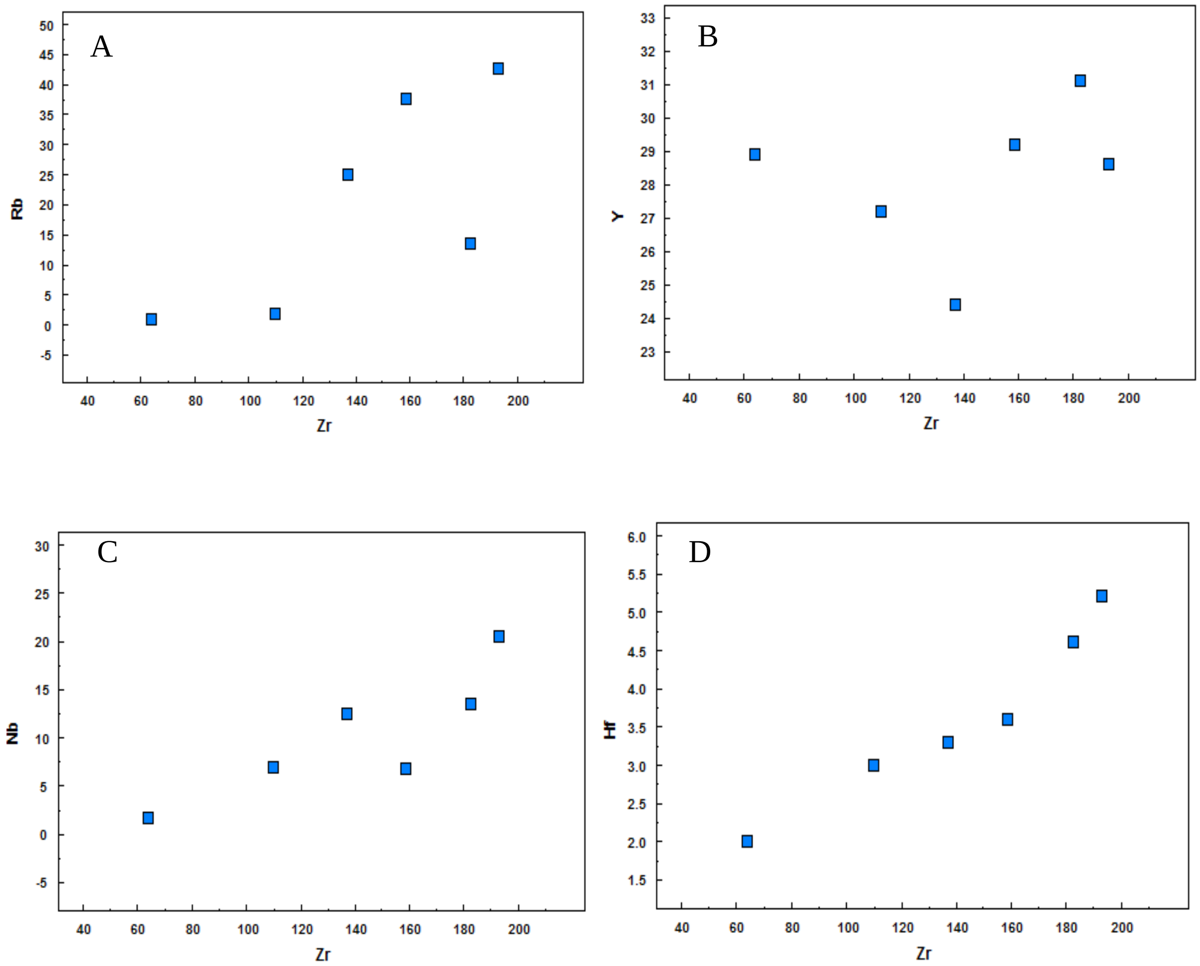

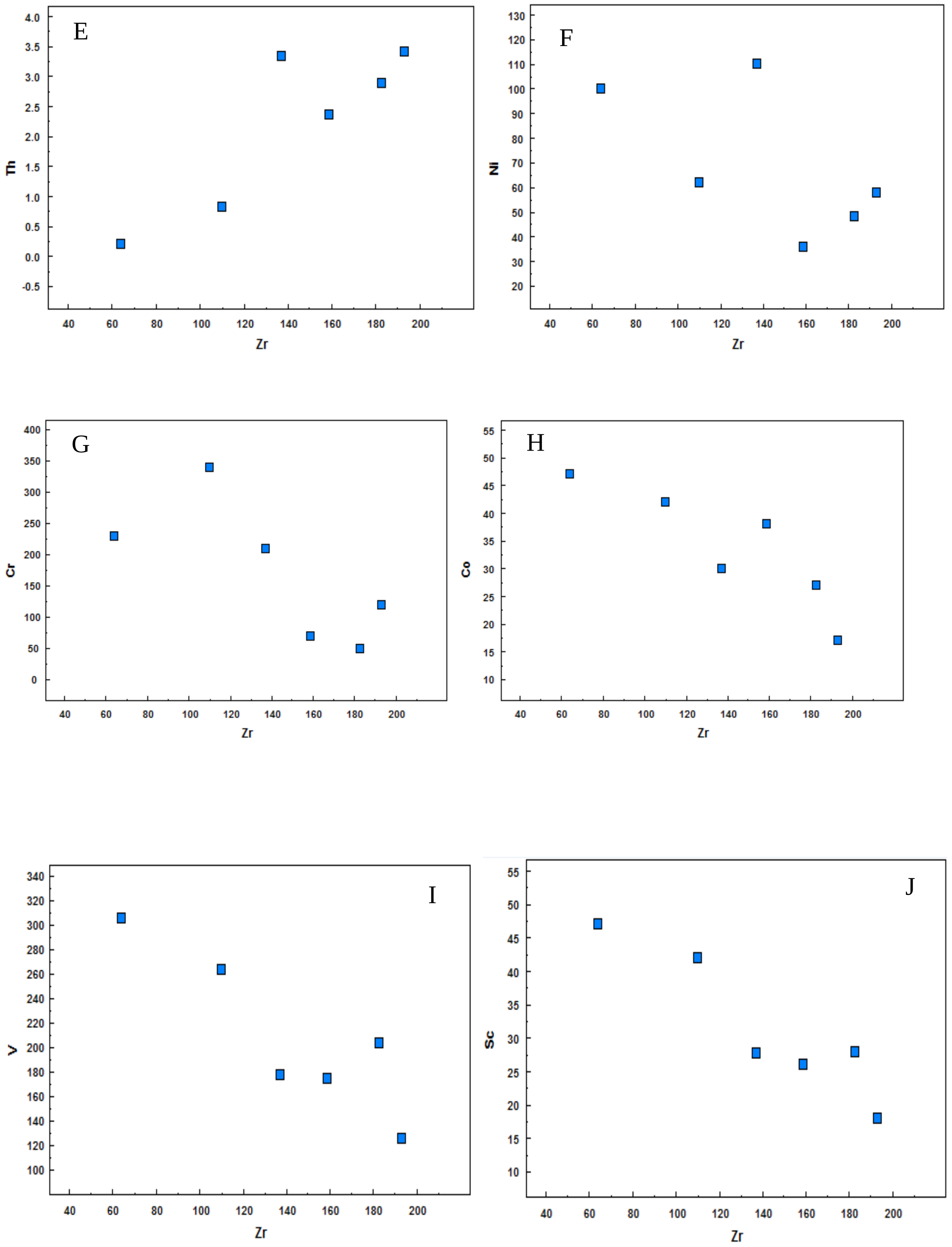

Figure 5.3 Zr variation diagrams for selected trace elements such as Nb, Cr, Co, Y, Hf, Th, U, Ga, Sc and Rb (in ppm) of the Bila metavolcanic rocks.

5.5 Trace Element Geochemistry

The abundances of trace elements are used to distinguish the crystals that were present during melting or fractional crystallization of the magma. To identify those trace elements involved in the melting or in fractional crystallization of the magma, chondritic normalized rare earth element (REE) abundance pattern (Fig.5.4) and multi-element variation diagram pattern (Fig 5.5) for Bila metavolcanic rocks are plotted.

The REE trend indicate slight enrichment in light rare earth elements (LREE) but, one sample from metavolcanic (BG-32) show depletion in LREE. However all rock samples from the Bila show slight depleted pattern for heavy rare earth elements (HREE). The enrichment of LREE and slight depleted pattern in HREE (Fig.5.4) indicates fractionations of the basic magma. From the Chondritic normalized diagram of REE (Fig.5.4) rock samples (BG-7 and BG-23) show slight negative anomaly in Eu which are 0.69 and 0.825 in terms of (Eu/Eu*) respectively. This may suggest fractionation of plagioclase feldspar in the magma. According to Valsami and Cann (1992) as cited in Woldehaimanot and Behrmann (1995) intense hydrothermal alterations result in positive Eu anomalies. In similar manor there were slight positive Eu anomalies in one sample (BG-16) which is 1.087 in terms of Eu/Eu*) of Bila rocks. This may reflect the effect of hydrothermal alteration in this sample particularly.

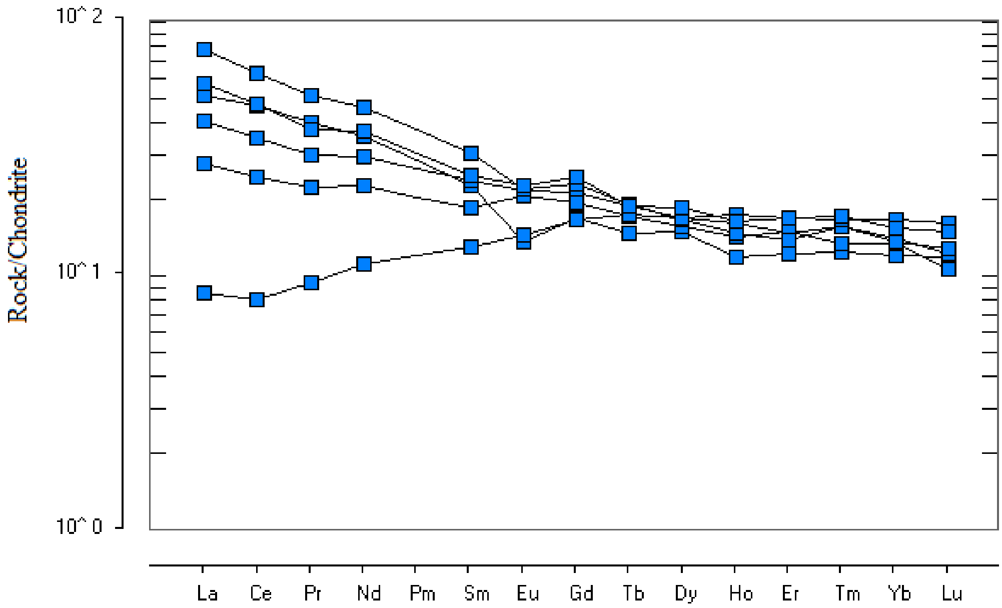

Figure 5.4 Chondrite-normalised REE pattern for representative metavolcanic rocks of Bila area (Boynton, 1984).

From the spider diagram pattern (Fig.5.5) samples (BG-7 and BG-13) of metavolcanic rocks show negative anomaly for Nb and Ti. These negative anomaly may related with fractionations of sphene and ilmenite present in the rocks (Rollinson, 1993). From this plot some samples of metavolcanic rocks shows negative anomaly for Rb, Pr and Sr which may suggests the removal of alkali feldspar and plagioclase feldspar from the magma. The negative anomaly of K in metavolcanic rocks indicate that the lower SiO_2 content in the magma. Additionally, slight depletion of Sr and Eu are commonly explained by fractionation of plagioclase and K-feldspar of Bila metavolcanic rocks (Ewart et al., 1985).

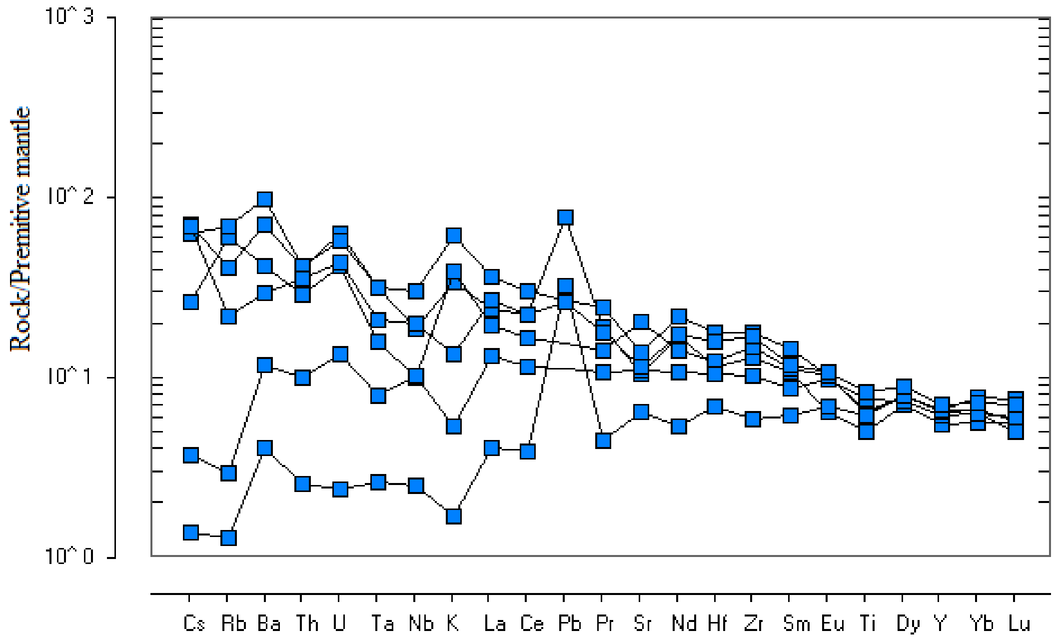

Figure 5.5 Multi-element variation diagram for metavolcanic rocks of Bila area (Primordial mantle-McDonough & sun, 1995).

5.6 Tectonic Setting

Since the rocks in the Bila area have been subjected to intense metamorphism, tectonic setting discrimination is based on the methods that use triangular discrimination diagrams of immobile trace elements. To determine geologic setting of metavolcanic rocks of the study area, the data is plotted on three immobile elements Zr-Y-Nb (Fig.5.6 A) and Th- Ta- Hf (Fig.5.6B) triangular discrimination diagrams. Based on these methods most of the samples are plotted within the volcanic arc basalt field. Such behaviour is the characteristic of back-arc basin basalts (Shervais, 2001).

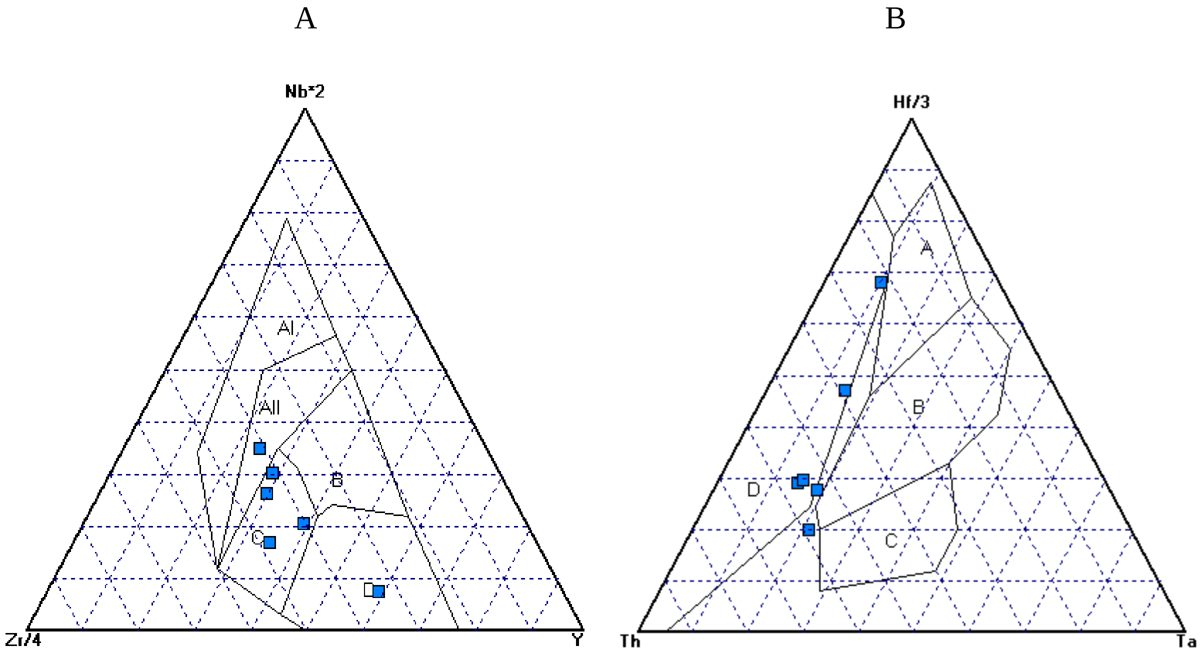

Figure 5.6 Tectonomagmatic discrimination diagrams of Bila metavolcanic rocks. A) Nb-Zr-Y triangular discrimination diagram (after Meschede, 1986). Within plate theoleiites plot in All, E-type MORB plot in B, Volcanic arc basalts plot in C and N-type MORB plot in D. B) Th- Ta-Hf triangular discrimination diagram (after Wood, 1980). N- Type MORB plot in A, E-type MORB plot in B, Alkaline within plate basalts plot in C and volcanic arc basalts plot in D field.

From tertiary discrimination diagram (Fig.5.6A and B) samples are plotted in volcanic arc and mid-ocean ridge basalts, this may give evidence for a back-arc basin type tectonic setting. These back-arc basin environments are characterised by the involvement of subduction-modified mantle components in the magma generation, producing spreading centre basalts with geochemical characteristics transitional to volcanic arc basalts (Saunders, 1984 as cited in Gebremedhin Tadesse and Allen, 2005).

5.7 Petrogenesis of Bila Metavolcanic Rocks

To describe petrogenesis of Bila metavolcanic rocks, major element and trace element variation diagrams as well as REE and multi element patterns are very important. Harker variation diagrams of major oxides like CaO, Al_2O_3, Fe_2O_5, Cr_2O_3, MnO, SiO_2, K_2O, P_2O_5, BaO, SrO and TiO_2 are plotted versus MgO. On the SiO2 versus MgO plot (Fig. 5.1D) most samples define a weak negative linear pattern, reflecting a decrease in silica with increasing MgO as would be expected for silica-poor rocks. Given the limited number of participating phases in tholeiitic magmas, this could reflect the effect of an under saturated mineral such as olivine on the fractionation of the parent magma. The Fe2O3 versus MgO plots (Fig.5.1F) also exhibit weak negative linear patterns, and may reflect involvement of ilmenite in the fractionation process. The CaO versus MgO plot (Fig.5.1C) shows a relatively tight positive linear pattern reflecting simultaneous removal of these two oxides from the parent magma, most probably accomplished by fractionation of clinopyroxene. The P2O5 versus MgO plot (Fig.5.1H) shows a tight strongly negative linear pattern between these oxides, possibly reflecting involvement of apatite in the fractionation process.

Trace elements such as Th, Hf, Nb, Ga, Rb and Zr are showing negative trend with MgO. However compatible trace elements like Co, Ni, V, Cr and Sc are showing positive trend with MgO. The positive and negative patterns of the compatible and incompatible elements with MgO may reflects the differentiation and fractionation of Mg and Fe bearing minerals such as olivine and pyroxene. The Mg and Fe are the accommodating elements for the compatible trace elements like Ni and Co. The Ni (Fig.5.2H) and Cr (Fig.5.2J) contents have positive correlation with MgO and negative correlation with Th (Fig.5.2A) indicating fractionation of the parental magma (Tadesse Yihunie et al., 2006).

The positive and negative correlations of major oxides and trace elements with MgO as well as the enrichment of LREE and slight depleted in HREE (Fig.5.4) infer that the differentiation and fractionations of Mg and Fe bearing minerals like olivine and pyroxene of basic magmas which are originated from the mantle sources (Saunders and Tarney, 1979 as cited in Gebremedhin Tadesse and Allen, 2005; Blade et al., 2015).

CHAPTER SIX

Conclusion and Recommendation

6.1 Conclusion

Bila metamorphic terrain encompasses metavolcano-sedimentary and meta-ultramafic rock groups. The metasedimentary group consists of slate, marble, phyllite, quartzite and graphite schist. The metavolcanic groups include: metabasalt and chlorite schist. While, the metaultramafic ones consist of serpentinite, talc schist and actinolite-tremolite schist. All the rock groups in the study area were affected by metamorphism. Textural change, grain size modification and recrystallization are observed in the rocks of the area with relict of some minerals from the pre-existing rock types. The metasedimentary rooks retained primary bedding and composed of mineral assemblages such as chlorite, mica, sericite, quartz and feldspar which show their origin may be came from pelitic rocks or clay rich rock materials. The presence of such mineral assemblages in the metasedimentary rocks of the study area indicate that the area were affected by low grade metamorphism of green schist facies. The abundance of mineral assemblages such as quartz, sericitized plagioclase, chlorite, epidote, actinolite, feldspar, opaque, calcite, talc and some relict of pyroxene and olivine in metaultramafic and metavolcanic rocks indicate that the area is experienced low grade green schist facies metamorphism.

Based on analysing the geometry of the rocks and their attitudes in the field and petrographic analysis, at least three deformational phases are recorded in the Bila area. The earlier deformation (D1) was responsible for the formations of parasitic, ptygmatic and similar folds as well as pervasive regional foliations. D2 deformational phases are mostly responsible for the formations of crenulation cleavage, crenulation lineation and open recumbent folds. The post D2 deformational phase may attributed to the later brittle deformational phase like veins, joints and faults.

Major oxides such as CaO, Al_2O_3, Fe_2O_5, Cr_2O_3 and MnO show increasing trend with increasing MgO and other major oxides like SiO_2, K_2O, P_2O_5, BaO, SrO and TiO_2 show negative correlation with MgO. The positive and negative correlation of major oxides with MgO indicate the fractionations of basic magma like olivine and pyroxene. The compatible trace elements increase with increasing MgO while incompatible trace elements decrease with increasing

MgO. This situations also reflects the differentiation and fractionation of Mg and Fe bearing minerals such as olivine and pyroxene. The major oxides and trace elements Harker variation diagrams, REE pattern and spider diagram of Bila metavolcanic rocks reflects the rocks are linked with fractional crystallization process. From Zr-Y-Nb and Th- Ta- Hf triangular discrimination diagrams most of the Bila rocks are within the volcanic arc basalt field.

6.2 Recommendation

Since the area recorded poly phase deformations, large scale structural mapping more than the present scale should be recommended for the further study of the tectonic evolution of the area.

Panning the gold by the local people is common. So, it is also recommended to study the genesis of base metals around the area for economic purpose.

Since this study covered a small area, further geochemical study on tectonic environment and geochronology around the area is also recommended.

Ultramafic rocks of the study area undergone intense hydrothermal alterations. So, care must be taken for the future geochemical survey while selecting representative rock samples around Bila area.

References

Abbate, E., Bruni, P. and Sagri, M. (2015). Geology of Ethiopia: A Review and Geomorphological Perspectives. 33-64 pp.

Abdelsalam, M.G. and Stern, R.J. (1996). Sutures and shear zones in the Arabian–Nubian Shield. *Journal of African Earth Sciences*, **23**:289–310.

Abraham, A. (1989). Tectonic history of the Pan-African low grade belt of western Ethiopia. Note No. 305, *Eth. Inst. Geol. Surv*., p. 15.

Mulugeta Alene, Ruffini, R. and Sacchi, R. (2000). Geochemistry and Geotectonic Setting of Neoproterozoic Rocks from Northern Ethiopia (Arabian-Nubian Shield). *Gondwana Research*, **3**: 333-347.

Allen, A. and Gebremedhin Tadesse (2003). Geological setting and tectonic subdivision of the Neoproterozoic orogenic belt of Tuludimtu, Western Ethiopia. *Journal of African Earth Sciences*, **36**: 329–343.

Allen, A. and Gebremedhin Tadesse (2005). Reply to Discussion of ''Geological setting and tectonic subdivision of the Neoproterozoic Orogenic Belt of Tuludimtu, Western Ethiopia''. *Journal of African Earth Sciences*, **41**: 333–336.

Asfawossen Asrat, Barbey, P., and Gleizes, G. (2001). The Precambrian Geology of Ethiopia: a review, *Africa Geoscience Review*, **8**: 271-288.

Beyth, M. (1972). The geology of central and western Tigray. Ph. D. Thesis Rheinische Friedrich Wilhems Universitat, Bonn, W. Germany, 200p.

Blades, M. (2013). Age and Origin of the Western Ethiopia Shield. *University of Adelaide*,

Blades, M.L., Collins ,A.S., Foden, J., Payne, J.L., Xu, X., Tadesse Alemu, Girma Woldetinsae, Clark, C. and Taylor, R.J.M. (2015). Age and Hafnium isotopic evolution of the Didessa and Kemashi Domains, western Ethiopia. *Precambrian Research*, **270**: 267–284.

Berhe, S.M. (1990). Ophiolites in Northeast and East Africa: implications for Proterozoic crustal growth. *Journal Geological Society of London*, **147**, 41–57.

Collins, A.S., Pisarevsky, S.A. (2005). Amalgamating eastern Gondwana: the evolution of the Circum-Indian Orogens. *Earth-Sci. Rev*. **71**: 229–270.

Cox, G.M., Lewis, C.J., Collins, A.S., Halverson, G.P., Jourdan, F., Foden, J., Nettle, D., Kattan, F. (2012). Ediacaran terrane accretion within the Arabian-Nubian Shield. *Gondwana Res*. **21**: 341–352.

de Wit, M.J. and Senbeto Chewaka (1981). Plate tectonic evolution of Ethiopia and the origin of its mineral deposits: An overview. In: Plate Tectonics and Metallogenesis: Some guidelines to Ethiopian Mineral Deposits. *Ethiopian Institute of Geological Surveys*, **2**: 115–119.

Fiori, M., Gabarino, C., Grillo, S., Tadesse, S. and Valera, R. (1988). Origin and evolution of th Lega Dembi primary gold deposit (Sidamo, Ethiopia). *Symposium in honour of Peiro Zuffardi, Cagliari (Italy)*, 10-15.

Fritz, H., Abdelsalam, M., Ali, K.A., Bingen, B., Collins, A.S., Fowler, A.R., Ghebreab, W., Hauzenberger, C.A., Johnson, P.R., Kusky, T.M., Macey, P., Muhongo, S., Stern, R.J., Viola, G.(2013). Orogen styles in the East African Orogen: a review of the Neoproterozoic to Cambrian tectonic evolution*. J. Afr. Earth Sci.*

Garland, C, R. (1980). Geology of the Adigrat Area. *Geological Survey of Ethiopia* **1**: 51p.

Gebremedhin Tadesse and Alistair Allen (2005). Geology and geochemistry of the Neoproterozoic Tuludimtu Ophiolite suite, western Ethiopia. *Journal of African Earth Sciences*, **41**: 192–211.

Green, T.H. (1980) Island arc and continent-building magmatism - A review of petrogenic models based on experimental petrology and geochemistry. In: Banks, M.R. and Green, D.H. (Eds.), Orthodoxy and creativity at the Frontiers of Earth Sciences (Carey Symposium). *Tectonophys*, **63**: 367-385.

Grenne, T., Pedersen, R.B., Bjerkgard, T.B., Braathen, A., Mulugeta Gebreselassie and Tadesse Worku (2003). Neoproterozoic evolution of Western Ethiopia: igneous geochemistry, isotope systematics and U–Pb ages. *Geol. Mag*, **140:**373–395.

Jakes, P. and White A. J. R. (1972). Major trace element abundances in volcanic rocks of orogenic areas. *Geol. Soc*, **83**: 29–40.

Johnson, P., Andresen, A., Collins, A.S., Fowler, A., Fritz, H., Ghebreab, W., Kusky, T., Stern, R. (2011). Late Cryogenian–Ediacaran history of the Arabian-Nubian Shield: a review of depositional, plutonic, structural, and tectonic events in the closing stages of the northern East African Orogen. *J. Afr. Earth Sci.* **61**:167-232.

Kazmin, V. (1971). Precambrian of Ethiopia. Nature, **230**: 176-177.

Kazmin, V. (1975). The Precambrian of Ethiopia and some aspects of the geology of the Mozambique Belt.- Bull. Geophys. Obs. Addis Ababa, **15**:27-18.

Kazmin, V., Alemu Shiferaw and Tilahun Balcha (1978). The Ethiopian basement: stratigraphy and possible manner of evolution. *Geologische Rundschau,* **67(2):**531-546.

Kazmin, V., Alemu Shiferaw, Mengesha Tefera., Berhe, S.M., Senbeto Chewaka (1979). Precambrian structure of western Ethiopia. *Annals Geological Survey Egypt,* **9**:1-8.

Kröner, A., Linnebacher, P., Stern, R., Reischmann, T., Manton, W., Hussein, I. (1991). Evolution of Pan-African island arc assemblages in the southern Red Sea Hills, Sudan, and in southwestern Arabia as exemplified by geochemistry and geochronology. *Precambrian Res***, 53**:99-118

Meert, J.G., 2003. A synopsis of events related to the assembly of eastern Gondwana. *Tectonophysics,* **362**: 1-40.

Meert, J.G., Lieberman, B.S., 2008. The Neoproterozoic assembly of Gondwana and its relationship to the Ediacaran–Cambrian radiation. *Gondwana Res,* **14:**5-21.

Mengesha Tefera, Tadiwos Chernet and Worklneh Haro (1996). Explanation of the Geological Map of Ethiopia. *Ethiopian Institute of Geological Surveys,* **2nd** edition.

Nureldin Hassan Lissan and Abdallah Kodi Bakheit (2010). The Geology and Geochemistry of Metavolcanic Rocks from Artoli Area, Berber Province, Northern Sudan: An Implication for Petrogenetic and Tectonic Setting. *Journal of American Science*, **6(8**).

Robinson, F., Foden, J., Collins, A. (2015). Geochemical and isotopic constraints on island arc, synorogenic, post-orogenic and anorogenic granitoids in the Arabian Shield, Saudi Arabia. *Lithos*.

Robinson, F., Foden, J., Collins, A., Payne, J. (2014). Arabian Shield magmatic cycles and their relationship with Gondwana assembly: insights from zircon U–Pb and Hf isotopes. *Earth Planet. Sci.*, **408**: 207–225.

Rodrigo Chaves Ramos and Edinei Koester (2015). Lithogeochemistry of the meta-igneous units from Arroio Grande Ophiolitic Complex, southernmost Brazil. *Brazilian Journal of Geology*, **45(1**): 65-78.

Rollinson, H.R. (1993). Using Geochemical Data: *Evaluation, Presentation, Interpretation*. Pearson Education limited, England.

Saunders, A.D. (1984). The rare earth element characteristics of igneous rocks from the ocean basins. In: Henderson, P. (Ed.), Rare Earth Element Geochemistry. *Elsevier*, Amsterdam, pp. 205–236.

Shervais, J. (2001). Birth, death, and resurrection: the life cycle of suprasubduction zone ophiolites. *Geochem. Geophys. Geosyst*. **2(1**).

Stern, R.J. (1994). Arc assembly and continental collision in the Neoproterozoic East African Orogen. *Ann. Rev. Earth Planet. Sci.* **22**:319–351.

Tadesse Alemu and Tsegaye Abebe (2007). Geology and Tectonic Evolution of the Pan-African Tulu Dimtu Belt, Western Ethiopia. *Online Journal of Earth Sc.,* **1**:24–42.

Teklewold Ayalew, Bell, K., Moore, J.M. and Parrish, R.R. (1990). U-Pb and Rb-Sr geochronology of the Western Ethiopian Shield. *Geol. Soc.* **102**:1309–1316.

Tadesse Yihune, Mamoru Adachi and Koshi Yamamoto (2006). Geochemistry of the Neoproterozoic metabasic rocks from the Negele area, Southern Ethiopia: Tectonomagmatic implications. *Journal of African Earth Sciences*, **44**:255-269

Teklewold Ayalew, (1997). Metamorphic and Structural evolution of the Gore - Gambella area, Western Ethiopia. *Ethiop.J.Sci*, **20(2):**235-259.

Teklewold Ayalew and Johnson, T.E. (2002). The Geotectonic Evolution of the Western Ethiopian Shield. *SINET*, **25**:227–252.

Tesfaye Kebede, Koeberl, C. and Koller, F. (1999). Geology, geochemistry and petrogenesis of intrusive rocks of the Wallagga area, western Ethiopia. *Journal of African Earth Sciences*, **29**: 715–734.

Tesfaye Kebede and Koeberl, C. (2002). Petrogenesis of A-type granitoids from the Wallagga area, western Ethiopia: constraints from mineralogy, bulk-rock chemistry, Nd and Sr isotopic compositions. *Precambrian Research***, 121**:1–24.

Valsami,E and Cann, J. R. (1992). Mobility of rare eath elements in zone of intense hydrothermal alteration in the Pindos ophiolites, Greece. In: Ophiolite and their Modern Oceanic Analogues (Edited by Parson, L. M., Murtan, B. J. and Browning, P.). *Geological Society Special Publication*, London, **60**, 219-232.

Woldehaimanot, B. and Behrmann B. J. (1995). A study of matebesite and metagranite chemistry in the Adola region (South Ethiopia): implications for the evolution of the East African orogeny. *Journal of African Earth Sciences,* **21**: 459-476.

Woldemichael, B.W., Kimura, J.-I., 2008. Petrogenesis of the Neoproterozoic Bikilal-Ghimbi gabbro, western Ethiopia. J. Mineral. *Petrol. Sci.* 103: 23–46.

Woldemichael, B.W., Kimura, J.-I., Dunkley, D.J., Tani, K., Ohira, H. (2010). SHRIMP U–Pb zircon geochronology and Sr–Nd isotopic systematic of the Neoproterozoic Ghimbi Nedjo mafic to intermediate intrusions of western Ethiopia: a record of passive margin magmatism at 855 Ma? Int. J. *Earth Sci*., **99**: 1773–1790.

Yibas, B., Reimold, W., Anhaeusser, C., Koeberl, C. (2003). Geochemistry of the mafic rocks of the ophiolitic fold and thrust belts of southern Ethiopia: constraints on the tectonic regime during the Neoproterozoic (900–700 Ma). *Precambrian Res.*, **121**: 157–183.

Appendix

Measured Structural Data from Bila area

No	Structural elements	Strike	Dip amount	Location	Lithologic units
1	Foliation	30˚	75˚ SE	E-0800776, N-1041136	Talc schist
2		40˚	70˚NW	E-0799913, N-1040549	Marble
3		30˚	80˚W	E-0801534, N-1042313	Marble
4		20˚	80˚SE	E-0801707, N-1041833	Slate
5		25˚	70˚SE	E-0823001, N-1042851	Slate
6		20˚	75˚SE	E-0802506, N-1041295	Slate
7		35˚	80˚SE	E-0802880, N-1041556	Phyllite
8		35˚	70˚SE	E-0802958, N-1041263	Phyllite
9		30˚	85˚SE	E-0803617, N-1042753	Phyllite
10		33˚	65˚SE	E-0803257, N-1043113	Phyllite
11		30˚	60˚SE	E-0803393, N-1043607	Phyllite
12		60˚	50˚W	E-0801100, N-1043872	Metabasalt
13		20˚	80˚NW	E-0798965, N-1042680	Graphite schist
14		30˚	65˚NW	E-0800175, N-1043520	Graphite schist
15		40˚	55˚NW	E-0802928, N-1042170	Marble
16		25˚	67˚E	E-0803189, N-1038240	Chlorite schist
17		35˚	70˚NW	E-0803473, N-1038433	Chlorite schist
18		20˚	70˚NW	E-0789750, N-1039850	Chlorite schist
19		30˚	72˚NW	E-0796539, N-1038638	Chlorite schist
20		35˚	75˚NW	E-0799652, N-1039561	Chlorite schist
21		30˚	65˚NW	E-0798450, N-1039550	Chlorite schist
22		25˚	70˚NW	E-0797400, N-1040251	Chlorite schist
23		35˚	65˚NW	E-0796774, N-1041811	Chlorite schist
24		30˚	77˚NW	E-0796684, N-1044048	Chlorite schist
25		25˚	75˚SE	E-0800625, N-1040359	Phyllite
26		30^0	67˚SE	E-0801483, N-1038887	Phyllite
27		20˚	80˚SE	E-0801186, N-1040938	Talc schist
28		35˚	65˚SE	E-0801483, N-1038887	Talc schist
29		20˚	75˚E	E-0801060, N-1042522	Phyllite
30		40˚	60˚SE	E-0800935, N-1043430	Phyllite
1	Fold axial plane	30˚	50˚SE	E-0802958, N-1041263	Phyllite
2		15˚	75˚E	E-0803617, N-1042753	Phyllite
3		30˚	60˚SE	E-0803681, N-1042803	Phyllite
4		35˚	55˚SE	E-0803393, N-1043607	Phyllite
5		20˚	70˚E	E-0798103, N-10044973	Marble
6		15˚	50˚E	E-0801483, N-1038887	Phyllite
7		25˚	80˚SE	E-0800625, N-1040359	Phyllite
1	Joint	320˚	85˚NE	E-0796684, N-1043300	Metabasalt
2		110˚	50˚W	E-0798877, N-1042534	Phyllite
3		240˚	65˚SE	E-0801100, N-1043872	Metabasalt
4		80˚	80˚S	E-0800935, N-1043430	Metabasalt
5		280˚	75˚NE	E-0801140, N-1043626	Metabasalt

1	Fault	330˚	75˚NE	E-0831760, N-1042313	Phyllite
2		280˚	50˚N	E-0803159, N-1042341	Phyllite
3		40˚	55˚SE	E-0831590, N-1042314	Phyllite
4		310˚	70˚NE	E-0803922, N-1043203	Phyllite